The Role of SLAM-Associated Protein in T Cell Signaling and Apoptosis

by

Melissa R. Eslinger

A dissertation submitted in partial fulfillment
of the requirements for the degree of
Doctor of Philosophy
(Cancer Biology)
in the University of Michigan
2015

Doctoral Committee:

Professor Colin Duckett, Chair
Professor Cheong-Hee Chang
Associate Professor Elizabeth Lawlor
Assistant Professor Andrew Rhim

Dedication

To my parents, no matter where in the world the path has led you have been the greatest source of inspiration and support. Thank you for everything.

Acknowledgements

This project required the cooperation of many agencies and individuals to accomplish an exceptionally challenging task. I thank Colin Duckett for accepting me into the program, serving as my advisor, and guiding me through its challenges. To the members of the Duckett Lab, Stefanie Galban and Andrew Kocab, I appreciate your support and experimental assistance. I am grateful for the guidance from my thesis committee members Cheong-Hee Chang, Elizabeth Lawlor, and Andrew Rhim.

Several collaborators have assisted with providing reagents or advice throughout. Jordan Shavit provided TALEN reagents and Niall Kenneth assisted protocols while Robert Lyons and Suzanne Gelnick assisted the CE screening. Cheong-Hee Chang and Yuenghyen Kim performed mitochondrial experiments, Andrew Snow assisted with SAP reagents and guidance, and Artur Veloso translated bioinformatics and was a perpetual sounding board. Thanks to Ann Savory and Zarinah Aquil who worked behind the scenes.

Finally, I thank my Army family for providing funding and support which allowed me to pursue this goal and return to the profession that is my passion. From USMA faculty, COL Leon Robert, Ken Wickiser, and Mike Labare to Army mentors BG Bill Burleson, III and LTC Matt Macneilly you have developed me as a leader, mentor, and teacher over the past 18 years. It has truly taken an army to raise this scientist and for everyone who has played a role, I am eternally grateful.

Table of Contents

List of Figures

List of Tables

Abstract

X-linked Lymphoproliferative type 1 (XLP1) disease is a rare inherited syndrome characterized by generalized immunodeficiency, an extreme sensitivity to viral infections and a predisposition to the development of lymphoma. The disease is caused by loss-of-function mutations in the gene encoding the SLAM-associated protein (*SAP*). SAP is a SH2-domain-containing protein that interacts with the cytoplasmic tail of signaling receptors and protein tyrosine kinases to promote T cell activation following stimulation of the T cell receptor (TCR). T cell signaling regulates the balance between cell activation and death, and defects contribute to the lymphoproliferative nature of the disease. Previous studies have examined the various roles of SAP in modulating T cell responses, but these influences require further investigation, and are the focus of this study. To clarify the role of SAP in T cell signaling, we took a gene editing approach to disrupt the *SAP* gene and created a *SAP*-null T cell line. Through this approach we identified *SAP*-specific effects, which included cytokine production, transcription factor activity, and calcium mobilization. Interestingly, *SAP*-null cells exhibited a decrease in IL-2 expression, attributable to defective nuclear factor of activated T cells (NFAT) activation, and increased IFN-γ production following TCR stimulation. Moreover, cells with *SAP* deficiencies have a heightened sensitivity to apoptotic stimuli. These results suggest that *SAP* defects drastically alter T cell activation and the cytokine environment,

making T cells more sensitive to apoptotic stimuli, potentially impeding their ability to respond to immune challenges. Together, these results identify specific *SAP*-dependent defects in T cell signaling that could contribute to the characteristic phenotypes of patients with XLP1 disease.

Chapter 1 X-Linked Lymphoproliferative (XLP) Disease

1.1 Introduction

X-linked Lymphoproliferative (XLP) disease is a rare inherited immune disorder resulting from respective mutations or loss-of-function in the SLAM-associated protein (*SAP*)[1–3] or X-linked inhibitor of apoptosis protein (*XIAP*)[4]. While these two genes co-occupy the Xq25 locus[5], they share no sequence homology, nor do their proteins appear to interact[6]. Affected children exhibit a spectrum of hematological defects, and these defects are often triggered by exposure to the Epstein-Barr Virus (EBV)[7].The lymphoproliferative nature of the disease suggests that the delicate balance between immune cell activation and death is disturbed[8]. While previous work has advanced the understanding of SAP's role as an adaptor protein, which modulates T cell signaling, the precise role of *SAP* in T cell signaling is not fully understood. The goal of this thesis is to investigate how *SAP* modulates T cell signaling and death to generate the phenotypes of XLP.

In this thesis a gene editing approach was taken to disrupt the human *SAP* gene in an established cell line to model the effects of *SAP* deficiencies (chapter 2). These *SAP*-deficient cells allowed the functional characterization of defects following T cell receptor (TCR) stimulation. Through this approach we identified *SAP*-specific effects, which included cytokine production, transcription factor activity, and calcium mobilization, and these results are presented in chapter 3.

Moreover, cells with *SAP* deficiencies have a heightened sensitivity to apoptotic stimuli, as discussed in chapter 4. Together, these results identify specific *SAP*-dependent defects in T cell signaling in a gene-edited model cell line, which could contribute to the characteristic clinical picture of patients with XLP1 disease.

1.2 Primary Immunodeficiencies and XLP

X-linked lymphoproliferative disease (XLP) is one of many rare primary immunodeficiencies (PIDs) where patients have genetic defects that predispose them to develop abnormal numbers or improperly functioning immune cells[9]. Although the diseases may differ, symptoms often manifest after exposure to viruses[10]. Advances in molecular genetics have led to the identification of many new PIDs and facilitated their diagnosis[11]. Table 1.1 identifies select primary immunodeficiencies along with their most commonly mutated genes within their respective disorder. Perhaps the most recognized PID is severe combined immunodeficiency (SCID) where patients exhibit severe reactions to infections due to low or absent numbers of T, NK, and B cells[12,13], immune cells described later. There are also primary conditions where inherited mutations cause cytotoxic defects such as autoimmune lymphoproliferative syndrome (ALPS) that stems from mutations in the *FAS* gene[14]. Mutations within the cytoplasmic tail of the receptor Fas impair the formation and activation of apoptotic signaling complexes and results in excessive proliferation of lymphocytes[14,15].

Disease	Defective Gene
Severe combined immunodeficiency (SCID)	*IL-2RG, RAG, CD3,* etc[13]
Autoimmune lymphoproliferative syndrome (ALPS)	*FAS*[16]
Hemophagocytic lymphohistiocytosis (HLH)	*PRF1, UNC13D*[17]
Wiskott-Aldrich syndrome (WAS)	*WASP*[18]
X-linked lymphoproliferative disease (XLP)	*SAP/XIAP*

Table 1.1 Select primary immunodeficiencies. Primary immunodeficiencies result in aberrant numbers or impaired function of immune cells due to inherited genetic defects. While these diseases can results from defects in several different genes, the most commonly mutated genes are listed with their respective disease.

Patients with hemophagocytic lymphohistiocytosis (HLH) inherit defects where cytotoxic lymphocytes are unable to kill virally infected cells. The cytotoxic capability is limited by defects that impair the ability to produce or transfer apoptotic inducing enzymes into virally infected cells[19]. The virally infected cells survive and produce elevated amounts of cytokines that activate macrophages which accumulate in the liver and spleen causing organ enlargement[17]. Another primary immunodeficiency, Wiskott-Aldrich syndrome (WAS), is associated with excessive immune cell proliferation due to abnormally low levels of regulatory T cells[20,21]. Lymphoma is identified in a portion of WAS patients with excessive T cell proliferation[22,23]. Other WAS patients exhibit defects in the ability of actin to mobilize during the formation of the immune synapsis, impairing activation[24]. Thus, WAS patients can exhibit either lymphoproliferation or impaired T cell activation. Similarly, a fraction of patients with XLP also develop lymphomas[25] and have impaired immune cell development and persistent infections due to defects in cytotoxic immune effector cells[26].

XLP1 also known as Duncan's disease[27], is caused by mutations in *SAP* (SLAM-associated protein)[5]. As shown in figure 1.2, these mutations are randomly

distributed and are a combination of missense and nonsense mutations[5,28,29]. *SAP* is a small 128 amino acid protein, largely comprised of a phosphotyrosine-binding SH2 domain[30] that is only expressed in T and natural killer (NK) cells[1,31,32]. Point mutations observed in XLP1 patients have been shown to affect the phospho-tyrosine binding pocket, the hydrophobic cleft, or the stability of the SAP protein[33].

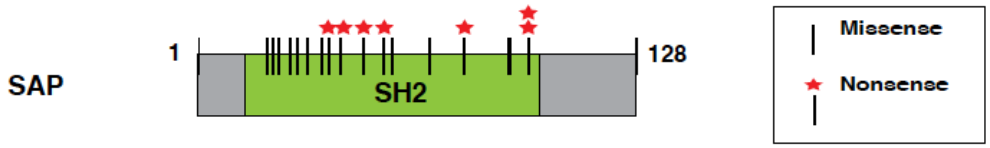

Figure 1.1 Structure and mutations of *SAP*. SAP is a small SH2 domain containing protein with mutations spanning the entire region of the gene[34]. Each line indicates an annotated patient mutation and the star denotes nonsense mutations. (Adapted from Blood (2010) 116:18.)

SAP defects manifests with a range of clinical presentations, outlined in table 1.2, and there is a general gap in the scientific evidence to why XLP1 patients develop these symptoms.

% of patients	(n=33)
55	Hemophagocytic Lymphohistiocytosis (HLH)
92	EBV triggered HLH
61	HLH associated lethality (HLH patients)
67	Hypogammaglobulinemia
7	Splenomegaly (w/o HLH)
30	Lymphoma

Table 1.2 The clinical picture of XLP1. XLP1 patients have a range of phenotypes including lymphoma[34]. (Adapted from Blood (2011) 117(5).)

HLH is the most common XLP morbidity and is characterized by excessive proliferation of lymphocytes and macrophages in response to infection[35], most

commonly triggered during the infection of B cells by EBV[36–38]. Moreover, HLH is associated with the abnormal production of cytokines[29] such as interferon-γ (IFN-γ) and interleukin-6 (IL-6), which stimulates the activation of many accessory cell types[39]. To counter the overproduction of cytokines and macrophage activation, the curative treatment for HLH and XLP is an allogeneic bone marrow transplant[40]. As previously mentioned, XLP is a rare disease[41], but the clinical burden may be under-diagnosed since *SAP* is not routinely screened in a pediatric setting. Notably, one-third of XLP1 patients develop lymphoma due to SAP-deficiencies[42].

1.3 XLP1 and B-cell lymphoma

The majority of *SAP*-mutated lymphomas are of B cell origin[43,44] and are classified as Burkitt's lymphoma[33]. Previous associations of EBV with cancer demonstrated that endemic EBV infection in African children contributes to the development of Burkitt's lymphoma, resulting from irregular B cell proliferation[45]. The comparison of endemic to sporadic Burkitt's lymphoma, shown in table 1.3, illustrates that there are worldwide differences in this disease. Both endemic and sporadic Burkitt's lymphoma are characterized by chromosomal translocations involving the c-MYC oncogene with over 80% of patients harboring t(8;14) involving the Ig heavy chain that results in rapidly proliferating B cells by over-activation of the cell cycle cell[46]. Orem, *et al.* (2007) proposed the model of the EBV-dependent development of B cell lymphoma where EBV infects African infants and T cells normally prevent the expansion of infected B cells. Exposure to other infections, such as malaria[47], suppress T cell activity and allow for the rapid

proliferation of B cells where chromosomal translocations can occur leading to the development of lymphoma.

	Burkitt's Lymphoma	
	Endemic (African)	Sporadic (Worldwide)
Onset	Childhood	Child (30%); Adult (70%)
Median age	7	30
Co-morbidity	Malaria	?; HIV
Tumor site	Face & jaw	Gastrointestinal
EBV status	100% +	30% +

Table 1.3 Comparison of endemic and sporadic Burkitt's lymphoma. While endemic African and sporadic Burkitt's lymphoma share similarities, they appear to be very different based on the age of onset and location of tumor development. The influence of additional co-morbidities and the correlation with EBV infection is unclear in sporadic lymphoma. XLP1-associated lymphoma patients have childhood onset but the contributions of additional co-morbidities are unclear. [Table is adapted from *African Health Sciences* (2007) 7(3): 166-175.]

XLP1-associated lymphoma shares similarities with both endemic and sporadic Burkitt's lymphoma patients. The age of onset is during childhood and is largely associated with EBV infection[48], similar to endemic cases, but the tumor sites are similar to sporadic cases involving the GI tract and kidneys[49]. It is possible that different strains of the virus exist and the interactions with unique co-morbidities contribute to the variation in endemic, sporadic, and XLP1 lymphoma patients. Although there have been studies[50] where SAP expression was measurable in B cells from EBV+ lymphoma patients, it is generally accepted that B cells do not express SAP[1,31,32]. This suggests that the development of lymphoma in XLP1 patients is due to non-cell autonomous roles of SAP in the cancer cell.

Lymphoma in XLP1 patients is thought to result from impaired immune surveillance of EBV infected B cells due to the absence of NKT (natural killer T) cells or impaired cytotoxic activity of CTLs (cytotoxic T lymphocytes) and NK (natural killer) cells[51]. NKT cells, a subpopulation of immune cells with NK like characteristics, express T cells receptors (TCRs). NKT cells contain an invariant TCR that recognizes the ligand α-galactosyl ceramide (α-GC)[52]. Upon binding α-GC, NKT cells release cytokines such as IFN-γ (interferon-γ)[52] that stimulate other lymphocytes during the adaptive immune response. In addition to a lack of NKT cells, XLP1 patients have defective NK cells[5]. NK cells are specialized innate immune cells that directly kill foreign pathogens by cytotoxic activity, similar to $CD8^+$ T cells. However, NK cells do not have TCRs, and their effects are executed when virally infected cells are not recognized as self by MHC-I (major histocompatibility class I)[53,54]. The persistence of virally infected cells within patients facilitates the transformation of infected B cells by the EBV genome[2,55,56] and the unopposed expansion of this population supports the neoplastic characteristics observed during the formation of XLP1-associated B cell lymphoma[49].

Relevant to XLP1 are two hallmarks of cancer that might be deregulated in the disease: genetic mutations contributing to genome instability, and the avoidance of immune surveillance[57]. As depicted in figure 1.2, immune cells identify mutant or precancerous cells and target them for destruction during immune surveillance. Pre-cancerous cells can acquire somatic mutations that facilitate their survival and neoplastic expansion. In the case of XLP1, the patients have an inherited genetic defect that increases the likelihood of cancer development. While EBV is primarily

asymptomatic in the normal healthy population, XLP1 patients have defects in their immune cells that contribute to the persistence of virally infected B cells. In this case, rather than a pre-cancerous cell acquiring capabilities to avoid immune surveillance the immune cells with SAP defects are ineffective at either the recognition of or the killing of infected B cells.

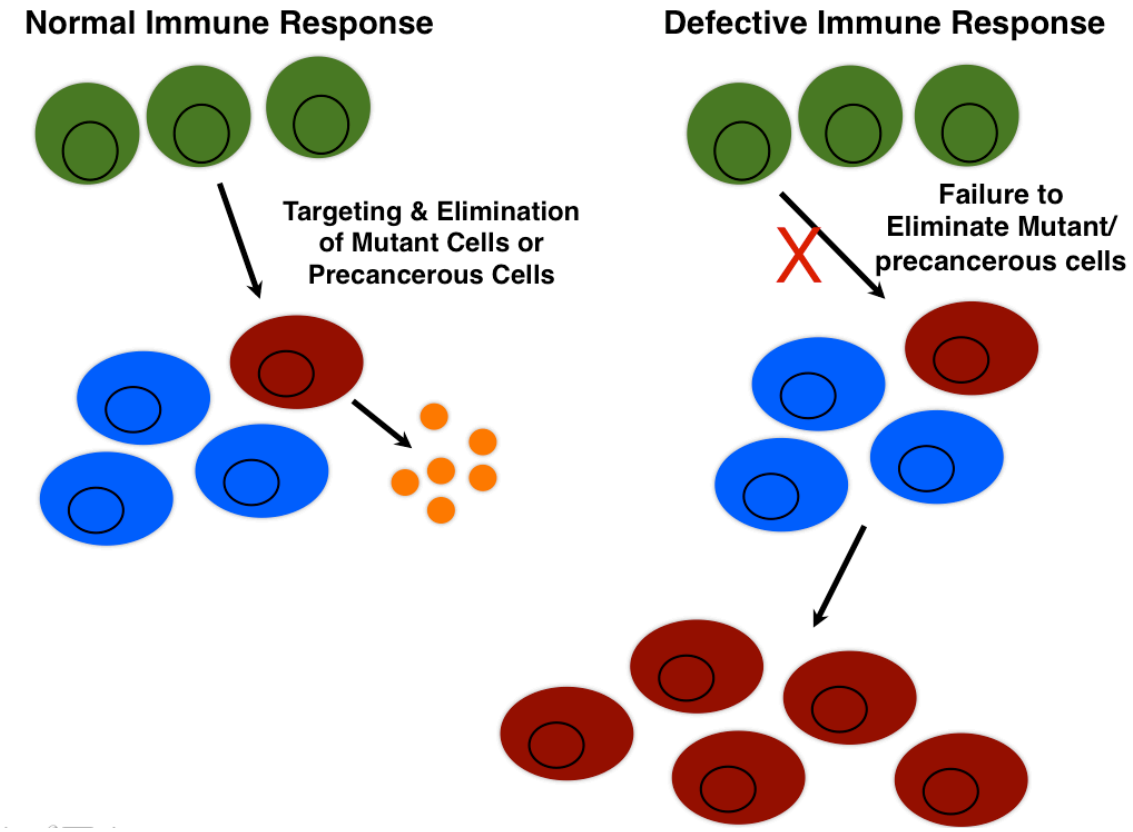

Figure 1.2. Immune surveillance defects contribute to cancer. The immune surveillance system identifies mutant or precancerous cells and targets them for destruction. When the immune system is defective, this permits the outgrowth and clonal expansion of cells to generate the formation of various neoplasms.

It is not well understood how cancer cells evade a fully functional immune system, but previous work has identified several possibilities. Studies have shown that tumors are able to downregulate major histocompatibility class I (MHC-I)

expression to escape T cell-mediated immune surveillance[58]. Anywhere from 40-90% of human tumors are deficient for MHC-I expression due to the partial or complete loss of the allele or by locus downregulation[58]. Virally infected cells that have lower levels of MHC-I expression are targeted by NK cells while cells with higher levels of MHC-I are recognized by TCR expressing CTLs[59]. Viral proteins are also capable inhibiting the production, movement, or formation of MHC-I and thus impair the ability for CTLs to recognize virally infected cells[60]. Following infection, viral proteins are encapsulated in endosomes and undergo proteasomal processing allowing the peptides to move to the ER, where they are loaded onto MHC-I components for movement through the Golgi forming secretory vesicles that migrate to the cell surface[60]. At the surface, the peptide within the MHC-I pocket is presented to cytotoxic T cells. For example, the HIV viral protein Nef down-regulates MHC-I on the cell surface by binding to the cytoplasmic tail of MHC-I causing it to migrate to the endosome for degradation[61] while Tat inhibits MHC-I promoter activity[62]. Similarly, the EBV latent member protein 2A (LMP2A) has been shown to impair the expression of MHC-II by impairing the class II transactivator (CIITA) protein[63]. In both cases, altered MHC expression restricts the types of immune cells that can respond to infected cells increasing oncogenic potential[64]. It is possible that XLP1 patients have downregulated MHC-I and, in particular following EBV infection, MHC-II. This would result in the inability of CTLs to target infected cells and impair the recognition of infected B cells and recruitment of the appropriate T cell help.

While tumor cells are capable of avoiding immune surveillance, it is plausible that cancer develops due to defects inherent in the immune cells themselves, maintaining a tumor permissive environment. This is supported by findings that the majority of viral induced cancers are within immunocompromised individuals[65] suggesting that the mechanisms that control viral infections must become deregulated in order for cancer to develop. Notably, the pathological examination of tumors have shown that immune cells are present within the tumors, sometimes at high numbers[66]. Innate immune cells, in particular, are thought to secrete tumor promoting growth factors[67,68] or secrete reactive oxygen species (ROS) that promote genetic mutations[69]. Lymphocyte activation signals would results in additional immune cell proliferation while additional mutations from exposure to ROS could convey a survival advantage within the pre-neoplastic or cancer cells in an inflammatory tumor microenvironment. Several studies using mouse models with defective $CD8^+$ cytotoxic T cells, $CD4^+$ T helper 1 cells, or natural killer cells demonstrated that animals with deficient immune cells have increased formation of tumors[70,71]. In the context of XLP1-associated lymphoma, it is possible that *SAP* mutations impair the ability of immune cells to effectively kill EBV infected B cells and the transformed B cells avoid destruction by altered expression of MHC on their surface. Therefore, non-autonomous influences of SAP contribute to the development of lymphoma. In this case, it is particularly important to understand how *SAP* defects impair immune cell activation as this could elucidate how XLP1 patients generate a permissive environment for the clonal expansion of EBV transformed B cells resulting in the development of lymphoma.

The burden of XLP1-associated B cell lymphoma may be under-represented in the population. A previous study[72] retrospectively analyzed the records of 158 males diagnosed with B cell-lymphomas and focused on patients with recurrent lymphoma, of which five were found to have undiagnosed *SAP* mutations. Thus, XLP1 may have a higher clinical burden and this disease, characterized by several phenotypes such as HLH and lymphoma, disrupts the normal immune response to infection[34]. As described in more detail below, T cells play a major role in the immune responses that are altered within XLP patients.

1.4 T cells and signaling

T cell activation involves the combination of stimulation of the T cell receptor (TCR) and modulation of the strength of the response by co-stimulatory receptors. The TCR is a complex of multiple $CD3^+$ subunits: the extracellular variant α and β chains, the transmembrane invariant γ, δ, and ε chains, and the intracellular ζ signaling chains[73]. The extracellular α and β chains recognize antigen peptides, while the invariant γ , δ, and ε chains assemble the rest of the TCR complex and the ζ chain, in conjunction with other signaling molecules, activates the T cell signaling cascade. Antigen-primed major histocompatibility (MHC) binds the TCR[74] and the ligation of additional co-stimulatory receptors, for example the well described CD28 receptor, induces T cell proliferation, differentiation, and cytokine production[75]. CD28 is expressed on T cells and interacts with the B7.1 (CD80) and B7.2 (CD86) receptor on antigen presenting cells during T cell activation[75]. Prior to activation, B7 binds with high affinity to the structurally similar inhibitory cytotoxic T-

lymphocyte-associated protein 4 (CTLA-4) expressed on inactive T cells[75]. Ligation of CD28 increases the expression of CTLA-4 to maintain homeostasis and prevent excessive T cell activation[76]. In cooperation with CD3, CD28 also has roles in the production of IL-2[77,78], discussed in detail below.

The two primary categories of T cells are classified by the presence of surface receptors CD4 or CD8[79]. CD4 expressing cells include the T helper (Th) and T regulatory (T_{reg}) lineages, while CD8 expressing cells are cytotoxic T cells. Initially, the thymic progenitors rearrange their α and β variable chains[80], in a process similar to VDJ recombination used in B cells to produce immunoglobulins[81], to recognize a large number of antigens[80]. Cells that successfully generate variant α and β subunits become double positive for CD4 and CD8 and proceed through self-recognition and selection before peripheral dispersal[82,83]. The differentiation of T cells into cytotoxic or T helper cells is guided by whether thymocytes bind MHC Class I or Class II ligands, respectively[80]. These single positive CD4 or CD8 T cells migrate to the periphery where they await activation based on cytokines and microenvironmental cues.

SAP was originally thought to bind to the intracellular domain of the signaling lymphocyte activation molecule (SLAM) family of receptors[84] to function as a termination signal. SLAM receptors contain an extracellular immunoglobulin-like domain, a transmembrane portion, and a cytoplasmic tail region[84,85] with variable numbers of immunoreceptor tyrosine-based switch motifs (ITSMs) that control the cell activation programs[33,86]. SAP recognizes the threonine/isoleucine-tyrosine-x-x-valine/isoleucine (T-I/Y-x-x-V/I) motif in the cytoplasmic tail of SLAM

receptor[86], and this binding can occur in the presence[87] or absence of phosphorylation[88]. However, further studies have ascribed SAP's role as an adaptor protein which not only binds the ITSMs but also recruits proteins such as protein tyrosine kinases (PTKs) to interact with the SLAM receptor family[53,54,89] linking SAP as a facilitator in T cell signaling.

T cells rely on various kinases to initiate multiple signaling cascades[90,91] and activate transcription factors that lead to cytokine production and T cell activation[92]. SAP binding to SLAM recruits PTKs that phosphorylate the cytoplasmic immunoreceptor tyrosine-based activation motifs (ITAMs) of the T cell receptor subunits[93]. During TCR stimulation two PTKs, lymphocyte-specific protein tyrosine kinase (LCK) and FYN, are recruited to the TCR complex [94,95], as shown in figure 1.3. Co-stimulation by CD28 has been shown to recruit LCK to the lipid raft[96], regions on the plasma membrane where signaling proteins are colocalized to facilitate their interactions[97]. LCK is associated with CD4 in T cells[98] whereas FYN is able to associate with multiple proteins, including SAP[94]. Structurally, LCK and FYN both contain SH3, SH2, and carboxy-terminal kinase domains[99]. The SH3 domains mediate binding to proline rich regions, while SH2 domains mediate interactions at phosphotyrosine residues[100]. As mentioned, disruption of the SAP/FYN interaction is shown to impair the development of NKT cells in mice[101] and this is thought to be why XLP1 patients do not develop NKT cells[5]. SAP has been shown to interact with FYN[95] to augment the phosphorylation of the SLAM receptor at tyrosine 307 and tyrosine 327[95].

The kinase domains of FYN and LCK are able to phosphorylate the ITAMs of the TCR and other target proteins during T cell signaling. One of the main functions of LCK is the phosphorylation of ζ-chain associated protein kinase of 70 kDa (ZAP-70) after TCR stimulation. ZAP-70 is normally bound in an inactive state to the ζ chain of the TCR at two phosphorylated residues. Following stimulation with CD3, CD28 recruits LCK to the TCR[96] where LCK phosphorylates and activates ZAP-70[102]. In turn, ZAP-70 phosphorylates other adaptors, such as the linker activator for T cells (LAT)[103,104]. LAT, in turn, activates several additional components including factors in the MAPK (mitogen activated protein kinase) and extracellular signal regulated kinase (ERK) pathways, as well as phospholipase C γ-1 (PLCγ–1)[105]. Studies examining the influence of co-stimulatory molecules have shown that CD28 also modulates the levels of PLCγ–1 in the presence of CD3 stimulation[106]. PLCγ–1 initiates calcium dependent and independent effects, discussed later.

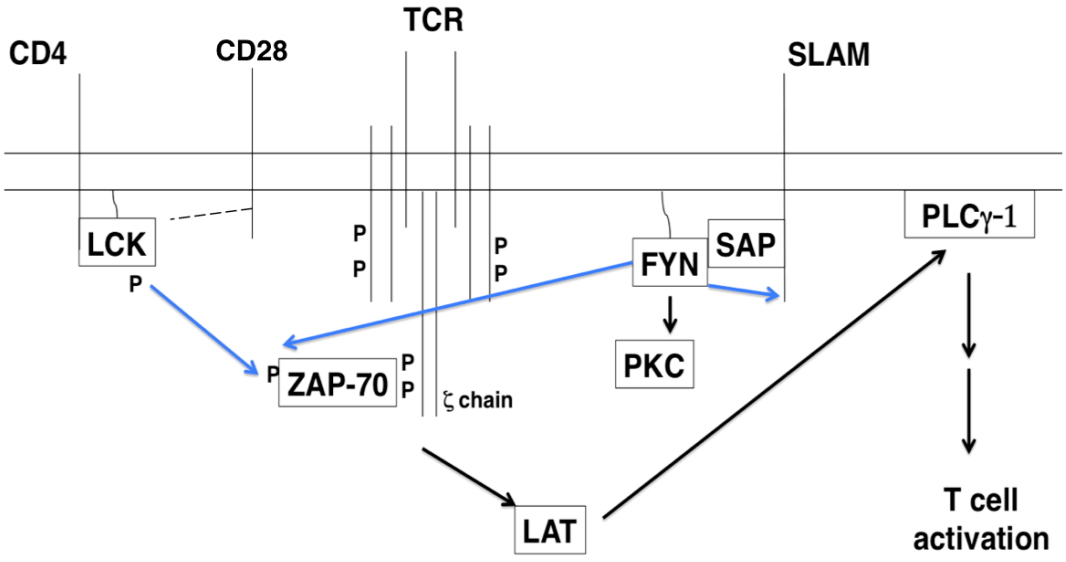

Figure 1.3 T cell activation and signaling cascades. The PTK LCK is associated with the CD4 receptor and, upon CD3 and CD28 stimulation, moves to the vicinity of the T cell receptor. LCK phosphorylates ZAP-70, which is bound to doubly phosphorylated ITAMs. This activates other proteins such as LAT and PLCγ–1 to stimulate T cell activation. SAP is bound to the co-stimulatory SLAM receptor and recruits the PTK FYN to the TCR. FYN activates several proteins, including ZAP-70, which can similarly activate PLCγ–1 and PKC–θ. Blue lines denote initial phosphorylation events upon TCR activation and co-stimulation. (PTK-protein tyrosine kinase; TCR-T cell receptor; LCK-lymphocyte-specific protein tyrosine kinase; ZAP-70-ζ chain associated protein of 70kD; LAT-linker activator for T cells; PLCγ1- phospholipase C γ-1; PKC–θ– protein kinase C-θ; SLAM- signaling lymphocytic activation molecule; SAP-SLAM-associated protein; ITSM- immunoreceptor tyrosine-based switch motif)[107].

T cell activation stimulates PLCγ–1 to affect the downstream activation of the transcription factor families nuclear factor-κB (NF-κB) and nuclear factor of activated T cells (NFAT). In turn, PLCγ–1 stimulates the hydrolysis of phosphatidylinositol-4,5-bisphosphate (PIP_2) into diacylglycerol (DAG) and inositol triphosphate (IP_3)[98]. Previous work in human primary $CD4^+$ cells has suggested that CD28 signaling regulates PIP_2 conversion[106]. The product of PIP_2, DAG, indirectly activates NF-κB by activating protein kinase C-θ (PKC-θ)[92,108] (figure 1.4). *Sap*-deficient mice exhibit impaired PKC-θ expression and NF-κB activation following TCR stimulation[109] and this has been attributed to decreased DAG production[110,111]. This suggests that CD3/CD28 stimulation requires T cells to express SAP in order for DAG to be produced. In the presence of SAP, activated PKC-θ phosphorylates CARMA-1 (CARD11 or caspase recruitment domain-and membrane-associated guanylate kinase-like domain-containing protein 1)[112], recruiting the constitutively-associated BCL10 (B-cell lymphoma/leukemia 10) and MALT1[113] (mucosa-associated lymphoid tissue lymphoma translocation protein 1) proteins to form the CARMA1/BCL10/MALT1 (CBM) complex[113]. The CBM complex phosphorylates the IκBα subunit causing its dissociation and proteasomal degradation[114] thus

liberating the nuclear localization signal of the remaining NF-κB subunits (p65 and p50)[115], allowing nuclear translocation.

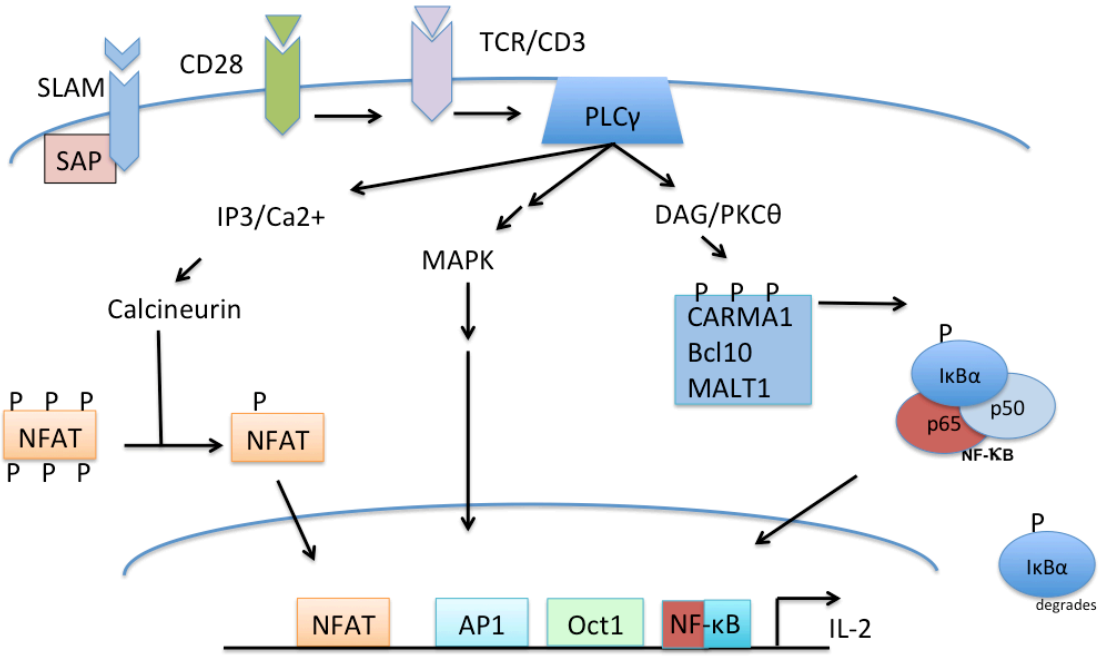

Figure 1.4 T cell activation leading to IL-2 transcription. T-cell receptor (TCR) signaling relies on primary and co-stimulation events that activate T cell responses through signaling cascades. Initial T cell activation, following TCR recognition of antigen, and co-stimulatory events, such as recognition by the SLAM-family of receptors, trigger a series of phosphorylation events that activate phospholipase C γ-1 (PLCγ-1). Once PLCγ-1 is activated, both the nuclear factor of activated T cells (NFAT) and nuclear factor kappa β (NF-κB) families of transcription factors are localized to the nucleus where they bind with the IL-2 promoter during T cell activation. In addition, TCR stimulation activates the MAPK (mitogen-activated protein kinase) pathway resulting in the formation of the AP-1 transcription factor, which also converges on the IL-2 promoter with the constitutively active Oct1.

For effective T cell activation, a sustained elevation of intracellular calcium is required, through a combination of receptor activation and ion channels, to activate the NFAT transcription factor family, as shown above. IP_3, generated by PIP_2 cleavage following CD28 co-stimulation[106], binds to the IP_3-receptor on the endoplasmic reticulum (ER), stimulating the release of calcium ions from intracellular stores[116]. The CRAC (Ca^{2+} Release-Activated- Ca^{2+}) channels at the cell

membrane are then opened to replenish calcium within the ER[117]. Within the cell, the free Ca^{2+} binds to four motifs within the calcium-modulated protein (calmodulin)[118], which interacts with the phosphatase calcineurin through a calmodulin binding domain[119]. Calcineurin dephosphorylates NFAT, allowing for its nuclear translocation[120], and modulates the formation of the CBM complex by dephosphorylating BCL10, which allows it to bind CARMA1[121]. Notably, there have been reports of excess intracellular calcium levels *in vitro* from TCR stimulated T cells from XLP1 patients[122]. Although this finding has not been thoroughly explored, calcium imbalances can be detrimental to T cells as it can lead to PLCγ–1 and PKC-θ degradation[123] or apoptosis[124].

TCR stimulation activates NFAT and NF-κB and these transcription factors converge on the IL-2 promoter (figure 1.3). IL-2 is of particular importance in T cell signaling, as it influences T cell proliferation. In addition to NFAT and NF-κB, TCR activation allows CD28 to bind growth factor receptor-bound protein 2 (GRB2)[125] which facilitates the stimulation of Ras and the serine/threonine mitogen-activated protein kinases (MAPK)[78] to activate c-Fos and c-Jun[126]. The transcription factor subunits c-Fos and c-Jun dimerize to form the AP1 transcription factor and bind to the IL-2 promoter[127] along with the constitutively active Oct1[128]. Studies have shown that T cells from XLP1 patients have decreased IL-2 production, suggesting impaired proliferation[122,129]. Taken together, the T cell signaling cascades involve the production of cytokines and the interaction of various proteins and these insights identified avenues to examine for specific *SAP*-dependent defects following TCR stimulation.

1.5 Models to study XLP1

Much of the understanding on how SAP influences the immune system is from previous work examining *Sap*-deficient mice and table 1.3 summarizes these findings in comparison to XLP1 patients. A striking similarity between the *Sap*-deficient mice and XLP1 patients is the lack of NKT development[130], a feature that has been previously attributed to the interaction of SAP and FYN during development[131]. Similarly, *Sap* defects are associated with impaired germinal center formation[132–135].

Germinal centers form in B cell follicles and is the location where long-term antibody memory is established[136]. B cell memory occurs following class switching of IgA, IgG, or IgE and hypermutation of the antigen binding variable chains[137]. $CD4^+$ T cells are required for the formation of germinal centers[138] and B cell function[139]. Specifically, follicular dendritic cells present antigen to follicular T helper cells (T_{FH})[140,141] which, in turn, signals the establishment of germinal centers and interactions with B cells[142]. It is this T:B interaction that stimulates class switching and B cells expansion and disruption is associated with hypergammaglobulinemia, impaired antibody production during the humoral response[142].

Exposure to various infections normally increases the production of specific antibodies but in the absence of Sap, mice have impaired antibody production. *Sap*-deficient mice have defects in T_{FH} cell production and secretion of IL-4, components required for B cell differentiation[143]. Similarly, following influenza infection, *Sap*-deficient mice have impaired expansion of B cells due to faulty $CD4^+$ T helper cell

activity[144,145] and restoration of Sap expression was able to rescue antibody production and germinal center formation[32].

Importantly, impairments to $CD4^+$ T cells from XLP1 patients have also been shown to affect T:B interactions, resulting in decreased antibody production[32] due to impaired GC formation[133–135] . Defective germinal center formation has been associated with immunodeficiency and the development of lymphoma, attributable to mutations or translocations involving the immunoglobulins and various oncogenes[146,147]. These mutations may confer proliferative advantages to infected cells or impair the release of antibodies in response to pathogens leading to persistent inflammation.

While some studies have shown that SAP is expressed in B cells [148–150] it is generally thought that SAP is restricted to T and NK lineages implying that GC formation and B cell induced antibody production depends on cues from SAP expressing T helper cells. $CD4^+$ T cells from *Sap*-deficient mice, *in vitro*, have decreased production of IL-4 which is required for Th2 development[32,151]. Together, these data suggest that SAP potentially regulates T:B cell interactions by the production of surface proteins or modulates the secretion of cytokines necessary for B cell development[32].

***Sap*-deficient mice**		**XLP1 patients**
	Cellular defects	
Impaired[130]	NKT cell	Not formed[130]
Impaired[132]	Germinal center formation	Impaired[133–135]
Impaired[32]	T_{FH}:B cell interactions	Impaired[32]
Impaired[32,143]	Th2 differentiation (IL-4)	Impaired[152]
Decreased[153,154]	Antibody (Ig) production	Decreased[155]
Increased[153,156]	$CD8^+$ T cells (after infection)	Increased[152]
Impaired[157,158]	CTL/NK activity	Impaired[159]
Decreased[160]	Apoptosis ($CD8^+$)	Decreased[159]
Increased (+MHV-68)[153,154]	Histiocytosis	HLH (+EBV)[161]
Increased (+LCMV)[152]	IFN-γ production	Variable

Table 1.4. Comparison of SAP defects in mice and humans. Studies in *Sap*-deficient mice have identified many similarities to defects observed in XLP1 patients. NKT-natural killer T cells; Th2-T helper 2 cells; CTL-cytotoxic T cells; NK-natural killer cell; T_{FH}-T follicular helper cells; and EBV-Epstein-Barr virus. *Mice cannot be infected by EBV and are infected by either lymphocytic choriomeningitis virus (LCMV) or murine gammaherpesvirus (MHV-68).

Both *Sap*-deficient mice and XLP1 patients have exhibited increased $CD8^+$ cells following viral infection and impaired cytotoxic killing abilities[6,84,91,133,152]. Infections increase the quantity of $CD8^+$ cells but studies have attributed defects in the killing of infected target cells to impaired interactions of SAP with the 2B4 receptor[157] and Ly-108 receptor[158]. The elevated quantities of $CD8^+$ cells exhibit increased resistance to apoptosis[160] suggesting that the accumulation of lymphocytes is SAP specific.

Previous studies infecting *Sap*-deficient mice with murine gammaherpesvirus-68 (MHV-68), used to mimic EBV infection, have shown that more $CD8^+$ T cells are produced compared to their Sap expressing controls[153]. The excessive quantities of CTLs generate a phenotype similar to HLH with evidence of tissue infiltration that is not observed in their control counterparts[154]. Studies have also shown that these expanded T cell populations produce excessive levels of

cytokines. *Sap*-deficient mice infected with lymphocyte choriomeningitis virus (LCMV) exhibit elevated levels of IFN-γ production by T cells[152]. Additionally, splenocytes from mice lacking Sap expression were shown to have increased IFN-γ production, independent of infection[152]. Correlations between *Sap*-deficient mice and XLP1 patients have enhanced the appreciation for the myriad of influences that SAP have on immune cell development and function. However, much remains to be understood as to how these defects contribute to the multiple phenotypes observed in XLP1 patients.

1.6 Summary and Dissertation Goals

XLP disease is a rare inherited immunodeficiency characterized by several phenotypes and an extreme sensitivity to infections, which results from mutations in either *SAP* or *XIAP*[34]. It is unclear why there is a range of phenotypes and how *SAP* and *XIAP* influence them. *SAP* defects result in the lack of NKT cell development[5,101] and disrupt T cell signaling[122,129], but there are many unanswered questions as to how these defects occur. The goal of this dissertation was to reveal insights into how *SAP*-deficiencies influence T cell signaling, using a cell-based model approach to affect targeting of the *SAP* gene.

To clarify the role of *SAP* in T cell signaling, we took a gene editing approach to disrupt the *SAP* gene and created a *SAP*-null cell line, as discussed in chapter 2. This *SAP*-deficient cell line was used to identify *SAP*-specific effects, which included cytokine production, transcription factor activity, and calcium mobilization, with results presented in chapter 3. Moreover, chapter 4 illustrated a *SAP*-dependent

heightened sensitivity to apoptosis. These results suggested that SAP defects drastically alter T cell activation and the cytokine environment, making T cells more sensitive to apoptotic stimuli, potentially impeding their ability to respond to immune challenges. Together, these results identified specific SAP-dependent defects in T cell signaling that could contribute to the characteristic phenotypes of patients with XLP1 disease.

Chapter 2 The Generation a *SAP*-deficient Cell Line

2.1 Introduction

Despite efforts over the past few years to understand how *SAP* defects impair immune cell responses, there are many unanswered questions. To further explore the role of *SAP* in T cell signaling, we chose to exploit an established SAP-expressing human cell line for analysis. The Jurkat cell line has been extensively used to characterize cytokine production and T cell signaling[107] and it was therefore selected as the model system to determine the impacts of *SAP*-deficiencies following stimulation of the T cell receptor (TCR). A common approach to this is to use RNAi technology to suppress gene expression, and these are powerful tools to assess the influences of a particular gene in a biological system. However, there are disadvantages to this approach as the effects are transient (siRNA) and stable suppression (shRNA) introduces the chance of an integration event. We chose to use transcription activator-like effector nucleases (TALENs) to edit the *SAP* gene and the construction and validation of this gene editing technology will be described within this chapter, culminating in the generation of a *SAP*-null model cell line.

The development of transcription activator like effectors (TALEs) comes from our understanding of the gram-negative members of the *Xanthomonas* genus[162]. These bacteria contain TAL effector (TALE) proteins that bind the host DNA and transcriptionally activate genes promoting bacterial survival. TALEs, the

DNA binding proteins, consist of repetitive sequences of 33-34 amino acids[163] and when fused with a nuclease (*FokI*) form a TALEN. TALENs function in pairs and each member of the pair contains one-half of the *FokI* nuclease. When bound to a target sequence, the activity of the *FokI* protein is reconstituted generating a specific break in the substrate DNA[164]. This process creates a DSB that is either repaired by homologous recombination (HR), if a template sequence is available, or non-homologous end joining (NHEJ)[165]. Herein, I describe the utilization of a TALEN gene editing approach to generate a *SAP*-deficient cell line to model the effects of SAP in T cells signaling.

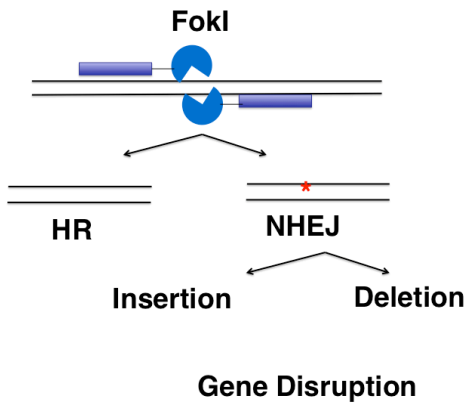

Figure 2.1 Concept of gene editing. A DNA binding protein binds to a specific nucleotide sequence and the corresponding nuclease activity generates a double strand break in the DNA sequence. This break is then repaired by either homologous recombination, if a suitable template is available, or through error-prone non-homologous end joining (NHEJ). NHEJ is the primary mechanism to generate insertions and deletions within the target sequence.

2.2 TALEN cloning

The TALEN-based approach presented here used a non-selection based plasmid that is transiently expressed by the cell after transfection and has a high degree of specificity for the target gene. Each TALEN recognizes 16 nucleotides and

the pair is separated by a 15-31 base pair spacer region[166]. The TALEN DNA binding domain is fused to the *FokI* wildtype nuclease, which is necessary for subsequent cleavage of the DNA. Considering the TALEN binding domains and spacer regions, it is estimated that a TALEN pair binds once in 6.2 billion base pairs[167], indicating high specificity. In the TALEN protocol described here, the TALEs were constructed using nested PCR followed by ligations into the final vector that contains the nuclease.

TALENs were constructed using nested PCR to assemble unique primers (TAL units), which specify binding to one particular target nucleotide[166,168]. As shown in figure 2.2, four TAL units combined to generate a module and four modules combined to form a TAL effector (TALE), capable of recognizing 16 nucleotides of a target sequence.

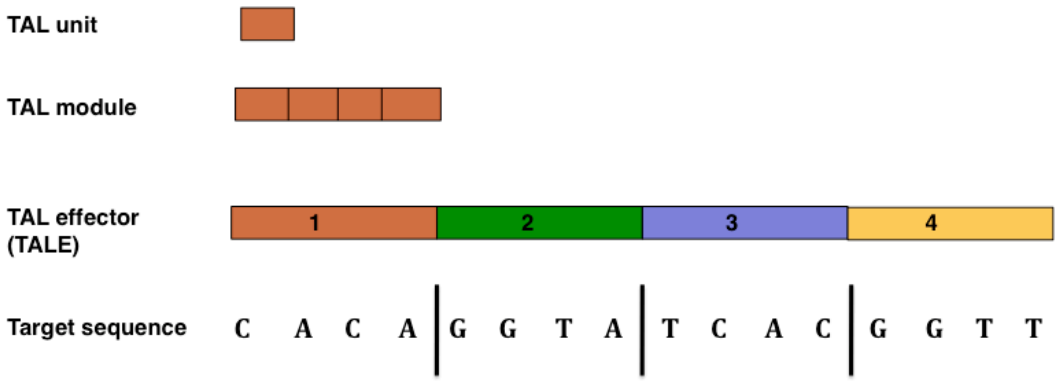

Figure 2.2 TAL Effector (TALE) composition. Each TALE consists of TAL units, a primer consisting of ~100 nucleotides, capable of recognizing one target nucleotide. Four TAL units were combined by PCR to generate a TAL module. The TALE was formed by the ligation of four TAL modules to generate a ~1600 nucleotide sequence that can recognize and bind 16 nucleotides of a target sequence. Finally, the TALE was incorporated into a nuclease containing plasmid to generate a TALEN.

2.2.1 Generation of the TAL modules

The initial step for designing a TALEN pair was to identify the specific nucleotide for editing within the gene of interest. A nucleotide that is often mutated in XLP1 patients, 163 C >T[169], was selected to target by gene editing. The Zinc Finger Consortium manages a web-based program, called ZiFiT, available at zifit.partners.org, to design gene editing systems[170,171] and is suitable for designing ZFNs, TALENs, or CRISPR/Cas9. Based on the specific nucleotide within a gene, the ZiFiT program recommended DNA binding domains for the TALENs to target within the flanking sequences and also generated a ZiFiT sequence, approximately 1600 nucleotides, which are the basis of the primers that construct the TAL units. Current versions of the ZiFiT program also specify which nuclease containing backbone (e.g. JDS vector for TALENs) to utilize for final assembly.

As mentioned, the TAL units are primers that confer binding specificity to one target nucleotide. The ZiFiT program identified TAL units that correspond to the target sequence, depicted in figure 2.3. For example, TAL unit 7 recognizes a cytosine and TAL unit 11 recognizes an adenine. These individual primers were joined in a nested PCR reaction to generate modules 1, 2, 3, and 4. An initial 3-part ligation joined modules 1 & 2 and 3 & 4. A subsequent 3-part ligation into the TALEN backbone joined all four modules to complete one side of the TALEN pair. The process was repeated for both the TALEN left and TALEN right and assembly of the modules will be outlined with more detail below.

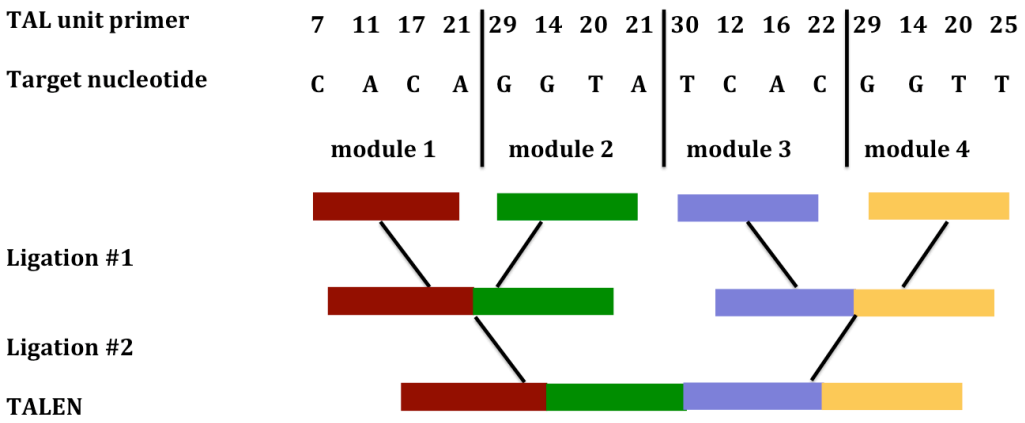

Figure 2.3 TAL module generation. The ZiFiT assembly program determines the order of specific TAL units to assemble into four modules. These modules are initially constructed by nested PCR reactions followed by several ligations to generate one side of the TALEN pair, capable of recognizing 16 target nucleotides. This process was repeated for both sides of the TALEN pair.

Each of the four TALE modules was generated by nested PCR reactions, illustrated in figure 2.4. The specified TAL units were combined with additional scaffolding primers that provided the ends for the modules during the PCR reaction. These scaffold primers differ for each module and contained specific 5'-restriction enzyme sites to allow subsequent restriction digests and ligation. The third primer type provided connectivity among the growing strands.

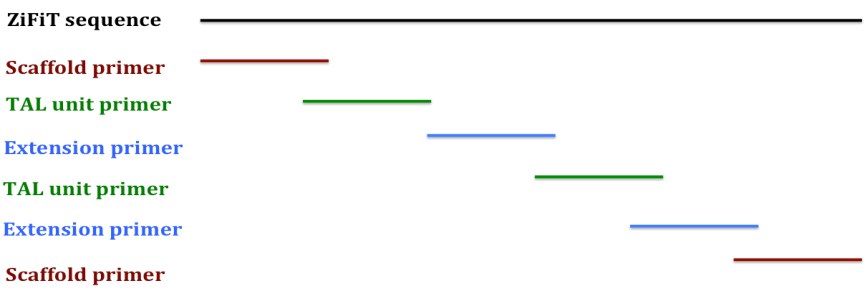

Figure 2.4 TAL unit scaffold. The nested PCR reactions generate TALE modules 1-4 using the ZiFiT sequence as a guide. The scaffold primers provides the framework for the beginning and end of the module while the connectivity primers join the TAL unit primers to provide continuity for the growing fragments.

2.2.2 Construction of the TALEN pair

Once the modules 1-4 were prepared and purified, the first 3-part ligation joined modules 1 & 2 and modules 3 & 4 into an intermediate vector (T-V0). To prepare for the ligation enzymes were specifically selected based on the nested PCR reaction primers. Figure 2.5 illustrates the digest of the module PCR fragments and initial ligation.

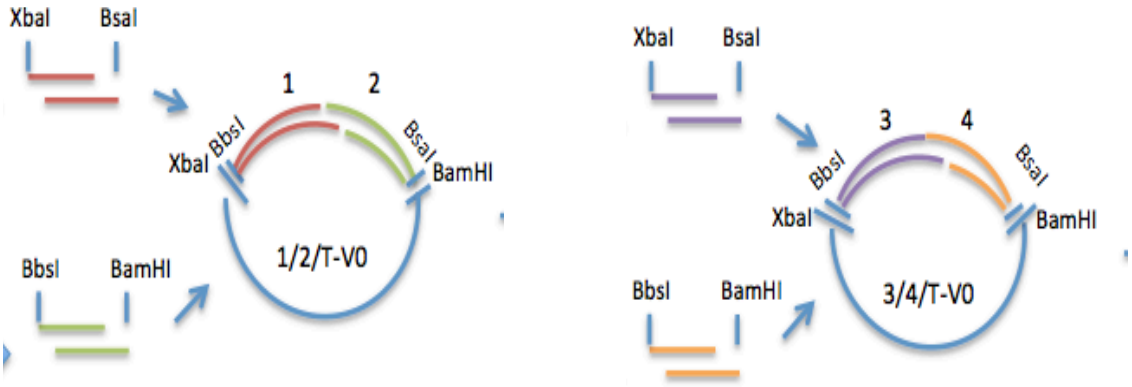

Figure 2.5 Digest & ligation of TALE modules. Modules 1&3 were digested with *XbaI* and *BsaI* while modules 2&4 were digested with *BbsI* and *BamHI*. The digested modules were then ligated into the intermediate TALEN vector (T-V0).

The initial 3-part ligation into T-V0 contained an 800 base pair insert that required sequencing. The ligation reactions were transformed and plated in preparation for in-well DNA preparations and PCR reactions prior to sequencing. Approximately 10-20% of colonies were expected to contain the correct size of 1kb band. Selected colonies were then prepared for sequencing. Homology for module 1/2 alignment began at 5'-GAAC and stopped at 5'-TTGA while homology for module 3/4 began at 5'-CTGA and stopped at 5'-C/TTGA. The purified 800 base pair modules were prepared for the final ligation by digest with *BbsI* and *BsaI*.

Figure 2.6, demonstrates the directional cloning strategy of the final 3-part ligation into vector (JDS70), thereby fusing the TALE DNA binding domain to the *FokI* nuclease. The JDS vector was cleaved by the exonuclease *BsmBI* at two sites creating a 6kb linear fragment with staggered overhangs that were complementary to the beginning nucleotides of modules 1/2 and the end of modules 3/4.

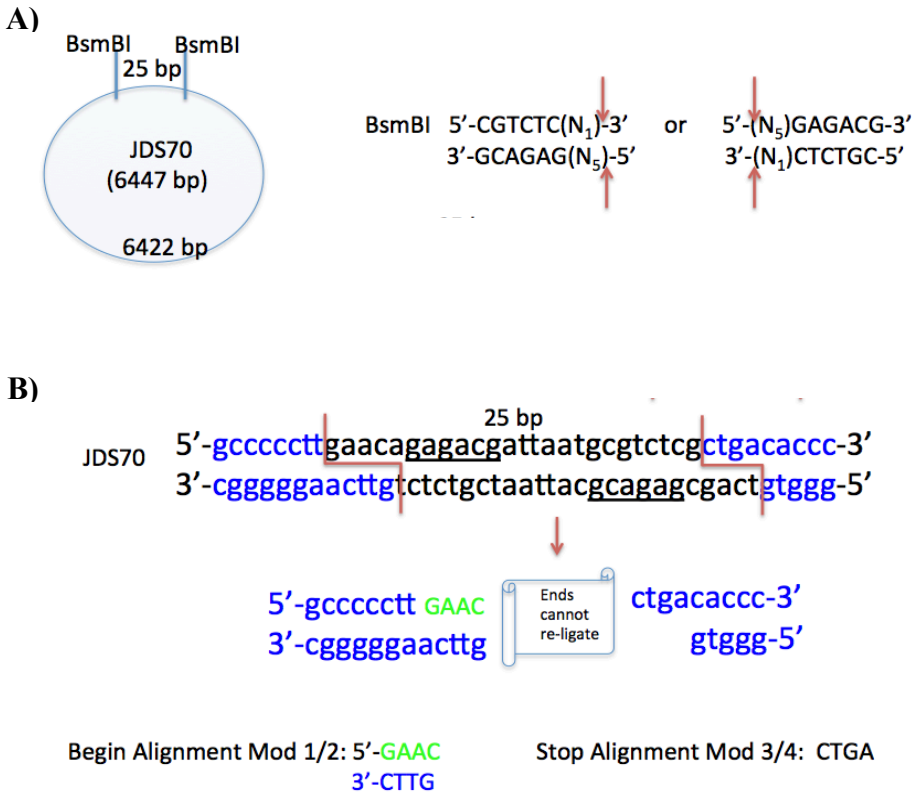

Figure 2.6 The final 3-part ligation. A) The final three-part ligation of modules into the TALEN vector was facilitated by digest with *BsmBI*. The JDS vector backbone contains two BsmBI sites, where the enzyme cleaved at the indicated nucleotides. **B)** *BsmBI* recognized the underlined nucleotides with cleavage at sites indicated by the red lines. This generated ends that were complementary to the alignments of modules 1&2 and modules 3&4 minimizing self- or inadvertent ligation of a single module.

After ligation, the 1600 base pair fragment was transformed into *E.coli* and plasmid construction was evaluated by a diagnostic restriction digest. As shown in figure 2.7,

the desired fragment size was 2400 base pairs (module 1/2 + module 3/4 + 500 base pairs to *ClaI* + 300 base pairs to *BamHI*), as depicted below. The plasmid preparations were sequenced and, at this point, the TALENs were ready for gene editing.

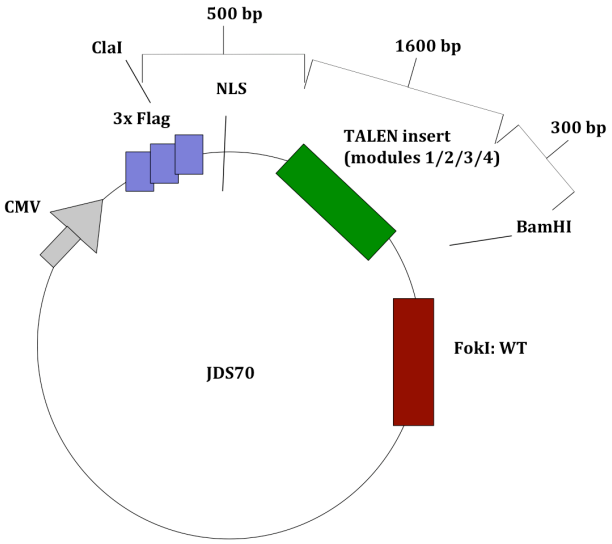

Figure 2.7 Restriction digest for final TALEN assembly. The final assembly of each side of the TALEN pair undergoes a confirmation restriction digest using *ClaI* and *BamHI.* The desired 2400 base pair fragment contained the JDS backbone and the correctly inserted module 1/2/3/4 ligation, which was then sequenced using T7 and NK49 primers for comparison to the ZiFiT homology.

2.3 Results

The *SAP* targeting TALEN pair was prepared but required demonstration of its effectiveness at inducing a DSB at the target nucleotide. To address the efficacy of the gene editing plasmids, the TALEN pair was transfected into Jurkat cells followed by the efficiency screen outlined in figure 2.8. One of the difficulties of this gene editing approach was distinguishing cells that had been edited from the

unaltered population. Distinguishing the altered population was often achieved through DNA isolation followed by PCR and sequencing.

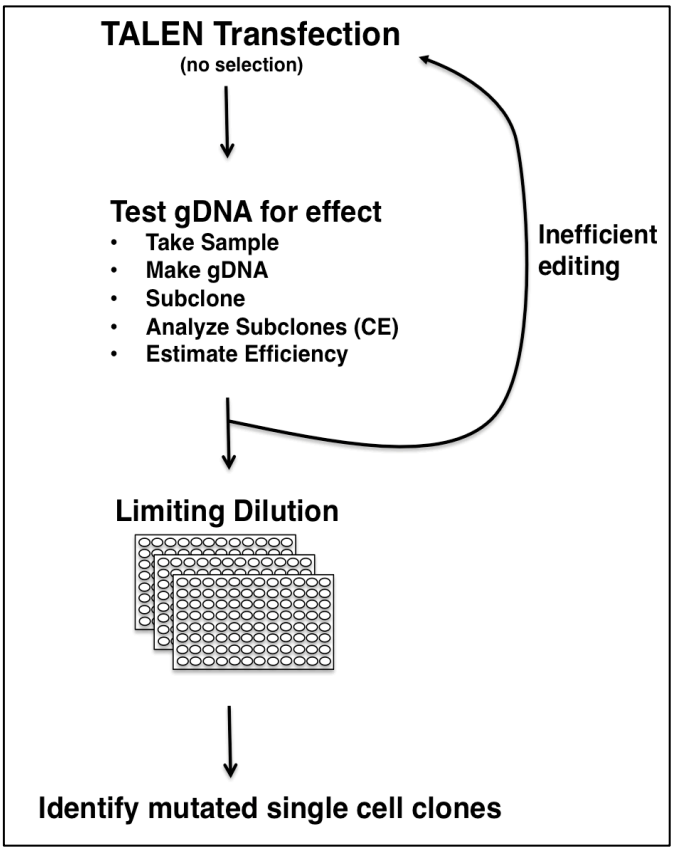

Figure 2.8 Determining TALEN efficiency and clonal isolation. To maximize workflow, the preparation of single cell clones from the TALEN transfected population was initiated while concurrently assessing the TALEN editing efficiency. Particularly for cells that require longer to recover from single cell isolation, this approach identified whether or not the TALENs were effective at editing the target cells. TALEN efficiency was determined by extracting genomic DNA from the transfected population and subcloning PCR fragments specific to the region of interest into a plasmid. These fragments were analyzed to identify mutations introduced within the targeted population. If the TALENs were inefficient, the transfection process was repeated. However, if insertions or deletions were identified, the single cell clones were screened for mutations.

To determine the efficacy of TALEN induced gene edits, genomic DNA from the transfected population was amplified by PCR using SAP specific primers (SAPEX2F/MEL2R) that surround the TALEN-binding domain targeting nucleotide

163 in *SAP* (R55 in SAP protein). These 286 base pair PCR fragments were then subcloned into a plasmid and analyzed by DNA gel electrophoresis for mobility changes. To confirm that the desired DNA region had been edited, sequencing was performed. However, the sensitivity of this approach was limited by resolution, which is based on fragment migration during gel electrophoresis.

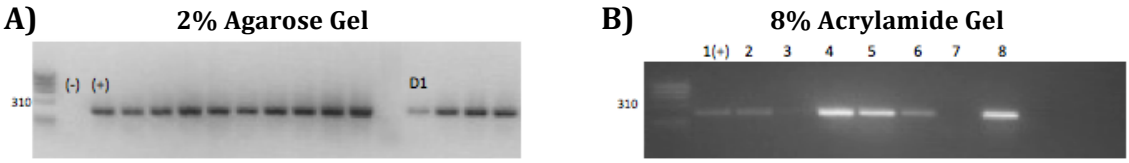

Figure 2.9 Challenges to screening using standard DNA electrophoresis. A) PCR fragments amplified for SH2DIA (SAP) exon 2 (286 base pair fragment) were analyzed on a 2% agarose gel. Visualization of band migration was difficult when insertions or deletions involved few nucleotides, resulting in unnecessary sequencing reactions. **B)** Visualization of PCR fragments on 8% acrylamide gels was also inefficient for resolving small changes in nucleotide content.

Standard agarose gel electrophoresis, figure 2.9, proved inefficient for identifying small gene edits, but was useful for the identification of select larger edits, as shown in figure 2.10. However, poor resolution by DNA electrophoresis continued to be a problem when screening, leading to the incorporation of capillary electrophoresis (CE) fragment size analysis.

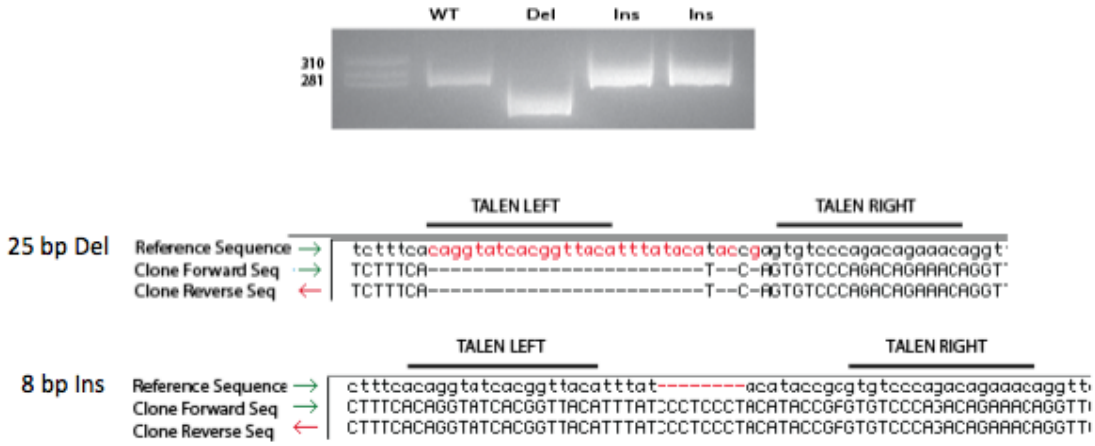

Figure 2.10 DNA electrophoresis is useful for resolving large gene edits. An 8% acrylamide gel resolved a 25 base pair deletion compared to WT. This deletion was sequenced using M13F/R primers and compared to the WT reference sequence. Smaller insertions were more difficult to identify by gel mobility. The 8 base pair insertion, confirmed by sequencing, was missed during gel electrophoresis.

Capillary electrophoresis (CE), used during forensic Short Tandem Repeat (STR) profiling[172,173], can quantify the size of a PCR fragment and identify nucleotide insertions or deletions by comparison to wild type controls, thereby eliminating the likelihood of overlooking gene alterations based solely on gel migration and, at the same time, minimize sequencing reactions. The PCR sample was loaded into a narrow capillary tube where it crosses electric fields, separating the sample by size, where a detector correlated the fragment size to an internal size standard[174]. The CE screening identified two mutations within the pooled population after TALEN transfection. Figure 2.11A illustrates the fragment sizes identified and demonstrated that the population contains the wild type (286 base pairs), and an insertion and deletion of 292 and 282 base pairs, respectively. DNA from the corresponding *E. coli* colonies with the aberrant fragment sizes were then

sequenced and indicated the generation of a stop codon at amino acid 69 and amino acid 52, for the insertion and deletion, respectively.

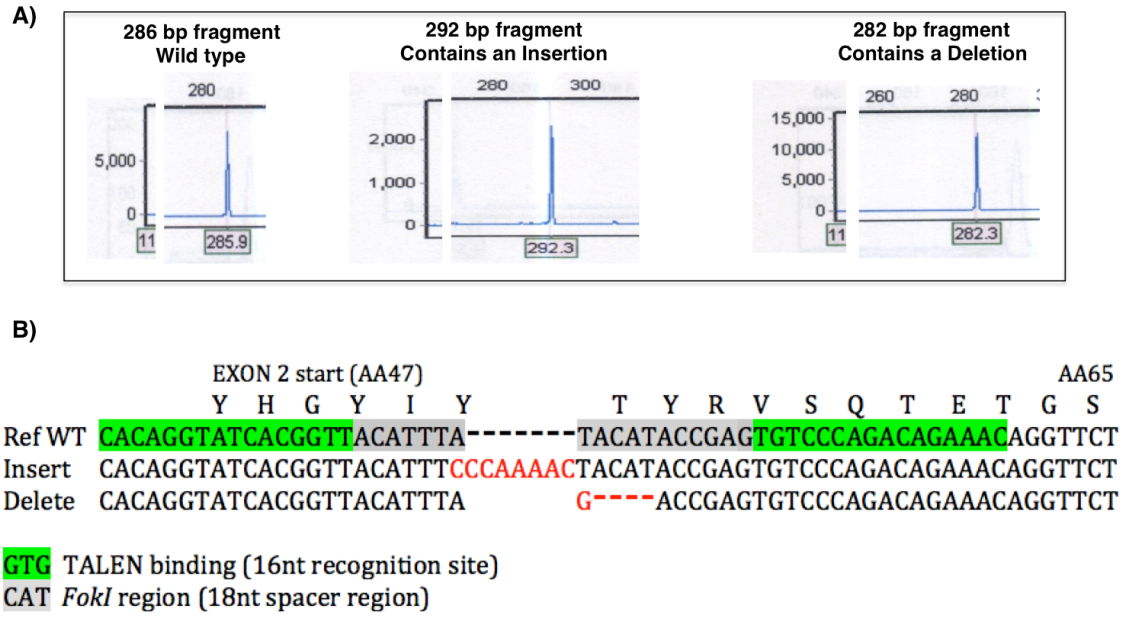

Figure 2.11 Identification of gene edits by Capillary Electrophoresis (CE). Genomic DNA was extracted from colonies cultured in a 96 well plate and PCR reactions using a 5'-6-FAM primer were analyzed by CE. **A)** The majority of colonies contained a 286 base pair (bp) fragment (WT), but variations also depicted a 292 bp and 282 bp fragment, indicative of a 6 bp insertion and 4 bp deletion, respectively. **B)** CE results were confirmed by sequencing, as shown. The reference sequence includes the TALEN binding site highlighted in green with the insertion and deletion generating stop codon through either frameshift or nonsense mutations at the point of editing, respectively.

Two mutations in the population of transfected Jurkat cells were identified during TALEN efficacy screening. CE analysis, illustrated in figure 2.12A, was subsequently performed on the clonally expanded Jurkat derivatives, identifying a population of cells with three different size fragments of 282, 286, and 292 base pairs. These fragments corresponded to wild type, the insertion, and the deletion

depicted in figure 2.11. Sequencing of the *SAP* exon 2 fragment in the TALEN binding region confirmed the previously identified edits.

A)

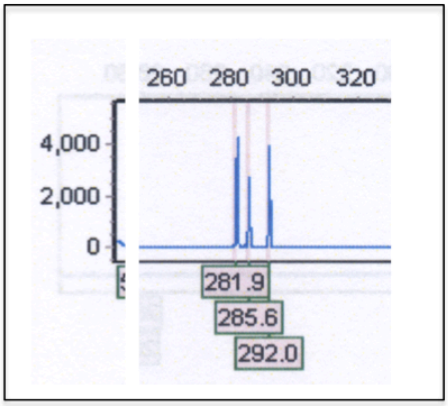

Figure 2.12 Capillary electrophoresis (CE) identifies mutant Jurkat clones. A) PCR fragments with 5'-6-FAM primer were analyzed by CE. One clone generated three different fragments with sizes of 282, 286, and 292 base pairs. The PCR fragments were sequenced. **B)** The deletion fragment sequence shows a T to G transition introducing a stop codon at amino acid 52. **C)** The insertion creates a frame shift introducing 17 amino acid variations before reaching a stop codon at amino acid 69.

B)

EXON 2 start (AA47)																AA65
Reference		Y	H	G	Y	I	Y	T	Y	R	V	S	Q	T	E	T	G	S
Wild-type	TATCACGGTTACATTTATACATACCGAGTGTCCCAGACAGAAACAGGTTCT															
Deletion	TATCACGGTTACATTTAG----ACCGAGTGTCCCAGACAGAAACAGGTTCT															

C)

EXON 2 start (AA47)															AA63
Reference		Y	H	G	Y	I	Y		T	Y	R	V	S	Q	T	E	T
Wild-type	TATCACGGTTACATTTA------TACATACCGAGTGTCCCAGACAGAAACA															
Insertion	TATCACGGTTACATTTCCCAAAACTACATACCGAGTGTCCCAGACAGAAAC															

A potential explanation for three peaks was that the limiting dilution generated a mixed, rather than a clonal, population. Thus, additional single cell isolation was performed on this population. Two fragments, 282 and 292 base pairs, were identified during the subsequent limiting dilution, figure 2.13C. As shown by Western blot, these cells no longer have evidence of SAP expression, lane C of figure 2.13D, while the populations from panels A and B, which contained the wild type peak during CE screening, also exhibited SAP expression. Two additional attempts of clonal expansion were attempted, but the deletion alone or the insertion alone could not be isolated. Notably, the unaltered (wild type) Jurkats used in

subsequent experiments have gone through the same selective influences of the TALEN transfection and clonal isolation.

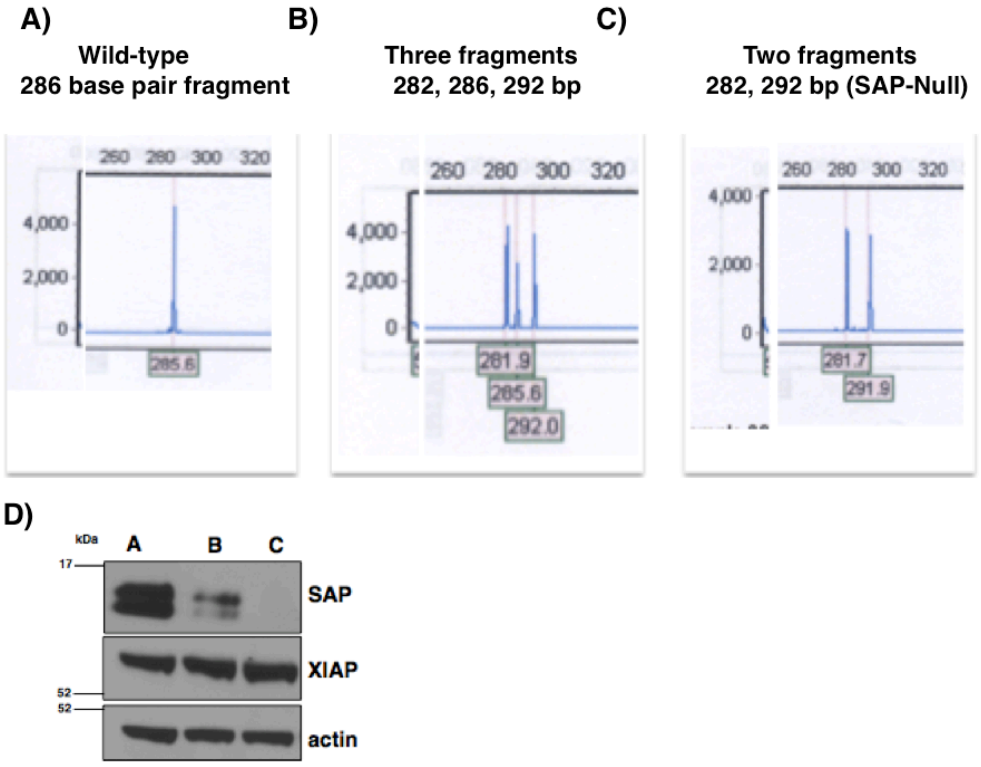

Figure 2.13 Generation of a *SAP*-null Jurkat. Clonal expansions of Jurkat cells transfected with the SAP-targeting TALEN pair were screened by capillary electrophoresis (CE). **A)** The unaltered 286 base pair fragment is shown. **B)** Analysis of a clonally expanded population demonstrated three fragments with sizes of 282, 286, and 292 base pairs. This population was further isolated by limiting dilutions and screened by CE. **C)** The CE screen of the newly isolated clone resulted in two fragments of 282 and 292 base pairs. **D)** Western blotting demonstrates SAP expression in the clones, corresponding to the CE fragments shown in A-C. The 282 and 292 size fragments shown in C show no evidence of SAP expression and are therefore classified as *SAP*-null Jurkat cells.

To further identify the clonal *SAP*-null population, the regions surrounding the TALEN binding site were sequenced using an internal *SAP* exon 2 sequencing primer (MES1) that is upstream of the TALEN left-binding site. The TALEN-binding site is indicated in blue on the chromatogram, shown in figure 2.14. The *FokI* cleavage generated a double-strand break within the spacer region, at nucleotide

155, indicated by the arrow. The *SAP*-null sequence corresponds to the colonies previously isolated and sequenced containing an insertion and deletion, both leading to stop codons within the *SAP* gene.

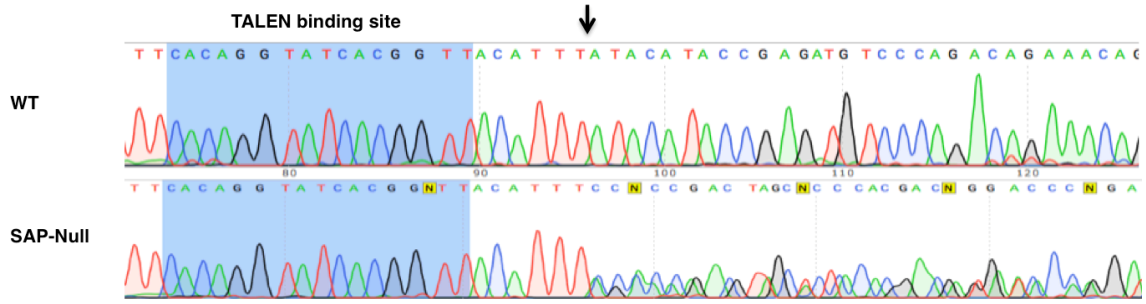

Figure 2.14 Sequencing results of the final iterations of clonal expansion. Genomic DNA from the wild type and *SAP*-null Jurkats was PCR amplified for the SAP exon 2 region targeted by the TALEN pair. The WT control and the *SAP*-null cells were sequenced using the MES1F primer. Chromatographs show that the *SAP*-null cells have overlapping chromatograms at the point of the double strand break, indicated by the arrow, downstream of the TALEN left binding site, highlighted in blue.

Gene editing facilitated the mutation of *SAP* to generate a *SAP*-null cell line. However, it was of concern whether the TALENs were still being expressed in the cell, where they could continually induce mutations. To address this question, and confirm that the TALENs were no longer present within the Jurkat cells, the wild type and *SAP*-null cells were examined for FLAG expression by Western blot. The TALEN plasmid backbone (JDS70) contains a FLAG-tag sequence, which would be detectable if the cells were still expressing the TALENs. For this experiment, the wild type and *SAP*-null Jurkats were transfected with an unrelated plasmid, while separate positive control transfections of *SAP*-null Jurkats with a FLAG-SAP-expressing plasmid and the wild type cells with a TALEN plasmid were prepared. As

shown in figure 2.15, there was no evidence of a FLAG-expressing protein in the wild type or *SAP*-null populations (lane 1 and lane 2, respectively), while the positive controls of the FLAG-SAP and new TALEN transfection demonstrated expression of FLAG–fusion proteins. This suggested that the *SAP*-deficient cell line had no residual evidence of TALEN expression. TALEN expression in the *SAP*-null Jurkats was transient and that there was no evidence of integration within the genome of the targeted cells.

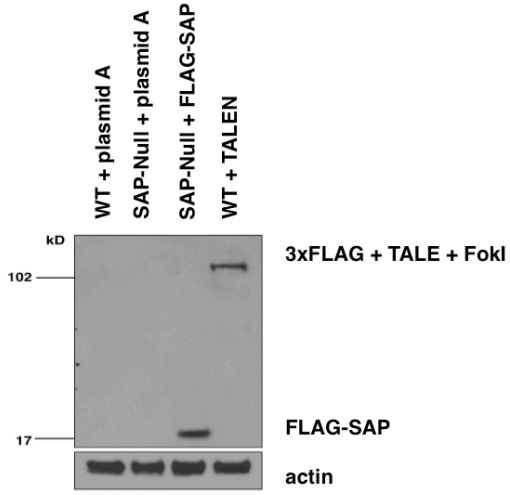

Figure 2.15 Transient expression of the TALEN pair. *SAP*-null Jurkat cells were transfected with an unrelated plasmid or a FLAG-SAP plasmid. Wild type Jurkat cells were transfected with an unrelated plasmid or one side of a FLAG-TALEN pair as a positive control. The TALEN generated *SAP*-null Jurkat line (lane 2) does not expresses FLAG protein while the control lanes, the transient SAP plasmid (lane 3) and the TALEN transfected into the WT Jurkat (lane 4) express the FLAG protein.

Considering that multiple iterations of clonal isolation did not separate the cell populations containing insertions and deletions within the *SAP* locus, it was concerning that this could be due to multiple X chromosomes. To determine if there was more than one copy of the X chromosome within the *SAP*-null Jurkats, short tandem repeat (STR) analysis[172,173] was performed. STR analysis is frequently used

to authenticate the identity of transformed cell lines in culture, as well as identify cross-contamination from unrelated cell lines. Performing STR analysis served two functions, it determined the number of X chromosomes within the population of cells, and confirmed the identity of the *SAP*-null cells compared to their parental Jurkat lineage. Guidelines[175] establish that in order to confirm cell line identity, >80% of loci must match and ranges below this threshold require further analysis, as they suggest cell line contamination. The percent match of alleles is determined by multiplying the number of shared alleles by two and dividing this product by the sum of the total alleles tested and the number of reference alleles compared [% match = (shared alleles x 2)/(total alleles tested + total reference alleles)]. Nine reference STRs obtained from the American Type Culture Collection (ATCC) STR database[176] were used to compare the WT and *SAP*-null Jurkat results. Compared to the original Jurkat cell line (Jurkat E6.1), the wild-type control Jurkats are a 93.8% match to the reference file, while the *SAP*-null Jurkats are an 89.7% match. Importantly, only one X chromosome was identified during this analysis. Having validated the identity of the SAP-null Jurkats, the final concern was the potential of TALENs to edit at unintended loci.

Despite the specificity inherent in the TALEN design process, the possibility remained that the TALENs may have bound at other regions within the genome. Aside from sequencing the entire genome to assess whether the TALENs disrupted at other loci, one method available to identify other regions where the TALENs may bind is by querying the NCBI BLAST nucleotide sequence program for the human genome[177]. The 50 nucleotides containing the TALEN binding domains and the

spacer region were entered into the NCBI BLASTn program and results demonstrated that *SAP* was the only gene to contain these sequences. While there are some fragments where one of the TALEN pairs could bind, there is no indication that the corresponding TALEN partner could bind within the proximity. Based on these results, it is unlikely that this particular *SAP* targeting TALEN pair will effectively bind and induce a genetic edit elsewhere within the human genome.

2.4 Discussion

To our knowledge, this is the first study in which gene editing technology was employed to generate an isogeneic cell line to directly compare the effects of SAP on T cell signaling. TALENs are one approach that has revolutionized the field of gene editing by introducing the ability to correct mutations or introduce specific point mutations in cells or animal models with relative speed. Other comparable gene editing approaches are available, such as CRISPR/Cas9 (clustered regularly interspaced short palindromic repeats), which are easier to generate and are guided to a specific sequence by 20 nucleotides[178], whereas TALENs are more difficult to produce but they have higher specificity by recognizing 32 target nucleotides[170]. CRISPRs are between 40-80% effective for targeting a specific region while TALENs range from 20-50%[179]. However, recent studies have shown that the CRISPR/Cas9, compared to TALENs, have higher off-target effects[180]. Given that the SAP TALEN pair was effective at targeting the SAP locus, it is possible that theses reagents could be used to repair hematopoietic stem cells from XLP1 patients with mutations within the targeted locus. This is an exciting option and proof-of-principle experiments have been done to correct a patient mutation for the type VII collagen

(*COL7AI*) gene in patient-derived primary fibroblasts[181], and mutations in the β-globin gene (*HBB*), which causes β-thalassemia, in induced pluripotent stem cells (iPSCs)[182].

Design, construction, and testing of a custom TALEN pair targeting *SAP* in Jurkat cells led to the generation of a *SAP*-null cell line in which the effects of SAP-defects in a $CD4^+$ cell lineage could be tested. Gene editing attempted to target a nucleotide, cytosine 163 with SAP[169], and generate a mutation observed in several XLP1 patients[183–185] using a single strand donor oligonucleotide. Studies have shown that ~50 homologous nucleotides flanking the site of correction are sufficient for use during gene editing to induce homologous recombination[186] and this was used as a guideline to design the SAP specific oligonucleotide. It was possible that the TALEN pair did not efficiently create a DSB to activate the HR machinery to incorporate the template or that the sequence homology was insufficient for recognition. Also, it is plausible that the correction was made but the population was unable to be recovered during clonal isolation. Screening for the correction was particularly challenging, as there was no difference in the size of the gene and the edits could not be resolved by CE screening.

Although the specific patient mutation was not generated, the *SAP* gene was effectively disrupted by NHEJ after the TALEN induced a DSB, which allowed the clonal isolation of a *SAP*-null cell line. While the TALEN plasmid utilized contained no selection markers, current generation plasmids contain fluorescent proteins which would facilitate separation and enrichment of transfected cells by fluorescence-activated cell sorting (FACS)[187]. This enriched population could then

be clonally isolated and analyzed by sequencing reactions to identify corrected cells. Gene editing also introduces the potential for random incorporation within the genome. While there was no evidence of the expression of a FLAG fusion protein in the *SAP*-null cells, a Southern blot would be required to formally exclude the presence of an integration event.

The TALEN was constructed using nested PCR followed by multiple restriction digests and ligations. Diagnostic restriction digests and sequencing of the assembled TALEN plasmids confirmed their nucleotide content prior to their use. The efficiency of TALEN editing was systematically analyzed using capillary electrophoresis to identify insertions and deletions with high resolution, and confirmed by sequence analysis. Analysis of single cell clones confirmed the acquisition of mutations within the *SAP*-null Jurkat cell line, which possessed both an insertion and deletion, thereby eliminating SAP expression. These cells provided an experimental system to analyze T cell signaling defects attributable to SAP. The validated *SAP*-null cells were functionally examined, as described in chapters 3 and 4, to characterize SAP-dependent defects in a T cell lineage and add insights into the biology of XLP1.

2.5 Materials & Methods

TAL primers. The following primers were used to construct the TAL unit modules during nested PCR reactions. The primers are listed in 5'-3' orientation.

(11) AGCAAGTCGTGGCCATTGCAAGCAACATCGGTGGCAAACAGGCTCTTGAGACGGTTCAGA
(12) AGCAAGTCGTGGCCATTGCATCCCACGACGGTGGCAAACAGGCTCTTGAGACGGTTCAGA
(14) AGCAAGTCGTGGCCATTGCAAATAATAACGGTGGCAAACAGGCTCTTGAGACGGTTCAGA
(15) AGCAAGTCGTGGCCATTGCAAGCAATGGGGGTGGCAAACAGGCTCTTGAGACGGTTCAGA
(16) ATCAAGTTGTAGCGATTGCGTCGAACATTGGAGGGAAACAAGCATTGGAGACTGTCCAAC
(17) ATCAAGTTGTAGCGATTGCGTCGCATGACGGAGGGAAACAAGCATTGGAGACTGTCCAAC
(19) ATCAAGTTGTAGCGATTGCGAATAACAATGGAGGGAAACAAGCATTGGAGACTGTCCAAC

(20) ATCAAGTTGTAGCGATTGCGTCCAACGGTGGAGGGAAACAAGCATTGGAGACTGTCCAAC
(21) CACAAGTGGTCGCCATCGCCTCCAATATTGGCGGTAAGCAGGCGCTGGAAACAGTACAGC
(22) CACAAGTGGTCGCCATCGCCAGCCATGATGGCGGTAAGCAGGCGCTGGAAACAGTACAGC
(24) CACAAGTGGTCGCCATCGCCAACAACAACGGCGGTAAGCAGGCGCTGGAAACAGTACAGC
(25) CACAAGTGGTCGCCATCGCCTCGAATGGCGGCGGTAAGCAGGCGCTGGAAACAGTACAGC
(26) ACCAGGTAGTCGCAATCGCGTCGAACATTGGGGGAAAGCAAGCCCTGGAAACCGTGCAAA
(27) ACCAGGTAGTCGCAATCGCGTCACATGACGGGGGAAAGCAAGCCCTGGAAACCGTGCAAA
(29) ACCAGGTAGTCGCAATCGCGAACAATAATGGGGGAAAGCAAGCCCTGGAAACCGTGCAAA
(30) ACCAGGTAGTCGCAATCGCGTCAAACGGAGGGGGAAAGCAAGCCCTGGAAACCGTGCAAA
(Extension 2)
TGCAATGGCCACGACTTGCTCCGGTGTAAGGCCGTGGTCTTGACAAAGGACCGGCAACAACCTTTGCACGGT
TTCCAGGGCT
(Extension 3)
CGCAATCGCTACAACTTGATCGGGAGTCAGCCCGTGGGCTTGACAGAGAACTGGGAGAAGTCTCTGAACCGT
CTCAAGAGCC
(Extension 4)
GGCGATGGCGACCACTTGTGCAGGCGTCAAACCGTGGGCTTGACACAACACGGGAAGGAGCCGTTGGACAGT
CTCCAATGCT
(Extension 5) TCCATGATCCTGGCACAGTACAGGCAGCAGGCGCTGTACTGTTTCCAGCGCC
(Scaffold 345)
GTACCTCGCGAATGCATCTAGAGAAGACAAGAACCTGACCCCAGACCAGGTAGTCGCAATCGCG
(Scaffold 346)
GTACCTCGCGAATGCATCTAGAGAAGACAACTGACCCCAGACCAGGTAGTCGCAATCGCG
(Scaffold 347)
ATGCAGGCCTCTGCAGTCGACGGGCCCGGGATCCGGTCTCTTCAGTCCATGATCCTGGCACAGTA
(Scaffold 384)
GTACCTCGCGAATGCATCTAGAGAAGACAATTGACCCCAGACCAGGTAGTCGCAATCGCG
(Scaffold 385)
ATGCAGGCCTCTGCAGTCGACGGGCCCGGGATCCGGTCTCTTCAATCCATGATCCTGGCACAGTA

PCR amplification and sequencing primers. The following primers were used for PCR amplification or sequencing reactions, as indicated. Sequencing reactions were performed by the University of Michigan DNA Sequencing Core.

SAPEX2F	5'-GGA AAC TGT GGT TGG GCA GAT ACA ATA TGG-3'	(PCR)
SAPEX2R	5'-GGC TAA ACA GGA CTG GGA CCA AAA TTC TC-3'	(PCR)
MEL2R	5'-ACC CCC AGA AGC AAA AAT AAA-3'	(sequencing & PCR)
BGHRev	5'-TAG AAG GCA CAG TCG AGG-3'	(sequencing)
NK49	5'-GGC CTG GAC AAT TGG GCT-3'	(sequencing)
MES1F	5'-CAC CAT ATA CGT GTG TCC-3'	(sequencing)

Nested PCR reactions for module construction. Four separate PCR reactions, one for each module were prepared as shown in table 2.2. PCR reaction conditions were: initial denaturation at 98°C for 3 minutes; followed by 35 cycles of 98° for 1 minute, 63° for 30 seconds, and 72° for 1 minute; and ending with 72° for 3 minutes.

The entire 400 base pair product from each module PCR reaction was visualized on a 1% agarose gel. These fragments were excised and purified using the QIAquick Gel Extraction Kit according to manufacturer's instructions and eluted in 50uL of water.

Component	Module 1	Module 2	Module 3	Module 4
5X Phusion Buffer	40uL	40uL	40uL	40uL
Phusion Polymerase	2uL	2uL	2uL	2uL
dNTP Mix (10 μM)	6uL	6uL	6uL	6uL
Extension 2-5 (0.5μM)	2uL	2uL	2uL	2uL
TAL Unit #X (0.5 μM)	2uL	2uL	2uL	2uL
TAL Unit #X (0.5 μM)	2uL	2uL	2uL	2uL
TAL Unit #X (0.5 μM)	2uL	2uL	2uL	2uL
TAL Unit #X (0.5 μM)	2uL	2uL	2uL	2uL
Scaffold (10 μM)	#345-4uL	#346-4uL	#384-4uL	#346-4uL
Scaffold (10 μM)	#347-4uL	#385-4uL	#347-4uL	#347-4uL
Ultra pure H2O	134uL	134uL	134uL	134uL
Total volume	**200uL**			

Table 2.1 Nested PCR reaction components.

Subcloning of modules 1 & 2 and module 3 & 4. PCR products of modules 1 and 3 were prepared with XbaI and BsaI, while modules 2 and 4 were digested with BbsI and BamHI and T-V0 was digested with XbaI and BamHI. Digests were incubated for 2 hours at 37°. The entire digest for each module was visualized on a 1% agarose gel ran at 100V for 45 minutes. The 400 base pair module fragments for each module and the 2.7kb fragment for T-V0 were excised and purified using the QIAquick Gel Extraction Kit according to manufacturer's instructions. Modules were eluted in 30uL and T-V0 eluted in 50 μL of water. Ligation reactions were prepared using 150ng of each module and vector DNA.

Component	Module 1	Module 2	Module 3	Module 4	T-V0
Module/Vector DNA	50uL	50uL	50uL	50uL	2.5uL
10X Digest Buffer	#4-10uL	#2-10uL	#4-10uL	#2-10uL	#4-10uL
10X BSA	10uL	10uL	10uL	10uL	10uL
Enzyme #1 (2uL)	XbaI	BbsI	XbaI	BbsI	BbsI
Enzyme #2 (2uL)	BsaI	BamHI	BsaI	BamHI	BamHI
Ultra pure H2O	26uL	26uL	26uL	26uL	23.5uL
Total volume	**100uL**				**50uL**

Table 2.2 Digest in preparation for ligation of modules 1 & 2 and modules 3 & 4.

Ligation reactions were transformed into XL-1 Blue cells and plated on agar plates. These colonies were further screened using in well DNA preparations and PCR reactions. Initially, colonies were selected and cultured on 96-well plates containing 150 µL of LB broth + carb (1:1000) with incubation at 37° overnight. A PCR reaction was prepared using 2 µL of the culture DNA, 5 µL of 5X Go-Taq buffer, 0.5 µL of (10 µM) dNTP mix, 1 µL (10 µM) of M13F, 1uL (10 µM) of M13R, 0.1 µL Go-Taq polymerase, and 15.4 µL ultra-pure water. PCR reaction conditions were: 98° for 3 minutes; 35 cyles of 98° for 1 minute, 63° for 30 seconds and 72° for 1 minutes; and 72° for 3 minutes. The colony PCR products were visualized on a 1% agarose gel ran at 100V for 30 minutes. Approximately 10-20% of colonies were expected to contain the correct size of 1kb band. Colonies were expanded to 5 mL LB + carbicillin (1:1000) in a 37° shaker incubator overnight. The following day cultures were prepared using the Qiagen Spin Mini Prep Kit according to manufacturer's instructions. Plasmids were sequenced by the University of Michigan Sequencing Core using M13 forward and M13 reverse primers and compared to the ZiFiT sequence. Homology for module 1/2 alignment began at 5'-GAAC and stopped at 5'-TTGA while homology for module 3/4 began at 5'-CTGA and stopped at 5'-C/TTGA.

TALE clones with precise alignments were then used for the final three-part ligation into the TALEN (JDS) vector backbone.

Final ligation into TALEN vector. The purified 800 base pair modules were prepared for cloning into the final TALEN vector (JDS70). Modules 1/2 and modules 3/4 were double digested with BbsI and BsaI while the TALEN JDS vector was digested with BsmBI. After two hours incubation at 37°, the entire volume was visualized on a 1% agarose gel at 100V for 45 minutes. The 800 base pair modules and the JDS fragment were excised and gel purified using the QIAquick Gel Extraction Kit according to manufacturer's instructions. Modules and vector were eluted to 30uL in water. Purified digests were prepared for ligation using 150ng of each module and 150ng of JDS vector.

Screen of final ligation into TALEN (JDS) vector. The overnight ligation of modules 1/2/3/4/JDS vector were transformed using 40 µL of XL1 Blue cells and one-half (10 µL) of the ligation reaction. After gentle mixing and incubation on ice for 15 minutes, the cells were heat shocked for 45 seconds at 42°. The transformation was transferred to 250 µL of SOC media in a 15 mL BD Falcon tube and placed in a shaking incubator at 37 degrees for one hour. Cells were plated on carbicillin- (1:1000) containing agar plates and incubated at 37° overnight. Colonies from plates grown overnight were selected and cultured on 96-well plates containing 150 µL of LB broth + carb (1:1000) with incubation at 37° overnight.

Eight to ten colonies were selected from the 96-well plate for preliminary screening and transferred to overnight 5 mL starter cultures + antibiotic in a 15 mL BD Falcon tube. Cultures were prepared using the Qiagen Spin Mini Prep Kit according to manufacturer's instructions. A diagnostic restriction digest was used to examine selected cultures after plasmid preparation using ClaI and BamHI. Digest reactions contained: 10 µL of plasmid preparation; 2.5 µL NEB Buffer 4; 2.5 µL 10X BSA; 1 µL BamHI; 1 µL ClaI; and 8 µL H2O and were incubated at 37° for one hour, followed by visualization on a 1% agarose gel ran at 100V for 30 minutes. The fragment sizes indicate whether the modules were correctly incorporated into the JDS backbone. The desired fragment size was 2400 base pairs (module 1/2 + module 3/4 + 500 base pairs to ClaI + 300 base pairs to BamHI). The plasmid preparations exhibiting the correct 2400 base pair fragment sizes were sequenced using T7 and specific reverse (NK49) primers and compared to the ZiFiT assembly sequence. Sequencing reactions were performed by the University of Michigan Sequencing Core.

Capillary Electrophoresis (CE). Genomic DNA extracts were prepared, followed by PCR using 5'-6 -FAM labeled primer (10 µM) forward with the corresponding anti-sense primer for SAP exon 2 (5'- /6-FAM/AAACTGTGGTTGGGCAGATACAATATGG -3' and 5'-GGCTAAACAGGACTGGGACCAAAATTCTC-3'). A 25 µL reaction was prepared using 2.5 µL of each primer, 0.25 µL dNTP (10mM mix), 5 µL of 5X colorless Go-Taq buffer, 0.125 µL of Taq polymerase, 12.6 µL of H2O, and 2.0 µL of gDNA. Reaction conditions were: 95° for 5 minutes; 35 cycles of 95° for 30 seconds, 56° for 30 seconds and 72° for 30 seconds; followed by 72° for 10 minutes. A

compatible 96-well plate containing GS500Rox standard dye for capillary electrophoresis was prepared by the University of Michigan Sequencing Core and PCR reactions were diluted to 1:150 with 1 μL of this dilution added to the CE plate. CE analysis was performed by the University of Michigan Sequencing Core with resulting data files interpreted using the GeneMaker Software program.

STR Analysis. Genomic DNA extracted from the cell, 0.1 ng/uL, was processed by the University of Michigan Sequencing Core using the Identifiler Plus PCR amplification kit, (Life Technologies ABI catalog number 4427368). Information on loci markers was analyzed by the GeneMapper ID-X Software (Applied Biosystems) program, and the profiles were compared to reference databases.

Media. Jurkat cells were cultured in RPMI 1640 (Corning 15-041-CV) supplemented with 1% GlutaMax (Gibco 35050-061) and 10% FBS (Atlas) with incubation conditions at 37° and 5% CO_2.

Transfection of Jurkat Cells. Jurkat cells were transfected using a BioRad Gene Pulser II (250 V and 975 uF) using 0.4 cm gap cuvettes (BioRad 1652088). 10^7 cells were transfected with 30 μg of each TALEN. Otherwise, 10 μg of expression plasmids were used for each transfection.

DNA extraction. Genomic DNA was extracted using the HotShot lysis method. Cells were centrifuged at 300 rpm for 5 minutes and resuspended in 50 µL of lysis buffer (14 µL of 50% NaOH, 14 µL of AccuGene 0.5M EDTA, 10mL H2O) and placed on a 95° heating block for 30 minutes. Samples were incubated on ice for 5 minutes followed by 50 µL of neutralization solution (40mM Tris-HCl). Samples were briefly vortexed and pelleted. Supernatant was stored at -20°.

Whole cell lysate preparation. Cells were harvested by centrifugation at 300 rpm for 5 minutes and resuspended in 100 µL of prepared radioimmunoprecipitation assay (RIPA) lysis solution per 10^6 cells. RIPA buffer consists of PBS containing 1% NP-40, 0.5% Na-deoxycholate, and 0.1% sodium dodecyl sulfate (SDS). To prepare lysis solution, 10mL of RIPA buffer was supplemented with 1 protease inhibitor tablet (complete Mini EDTA-free Roche 11836170001), 100 µL Na_3VO_4 (BioLab P0758S 100mM), of 1mM DTT, and 10 µM PMSF, and 20 µL NaF (BioLab P0759S 500mM). Suspension was incubated on ice for 10 minutes, followed by a 10 minute centrifugation at 13000 rpm at 4°. Supernatants were stored at -80°.

Western blotting. Protein concentration was determined by using the Pierce BCA kit. Cytoplasmic extracts (25 µg) were prepared in LDS sample buffer (Invitrogen) and loaded on a 4-12% NuPage gel in MES running buffer. Following transfer, nitrocellulose membranes were blocked in 5% milk with TBS 0.1% Tween, followed by overnight incubation at 4° with the appropriate antibody. After washing, membranes were incubated with horseradish peroxidase-conjugated antibody for 1

hour at room temperature followed by visualization on chemiluminescence film. The following antibodies were used for Western blotting: rat anti-SAP (Cell Signaling #2805); goat-anti rat IgG-HRP (sc-2006); mouse anti-FLAG M2 (Sigma 088K6018); anti-mouse IgG-HRP (Cell Signaling #7076S); HRP-conjugated actin (Abcam 20272); and mouse anti-XIAP (BD 610717).

Chapter 3 Analysis of T Cell Signaling in *SAP*-null Jurkat Cells

3.1 Introduction

While previous studies have examined the role of SAP in signaling, there is much to be learned, and SAP's influence on T cell signaling remains unclear. To further understand these roles, the gene edited cell line, discussed in chapter 2, was used to identify specific *SAP*-dependent effects in T cell signaling. More specifically, we examined the influences of SAP on cytokine production, transcription factor activation, and calcium mobilization following stimulation of the T cell receptor.

SAP-dependent T cell activation is influenced by protein interactions with the cytoplasmic tail of the SLAM-family of receptors[91]. For example, SAP binds the adaptor protein FYN, a protein tyrosine kinase (PTK) that contains a SH3, SH2, and kinase domains, which allows FYN to phosphorylate the SLAM receptor[31,94,95]. The interaction of SAP and FYN with the SLAM receptor has been associated with Th2 differentiation and NKT cell development [101,188]. Conversely, in the absence of SAP, SLAM is bound to the inhibitory Src-homolgy-2-containing inositol phosphatase 1 (SHIP-1) at the switch motif[54,89], which inactivates other T cell signaling proteins such as ZAP-70 and LCK[109,189]. Notably, SAP binding to SLAM can displace SHIP-1, allowing for TCR activation[54,89].

SAP binds numerous members of the SLAM family of receptors through their immunoreceptor tyrosine switch motif (ITSM), including SLAM (CD150), CD84,

NTB-A (Ly108), and Ly9 (CD229)[1,94,95], all of which have important immunological functions. For example, SAP interaction with CD84, expressed on $CD4^+$ T cells, stabilizes T and B cell interactions and promotes germinal center development, B cell differentiation, and antibody production[139,190]. Additionally, while the impact of SAP engaging Ly9, a receptor constitutively expressed on $CD4^+$ T cells, is unclear[191], SAP interacting with the NK, T and B cell antigen (NTB-A) receptor stimulates Th1-type cytokine production[192] and is reportedly involved in the death of activated T cells[159]. Thus, SAP/SLAM interactions in $CD4^+$ T cells regulate T cell activation, cross-talk between other immune cells, and apoptosis.

Defective SAP in T cells is best characterized by the clinical manifestations observed in XLP1 patients, who harbor mutation in the *SAP* gene. As mentioned above, together with TCR stimulation, SAP binding to SLAM modulates T cell signaling, which results in the production of various cytokine. Notably, XLP1 patients have abnormal amounts of cytokines that induce immune cell proliferation and differentiation, such as IL-2[193], suggesting that SAP regulates cytokine production. One proposed mechanism for decreased IL-2 production in XLP1 patients has been described, resulting in elevated levels of diacylglycerol kinase α (DGKα)[194], which phosphorylates diacylglycerol (DAG) to form phosphatidic acid (PA) and prevents the activation of PKC-θ and NF-κB (figure 3.1).

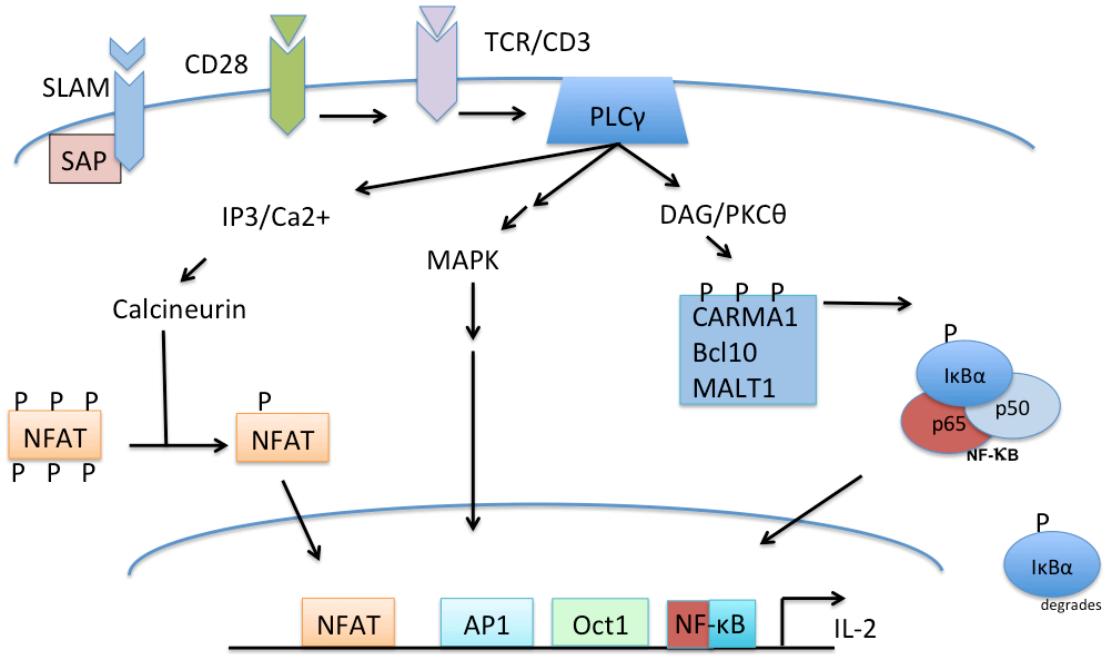

Figure 3.1 Activation and co-stimulation of the T cell receptor. Stimulation of the T cell receptor and SLAM, a co-stimulatory receptor, results in the activation of PLCγ–1 which activates DAG and PKC-θ to cause the CBM complex to phosphorylate IκBα which marks it for degradation, allowing for the nuclear translocation of NF-κB. Similarly, PLCγ–1 stimulates the release of calcium, activating the phosphatase calciuneurin to activate NFAT and allowing for its nuclear translocation. In addition, TCR stimulation activates the MAPK (mitogen-activated protein kinase) pathway resulting in the formation of the AP-1 transcription factor, which also converges on the IL-2 promoter with the constitutively active Oct1.

Through an unknown mechanism, SAP decreases the activity of DGKα, allowing for NF-κB activation following TCR stimulation and production of cytokines like IL-2. *In vitro* studies demonstrated that inhibition of DGKα in *SAP*-deficient cells partially restored PKC-θ activity and IL-2 production, suggesting that a potential role for SAP is to inhibit DGKα during T cell activation[190].

In addition to IL-2, another cytokine that influences immune cell activation is IFN-γ. IFN-γ has pleiotropic effects and is produced by various cells, including T and NK cells[195]. Elevated IFN-γ production leads to increased macrophage activation, a

characteristic of HLH patients[196] and there are cases of elevated IFN-γ levels in XLP1 patients[197]. Additionally, previous reports demonstrated that splenocytes from *Sap*-deficient mice produced elevated levels of IFN-γ following TCR stimulation[152] and this has directed naïve $CD4^+$ T cells to develop towards a Th1 cell phenotype[198], which suggests that elevated IFN-γ expression disturbs the balance of the other T helper and regulatory cells.

A key clinical observation is that patients with XLP1 frequently present to the emergency room with infections. Previous studies have explored the relationship between SAP expression and cytokine production upon exposure to several infectious agents. More specifically, SAP expression in human $CD4^+$ T cells inversely correlates to IFN-γ levels after tuberculosis infection, suggesting that the presence of SAP disrupts IFN-γ production[199]. Furthermore, these results suggest that SAP deregulation has implications in T cell signaling and subsequent effects in T cell activation, and cytokine production.

3.2 Results

XLP1 patients are diagnosed by measuring SAP expression by flow cytometry and sequencing the *SAP* gene. To assist future efforts in primary T cells and provide a rapid mechanism to assess SAP expression, an intracellular staining protocol was developed to analyze SAP expression. The wild type and *SAP*-null cells were analyzed by flow cytometry, as shown in figure 3.2, to compare SAP expression.

.

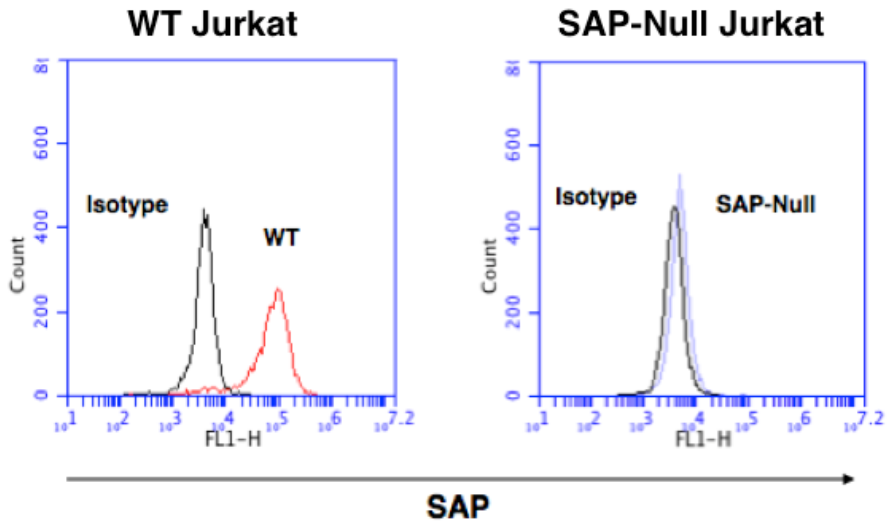

Figure 3.2 Development of a flow cytometric assay for intracellular SAP expression. The wild type and *SAP*-null Jurkats were analyzed by flow cytometry for SAP expression. The isotope control for both the WT and *SAP*-null cells are shown in black along with the corresponding peaks for SAP.

These Jurkat cells were used as a representative model of $CD4^+$ T cells, to evaluate the influences of *SAP* in T cell signaling. TCR stimulation results in the downstream production of cytokines and activates various transcription factors, which together regulate T cell proliferation and differentiation programs. Two cytokines that have been examined in XLP1 patients are IL-2 and IFN-γ and studies have shown that IL-2 mRNA production is decreased in XLP1 patient T cells[122], while IFN-γ production varies[152]. To assess whether IL-2 and IFN-γ mRNA production differed in a *SAP*-deficient cell, the Jurkat cells were stimulated for 6 hours with activating CD3 and CD28 antibodies, a biological approximation of TCR stimulation. RNA from unstimulated and stimulated cells was collected and prepared for qRT-PCR analysis for IL-2 and IFN-γ. IL-2 transcription was decreased in *SAP*-null Jurkats upon stimulation with CD3 and CD28 compared to the wild type cells (figure 3.3). Conversely, IFN-γ transcription was increased upon TCR

stimulation in *SAP*-null cells, suggesting that SAP modulates IFN-γ production. While IL-2 production was extremely low and sometimes below the threshold of detection in unstimulated Jurkat cells, there was measurable production of IFN-γ in unstimulated wild type and *SAP*-null cells. To assess the extent of IFN-γ production in the *SAP*-null cells with and without TCR stimulation, the *SAP*-null samples were also normalized to the wild type unstimulated samples, as described in figure 3.3B. This illustrated that the fold changes in expression were measurable with or without stimulation, indicating that these were basal differences in IFN-γ expression, and that the fold change was even more pronounced in the *SAP*-deficient cells when comparing the transcription levels to the wild type cells after TCR stimulation.

A)

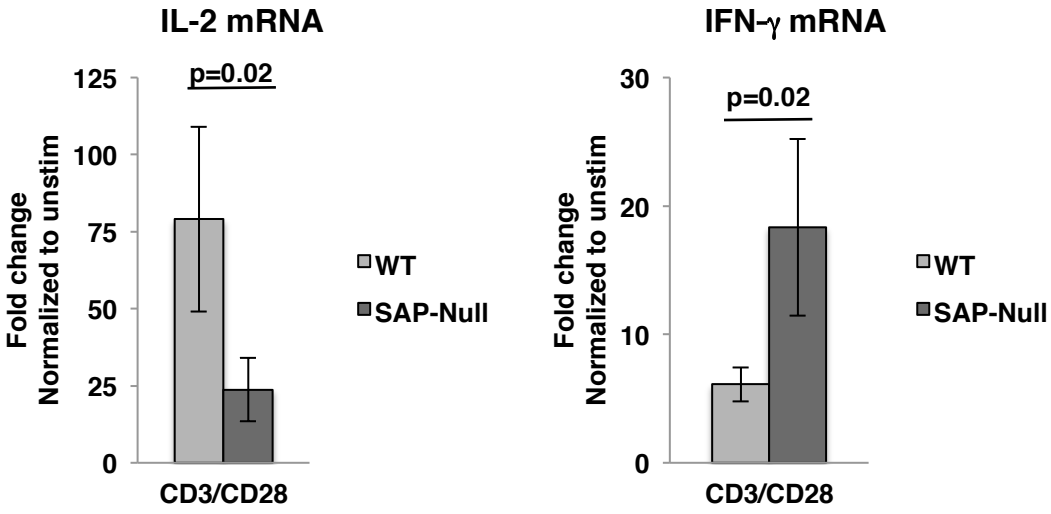

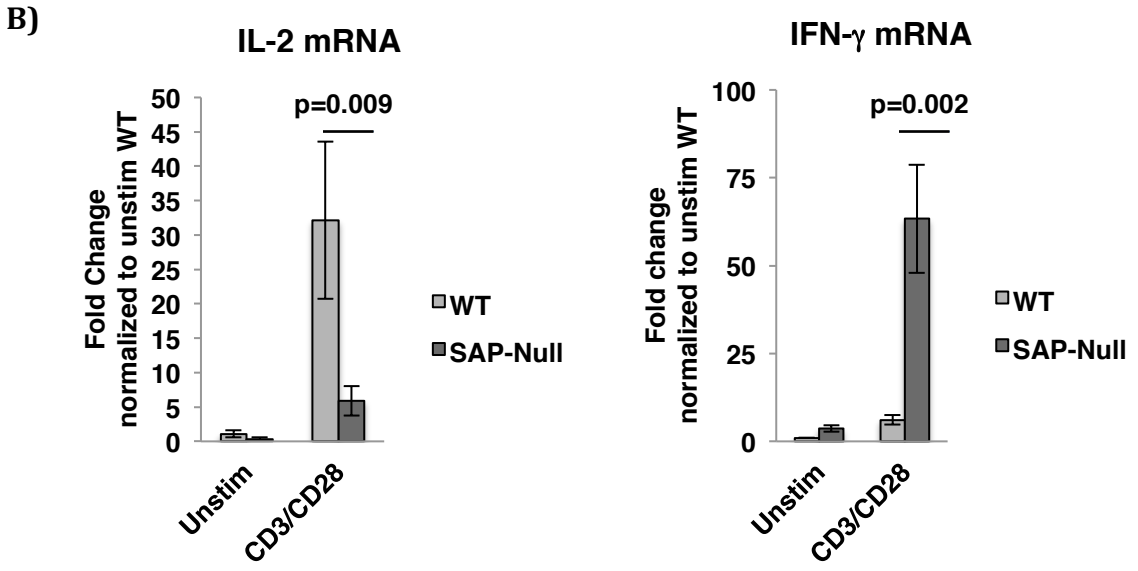

Figure 3.3 Altered cytokine production in *SAP*-null Jurkats. Jurkat cells were stimulated for 6 hours with activating CD3 and CD28 antibodies (4 μg/mL; 4 μg/mL). RNA was harvested and analyzed by qRT-PCR and Ct values were normalized to GAPDH. Fold change was calculated by normalizing to unstimulated of same cell type **A)** or to wild type **B),** as indicated. Statistical significance was calculated using a one-sided t-test and values are indicated. Data represent three independent experiments performed in triplicate.

NFAT is a key transcription factor that is required for IL-2 production. To assess the activity of NFAT in *SAP*-deficient cells, a luciferase reporter plasmid was transfected into the cells, which were subsequently treated with CD3 and CD28 for 18 hours and analyzed, as shown in figure 3.4. The wild type cells exhibited elevated levels of NFAT reporter activity following stimulation, while the *SAP*-null cells had negligible activity above the unstimulated levels, suggesting that *SAP* defects impair NFAT activity resulting in decreased IL-2 production.

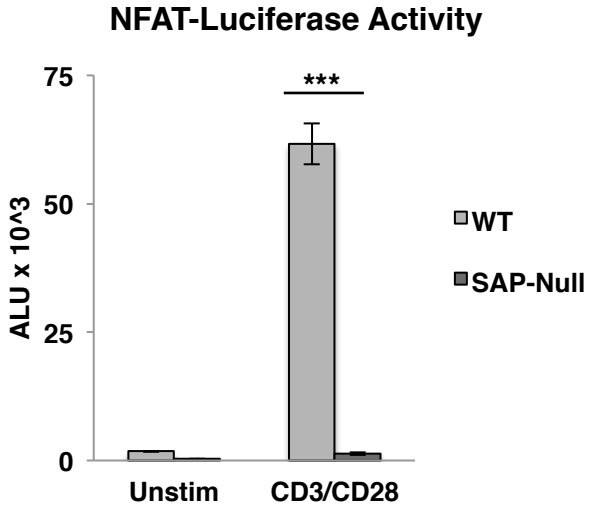

Figure 3.4 NFAT activation in Jurkat cells. Wild type and *SAP*-null Jurkat cells were transfected with a NFAT-luciferase reporter. Two days post-transfection cells were treated with CD3/CD28 (4 µg/mL; 4 µg/mL) for 18 hours prior to measuring luciferase activity. Data represent one of three independent experiments performed in triplicate with error bars indicating standard deviation ($p<0.00005$).

Given that the relative activity of the reporter was decreased in the *SAP*-null cells, it was possible that this was an artifact of transfection efficiency rather than a representation of transcription factor activity. To address this question, the wild type and *SAP*-null Jurkats were co-transfected with a fluorescent plasmid and the reporter plasmid, followed by microscopy and flow cytometry to assess transfection efficiency. Results from these experiments indicated that the wild type cells had a slightly higher transfection efficiency compared to the *SAP*-null cells as determined by fluorescent microscopy (figure 3.5A) and flow cytometry (figure 3.5B). These data suggest that the impaired NFAT reporter activity illustrated in figure 3.4 was not largely attributable to differences in transfection efficiencies, although this cannot be definitively excluded.

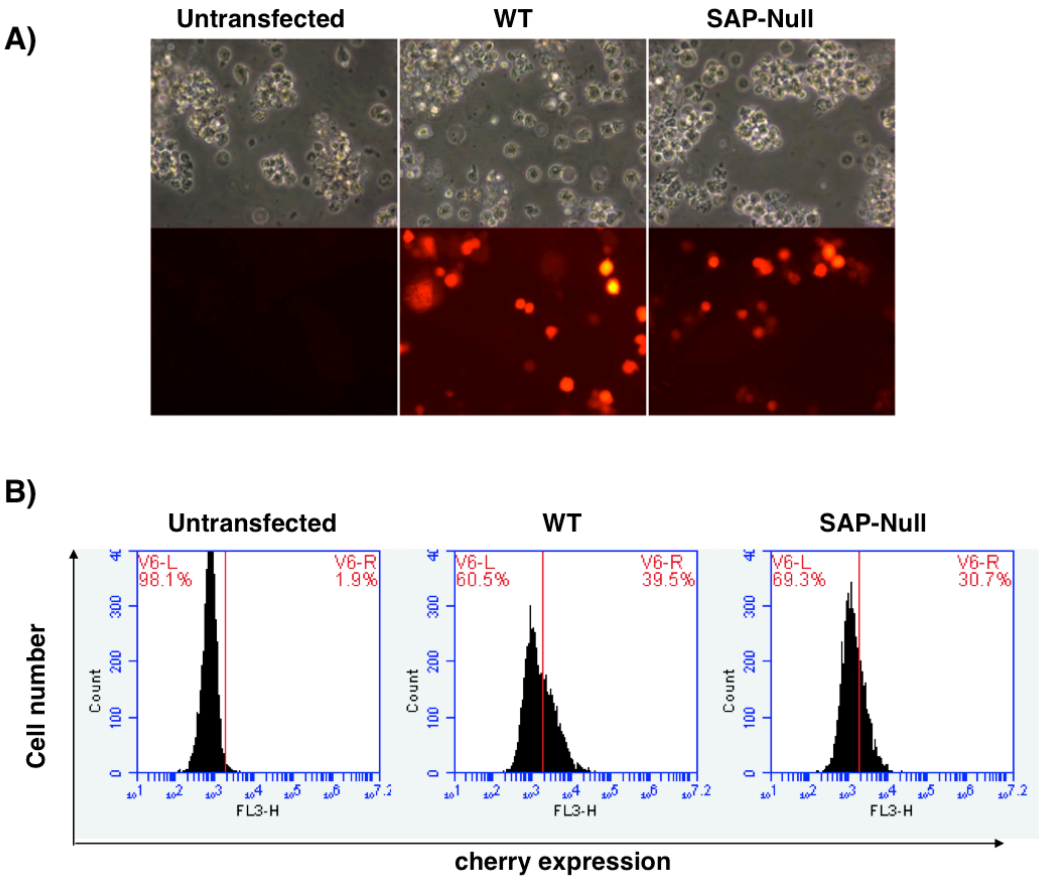

Figure 3.5 Transfection efficiency in Jurkat cells. A) Wild type and *SAP*-null Jurkat cells were co-transfected with a reporter plasmid and pEBB-cherry. Images represent untransfected and transfected cells at 48 hours with representative quantification by flow cytometry shown **B).**

The evidence of both decreased NFAT reporter activity and IL-2 mRNA production in the *SAP*-null cells suggested that a *SAP*-dependent defect occurred upstream of NFAT activation. NFAT activity is dependent on calcium mobilization from the ER to the cytoplasm to stimulate the phosphatase calcineurin[200]. It was possible that *SAP*-deficiencies alter calcium mobilization within the cell, and this has

been observed in at least one study of XLP1 patients, who exhibited excess intracellular calcium[122]. To assess whether there was a *SAP*-dependent defect on calcium mobilization, the wild type and *SAP*-null Jurkats were stained with a dye that binds free calcium ions, followed by TCR stimulation. Mobilized intracellular calcium ions were measured by fluorescence, and the results indicated that *SAP*-deficient cells had increased levels of free calcium compared to the wild type cells after stimulation (figure 3.6). This suggested that *SAP*-null cells have either defects in calcium ion processing upon release from the ER or that there were defects in the ion channels that replenish calcium ions within the cell.

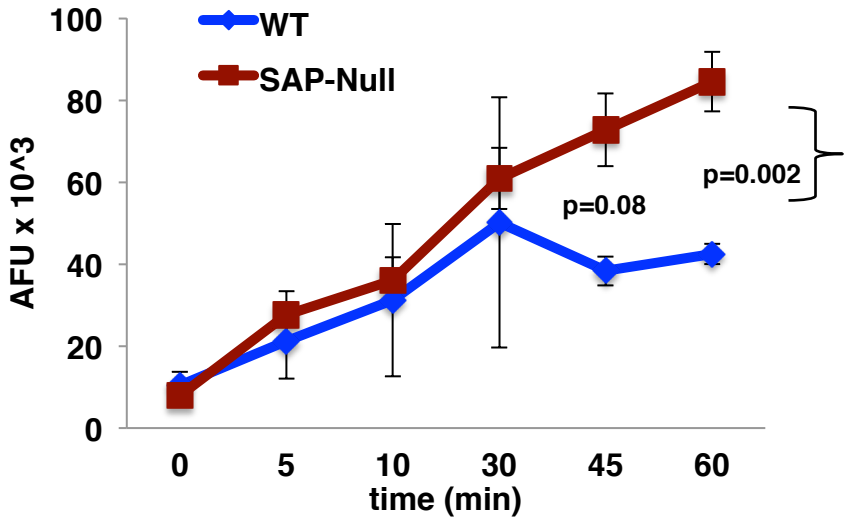

Figure 3.6 Intracellular calcium mobilization in Jurkat cells. Cells were stained with fluor-4-direct dye, followed by stimulation with CD3 and CD28 (4 µg/mL; 4 µg/mL) and measurement of intracellular calcium. Representative data are shown from two independent experiments with bars indicating standard deviation.

The results described above suggested that TCR stimulation in *SAP*-deficient cells impaired the transcription of IL-2 activity by altering the activity of NFAT and maintaining excess free calcium within the cells. However, to attribute these defects to SAP, it was necessary to restore SAP expression in the *SAP*-null cells by co-transfecting a FLAG-SAP plasmid (*SAP*-null + pSAP) and an antibiotic resistance plasmid into the *SAP*-null cells followed by continual growth in selection media. These cells, with restored SAP expression, were analyzed by flow cytometry (figure 3.7A) and Western blot analysis (figure 3.7B) to verify the reconstitution of SAP expression within the cell population. The flow cytometry results illustrated that the FLAG-SAP population had two peaks, indicated by the red lines, and one of these peaks overlaid the isotype control, similar to the *SAP*-null cells. This suggested that the *SAP*-null + pSAP population is a combination of the *SAP*-null cells and cells ectopically expressing SAP. Additionally, the Western blot demonstrated that SAP expression is restored in the *SAP*-null cells, as shown by the FLAG-SAP fusion protein.

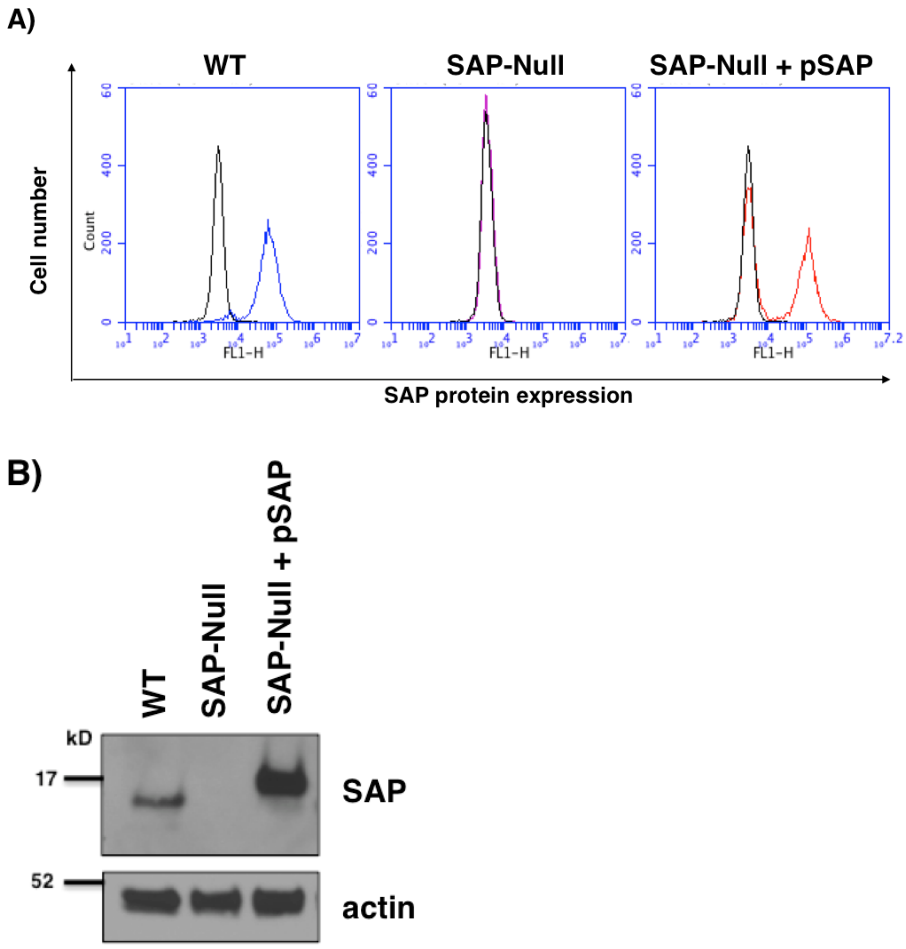

Figure 3.7 Reconstitution of SAP expression in *SAP*-null Jurkats. A) *SAP*-null Jurkats were co-transfected with pEBB-FLAG-SAP (10 μg) and 1 μg of pBABE-puromycin followed by antibiotic selection with 0.5 μg/mL puromycin. Intracellular SAP staining was analyzed by flow cytometry for the wild type, *SAP*-null, and reconstituted SAP expressing cells, with black lines indicating respective isotype controls. **B)** The restoration of SAP expression was further confirmed by Western blotting as illustrated by the presence of the FLAG-SAP fusion protein in lane 3. Jurkat-derived cells were analyzed by Western blot using anti-SAP antibody.

Reconstituting SAP expression in the *SAP*-null cell line allowed us to determine if the measured cytokine defects upon TCR stimulation were SAP-dependent. The wild type, *SAP*-null, and *SAP*-null + pSAP cells were stimulated with CD3 and CD28 for six hours prior to RNA harvest, followed by qRT-PCR to measure IL-2 and IFN-γ production. Reconstitution of SAP in the *SAP*-deficient cells partially

restored the levels of IL-2 production after CD3 and CD28 stimulation, compared to the wild type (figure 3.8). Again, one explanation for the partial restoration of IL-2 transcription is that the cell line contained a mixture of stably expressing SAP cells and *SAP*-null cells, suggesting that only a portion of the cells, the ones with ectopic SAP expression, have elevated IL-2 levels. Additionally, the level of IFN-γ production was decreased in the cell line where SAP is reintroduced and approximated that of the wild type. Together, these results suggested that the cytokine abnormalities in the *SAP*-null cells after TCR stimulation were a *SAP*-dependent effect.

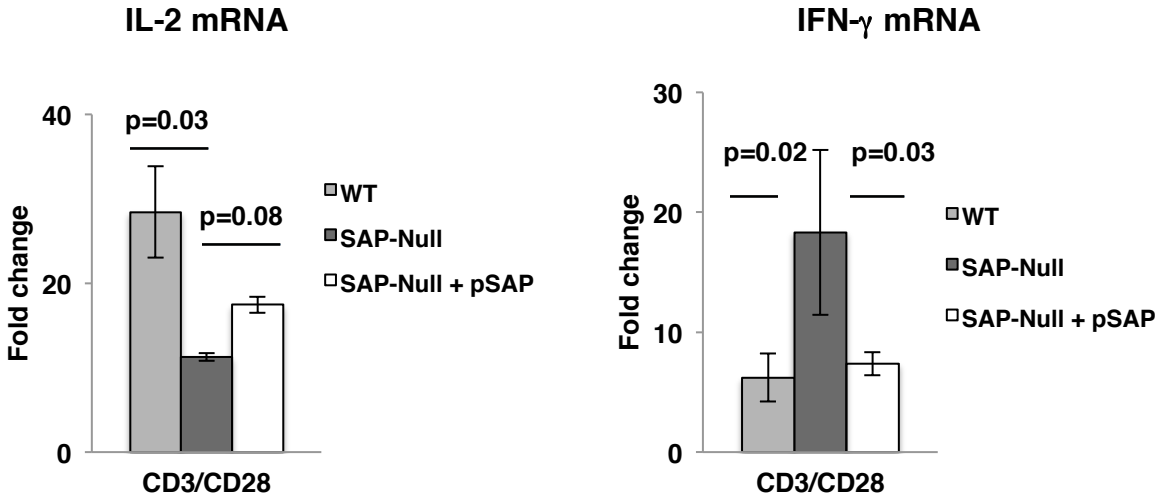

Figure 3.8 SAP reconstitution partially restored cytokine production. Wild type, *SAP*-null, and *SAP*-null + pSAP cells were stimulated for six hours with CD3/CD28 (4 μg/mL; 4 μg/mL). RNA was harvested and analyzed by qRT-PCR and Ct values normalized to GAPDH. Fold change was calculated by normalizing to the unstimulated sample of the same cell type. Data represents two independent experiments performed in triplicate.

3.3 Discussion

The gene editing derived *SAP*-deficient T cells, when stimulated by CD3 and CD28, led to altered cytokine production, impaired NFAT transcription factor activity, and increased free intracellular calcium compared to the wild type. The wild type and *SAP*-deficient cells were examined for cytokine deficiencies and the *SAP*-null cells had impaired IL-2 mRNA production and increased IFN-γ mRNA levels compared to the wild type cells following TCR stimulation. Restoration of SAP expression in the *SAP*-null cell line demonstrated that IL-2 transcription after TCR stimulation was partially restored, as shown by increased IL-2 levels compared to the *SAP*-null cells. Similarly, the cells with ectopic SAP expression had reduced levels of IFN-γ, compared to the *SAP*-null cells, to approximate the same levels as expressed by the control cells. The activity of NFAT was also examined, finding that the *SAP*-null cells did not exhibit measurable NFAT reporter activity following TCR stimulation, suggesting an NFAT defect. Additionally, an intracellular SAP staining protocol was developed to confirm the loss of SAP expression in the *SAP*-null Jurkat cells and is available for future lines of inquiry using primary cell lines. Finally, the decreased NFAT activity supported the idea that calcium mobilization is altered in *SAP*-null cells as indicated by increased free intracellular calcium levels after TCR stimulation. These results may be clinically relevant since XLP1 patients have been shown to exhibit similar characteristics with decreased IL-2 production and excess calcium mobilization within the cell[193]. Together, these results provided additional insights to the SAP-dependent effects in T cell signaling, and may have important clinical implications in the diagnosis of XLP1.

A key consequence of T cell activation is IL-2 production, and prior studies have demonstrated that T cells from XLP1 patient have impaired IL-2 production following TCR stimulation[122,129], although the mechanism was unclear. Consistent with these studies, (figure 3.3) illustrated that IL-2 production was decreased in the *SAP*-null Jurkat cells, compared to the wild type control cells. IL-2 expression was measured at the transcriptional level by assessing mRNA production. While it was assumed that transcriptional differences equate to expression differences, it was not conclusively proven to be the case. Two approaches would confirm the expression of cytokines: measuring the secretion by an enzyme-linked immunosorbent assay (ELISA) and intracellular staining and quantification by flow cytometry.

It is also possible that the IL-2 mRNA is transcribed in the wild type Jurkat cells but there is a difference in the stability of the transcripts, potentially equalizing the amounts of IL-2 expressed or secreted. Cytokines have been observed to have short mRNA half lives in response to stimuli[201]. Although there is increased transcription of IL-2 in the wild type Jurkat cells, the mRNA could be unstable due to deadenylation, removal of the 3'-poly(A) tail, or directed by AU-rich sequences within the 3'-untranslated region[202]. Genes with AU-rich sequences are targeted, through unknown mechanisms, for decay upon recruitment of AU-binding proteins[203] and analysis of the adenylate-uridylate-rich elements (AREs) within the 3'-untranslated region of the mRNA would determine stability of the IL-2 message. An experimental approach to examine this would be accomplished by a nuclear run-on experiment. The IL-2 transcript would be *in vitro* labeled by the incorporation of radionucleotides, which can then be isolated and hybridized to a complementary

probe and quantified by radiography. Should the IL-2 mRNA be stable, this would support that SAP defects impair IL-2 transcription and expression.

The decreased IL-2 transcription in the *SAP*-deficient cells is partially due to impaired NFAT activation and calcium mobilization. NFAT is a family of transcription factors that regulate not only T cell activation but also influence thymocyte development and T cell differentiation[204]. The functional contributions of each NFAT isoform are not well understood[205] and isoform reduction using RNAi in conjunction with SAP expressing and SAP-deficient cells would identify what characteristics, such as cytokine production and the regulation of other genes, are ascribed to each variant. An intriguing possibility that might account for impaired NFAT activation and the calcium processing defects observed in the *SAP*-deficient cells is abnormal expression of carabin, the negative regulator of calcineurin's phosphatase activity[206]. While little is known about its regulation, carabin binds with and inhibits the activation of calcineurin[206]. *Carabin*-null mice were shown to exhibit normal T cell development, however, upon TCR stimulation demonstrated increased proliferation and NFAT activation, implicating carabin as a negative regulator of TCR signaling[207]. Although analysis of the mechanism of calcium mobilization defects are beyond the scope of this study, it is possible that SAP regulates carabin expression, and when *SAP* is deficient carabin levels may increase, impeding calcineurin's activity and accounting for the decreased NFAT activation and calcium mobilization observed in the *SAP*-null cells.

Aside from IL-2, *SAP*-null Jurkats exhibited increased IFN-γ expression following TCR stimulation. IFN-γ has pleiotropic effects and is produced by various cells, including T and NK cells[195]. Additionally, the influence of elevated IFN-γ levels on macrophage production is of clinical interest for potential therapeutic intervention in XLP1 patients, because they exhibit excessive macrophage activation[196]. A phase II clinical trial has been initiated to investigate the efficacy of using neutralizing IFN-γ antibodies to decrease macrophage activation in HLH patients[208]. Characterizing the extent of macrophage activation by T cells with *SAP* defects would be of interest to determine whether XLP1 patients are likely to benefit from this treatment.

The impact of excess IFN-γ production has been observed in splenocytes from *Sap*-deficient mice, preferentially differentiating into Th1 cells after TCR stimulation[152], and previous work suggested that SAP's interaction with FYN is necessary for Th2 differentiation[101,188,209]. It is reasonable to speculate that disruption of the SAP/FYN interaction may result in the observed increase in IFN-γ production and that this preferentially differentiates T helper cells toward a Th1 fate in human cells. Importantly, the implications of elevated IFN-γ levels and decreased Th2 cell development would be impaired release of IL-4 by Th2 cells, which could impede B cell proliferation and antibody production during humoral immunity[209].

Previous work has shown that IFN-γ production by CD4 cells is modulated by T-bet[210] (T-box family of transcription factor) and Bcl-6[211]. T-bet and Bcl-6 associate on the IFN-γ promoter and when Bcl-6 expression is high there is less IFN-γ

expression[212]. T helper cells express Bcl-6, which is expressed at high levels in germinal center B cells [213]. Since SAP defects impair the development of GCs, it is plausible that this contributes to decreased Bcl-6 expression and the elevated IFN-γ transcription identified in the *SAP*-null Jurkat cells. To further test this, measurement of the levels of T-bet and Bcl-6 expression followed by selective targeting of each gene would confirm which components are modulated by SAP.

An area relatively unexplored in *SAP*-deficiencies is the activation of T regulatory cells, which modulate the proliferation of other T cells. NFAT is required, in addition to the transcription factor FOXP3, to affect T_{reg} differentiation[214]. As *SAP*-null cells exhibit impaired TCR-mediated NFAT activity (figure 3.4), this may suggest that naïve T cells are insufficiently differentiated into T_{reg} cells, potentially contributing to the lymphoproliferative phenotype observed in XLP1 patients. To test this hypothesis, future studies may include siRNA mediated silencing of *SAP* in naïve primary T cells from healthy donors, followed by TCR stimulation to determine whether the differentiation of T_{reg} cells differs based on reduced SAP expression. Moreover, cytokine production may not only impact T cell differentiation, but also influence the premature death of immune cells, which could impair the ability of XLP1 patients to clear infections.

3.4 Materials & Methods

Media. Cells were cultured in RPMI 1640 (Corning 15-041-CV) supplemented with 1% GlutaMax (Gibco 35050-061) and 10% FBS (Atlas) with incubation conditions at 37° and 5% CO_2.

SAP Reconstitution. The *SAP*-null Jurkat cells were transfected using a BioRad Gene Pulser II (250 V and 975 uF) using 0.4 cm gap cuvettes (BioRad 1652088). 10^7 cells were transfected with 10 μg of pEBB-SAP-FLAG and 1 μg of pBABE-puro selection plasmid and 48 hours after transfection, cells were continually maintained in 0.5 μg/mL of puromycin containing selection media.

Whole cell lysate preparation. Cells were harvested by centrifugation at 300 rpm for 5 minutes and resuspended in 100 μL of prepared radioimmunoprecipitation assay (RIPA) lysis solution per 10^6 cells. RIPA buffer consists of PBS containing 1% NP-40, 0.5% sodium-deoxycholate, and 0.1% sodium dodecyl sulfate (SDS). To prepare lysis solution, 10mL of RIPA buffer was supplemented with 1 protease inhibitor tablet (complete Mini EDTA-free Roche 11836170001), 100 μL Na_3VO_4 (BioLab P0758S 100mM), 10 mM DTT, and 20 μL NaF (BioLab P0759S 500mM). Suspension was iced for 10 minutes followed by a 10 minute centrifugation at 13000 rpm at 4°. Supernatants were stored at -80°.

Western blotting. Protein concentration was determined by using Pierce BCA kit against a known standard. Cytoplasmic extracts (25 μg) were prepared in LDS sample buffer (Invitrogen) and loaded on a 4-12% NuPage gel in a 1:20 MES running buffer. Following transfer, nitrocellulose membranes were blocked in 5% milk with TBS 0.1% Tween, followed by overnight incubation at 4° with the appropriate antibody. After washing, membranes were incubated with horseradish peroxidase-conjugated antibody for 1 hour at room temperature followed by

visualization on chemiluminescence film. The following antibodies were used for Western blotting: rat anti-SAP (Cell Signaling #2805); goat-anti rat IgG-HRP (sc-2006); mouse anti-FLAG M2 (Sigma 088K6018); anti-mouse IgG-HRP (Cell Signaling #7076S); HRP-conjugated actin (Abcam 20272); and mouse anti-XIAP (BD 610717).

qRT-PCR. RNA was extracted using the RNeasy Mini Kit (Qiagen 74104) according to manufacturer's instructions. High-capacity cDNA reverse transcription kit (Applied Biosystems 4368814) was used to prepare cDNA from 1 μg of isolated RNA. The following Taq-Man primers were used for qRT-PCR on Applied Biosystems platform ABViiA7: IFN-γ Life Technologies ABI Hx00174143_m1 and IL-2 Life Technologies ABI hs00174114_m1. Samples were standardized to GAPDH and normalized to the unstimulated samples using the ΔΔCt method.

Reporter Assays. Jurkat cells (10^7) were transfected using a BioRad Gene Pulser II (250 V and 975 uF) with 0.4 cm gap cuvettes (BioRad 1652088). 10^7 cells were transfected with 10 μg of NFAT-Luc reporter or 2kB-Luc reporter plasmids and 1 μg of pEBB-cherry. After 44 hours, cells were stimulated as indicated for 6 hours. Luciferase was measured with the dual-luciferase reporter assay system (Promega E1910). Briefly, 10^6 cells were harvested and washed in 1x PBS prior to adding 100 μL of 1x Passive Lysis buffer (PLB#E1941) with a brief vortex. Twenty microliters of this was transferred per well of a 96-well Costar white bottom plate. Just prior to measurement, 100 μL of prepared Luciferase Assay Reagent (LAR) was added per well. Luciferase readings were performed on a Biotek Plate Reader for

luminescence using the AutoGain option. Fold changes, where indicated, are normalized against unstimulated readings by cell type.

Intracellular SAP staining with flow cytometry analysis. Cells were fixed and permeabilized using eBioscience Intracellular Fixation & Permeabilization Buffer Set (88-8824). Approximately 750,000 cells were centrifuged at 300g for 10 minutes. Cells were fixed in 100 µL of IC fixation buffer and pulse vortexed. After incubation in the dark at room temperature for 30 minutes, cells were washed twice by resuspending in 2mL of 1X permeabilization buffer and centrifuged at 300g for 5 minutes at room temperature. Cells were resuspended in 100 µL of 1X permeabilization buffer, and 1 µg of SAP antibody or isotype control was added with incubation in the dark at room temperature for 15 minutes (Mouse Anti-SH2D1A Abnova H00004068-M01 or Purified Mouse IgG2a BioLegend 41502). Cells were washed in 1X permeabilization buffer followed by centrifuge 300g for 5 minutes. Cells were resuspended in 100 µL of 1X permeabilization buffer and 1 µg of secondary fluorochrome-labeled antibody was added with incubation in the dark at room temperature for 15 minutes (Goat Anti-Mouse IgG2a-FITC Southern Biotech 108-02). Cells were washed in 1X permeabilization buffer followed by centrifuge 300g for 5 minutes. Cells were resuspended in 500 µL of FACS buffer and processed on an Accuri C6 flow cytometer with a 500,000 threshold collecting 10,000 events.

Calcium mobilization assay. The fluo-4 direct calcium assay kit (Life Technologies F10471) was used to measure free intracellular calcium levels according to manufacturer's instructions. Briefly, loading solution was prepared with 250nM probenecid stock in the fluo-4 direct calcium assay buffer. 125,000 cells were plated in 50 μL of media on a black-sided, clear bottom, 96-well plate followed by 50 μL of the prepared loading solution, with incubation at 37° for 30 minutes followed by 30 minutes at room temperature. Stimulation was added just prior to fluorescence measurement on a Biotek plate reader using 494 nm excitation and 516 nm emission.

Chapter 4 Characterization of Apoptosis in *SAP*-null Jurkat Cells

4.1 Introduction

X-linked Lymphoproliferative disease (XLP) is caused by mutations in *SAP* (XLP1) or *XIAP* (XLP2)[5]. *SAP* and *XIAP* are structurally unrelated and the expression of SAP is restricted to T and natural killer (NK) cells while XIAP is ubiquitously expressed[1,31,32]. *SAP* is a small 128 amino acid protein largely comprised of a SH2 domain[1], while *XIAP* is a 497 amino acid residue with three baculovirus inhibitor of apoptosis protein repeat (BIR) domains, capable of binding and inhibiting caspase activity, and a RING E3 ubiquitin ligase domain[5].

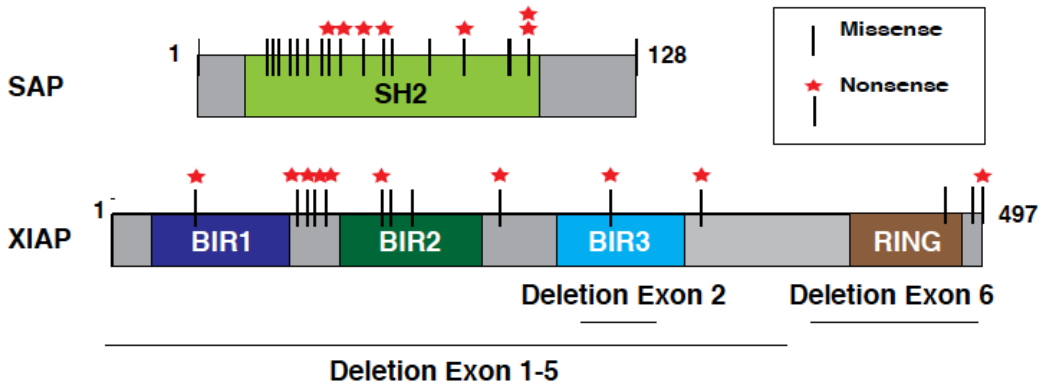

Figure 4.1 Structure and mutations of *SAP* and *XIAP*. *SAP* is a small SH2 domain containing protein while *XIAP* has three caspase binding domains and enzymatic activity. Mutations associated with XLP span the entire regions of *SAP* and *XIAP*[34]. Each line indicates an annotated patient mutation and the star denotes nonsense mutations. (Adapted from Blood (2010) 116:18.)

Previous studies examining Sap and Xiap expression in mouse models determined that *Sap*-deficient cells have normal levels of Xiap expression and vice versa[6]. At first glance, SAP and XIAP appear to be functionally unrelated as SAP binds the SLAM family of receptors, while XIAP binds and inhibits caspase activity. Patients with XLP1 and XLP2 have similar, but not identical, clinical presentations, as shown in table 4.1.

XLP1 (*SAP*) n=33 % of patients		**XLP2 (*XIAP*)** n=30 % of patients
55	Hemophagocytic Lymphohistiocytosis (HLH)	76
92	EBV triggered HLH	83
61	HLH associated lethality (HLH patients)	23
67	Hypogammaglobulinemia	33
7	Splenomegaly (w/o HLH)	87
30	Lymphoma	0
0	Colitis	17

Table 4.1 The clinical picture of XLP. XLP patients have a range of phenotypes associated with XLP1 and XLP2[34]. However, a unique feature of XLP1 (*SAP*-deficient) patients is lymphoma development, while only XLP2 (*XIAP*-deficient) patients exhibit colitis. (Adapted from Blood (2011) 117(5).)

As described in chapter 3, there is strong evidence to suggest that SAP is involved in TCR signaling. T cell activation involves the proliferation and clonal expansion of immune cells and is followed by cell death. Studies from Katz *et.al*, (2014) provided evidence that SAP is involved in apoptosis but the mechanism is not well characterized. To further understand the influences of *SAP* on apoptosis, S*AP*-null Jurkat cells were examined for their sensitivity to cell death. Furthermore, a comparative approach to analyze sensitivity to apoptotic stimuli in cells with

decreased SAP and XIAP expression was investigated to understand immune cell death in XLP.

Apoptosis is an orchestrated cellular process where dying cells are consumed by neighboring cells. In contrast, other cell death programs such as necrosis result in enlarged cells that release their cellular contents into the microenvironment causing inflammation and the recruitment of other immune cells to the necrotic sites[215,216]. Thus, tumors with a component of necrotic tissue have been shown to release cytokines that further stimulate immune cell proliferation [69]. Necrotic cells appear to foster an inflammatory environment whereas apoptosis does not appear to introduce additional inflammation within the microenvironment.

Apoptosis, as shown in figure 4.2, can be initiated by cell surface receptors or by the sensing of a plethora of cellular stresses that result in the activation of effector proteins called caspases (cysteine aspartate-specific proteinases), in particular, Caspase-3[217,218]. In receptor-induced apoptosis, cell death can be initiated by members of the TNF (tumor necrosis factor) receptor superfamily, which contain a cysteine-rich extracellular domain, a transmembrane region, and variable cytoplasmic tails that govern the specific functions of the receptor[219]. Certain TNF receptors contain death domains (DDs) in their cytoplasmic tails, which help trigger apoptotic signaling pathways following ligand activation. A well characterized death receptor is Fas (CD95/APO-1)[219], which is activated by binding of Fas ligand (FasL). Ligation recruits the Fas-associated death domain (FADD) protein to the death domain (DD) in the cytoplasmic tail of Fas[220]. Additionally, pro-Caspase-8[221] is recruited to the receptor complex, forming the death-inducing signaling complex

(DISC)[222]. Once formed, the complex induces the cleavage and activation of pro-Caspase-8 which, in turn, activates Bid[223,224].

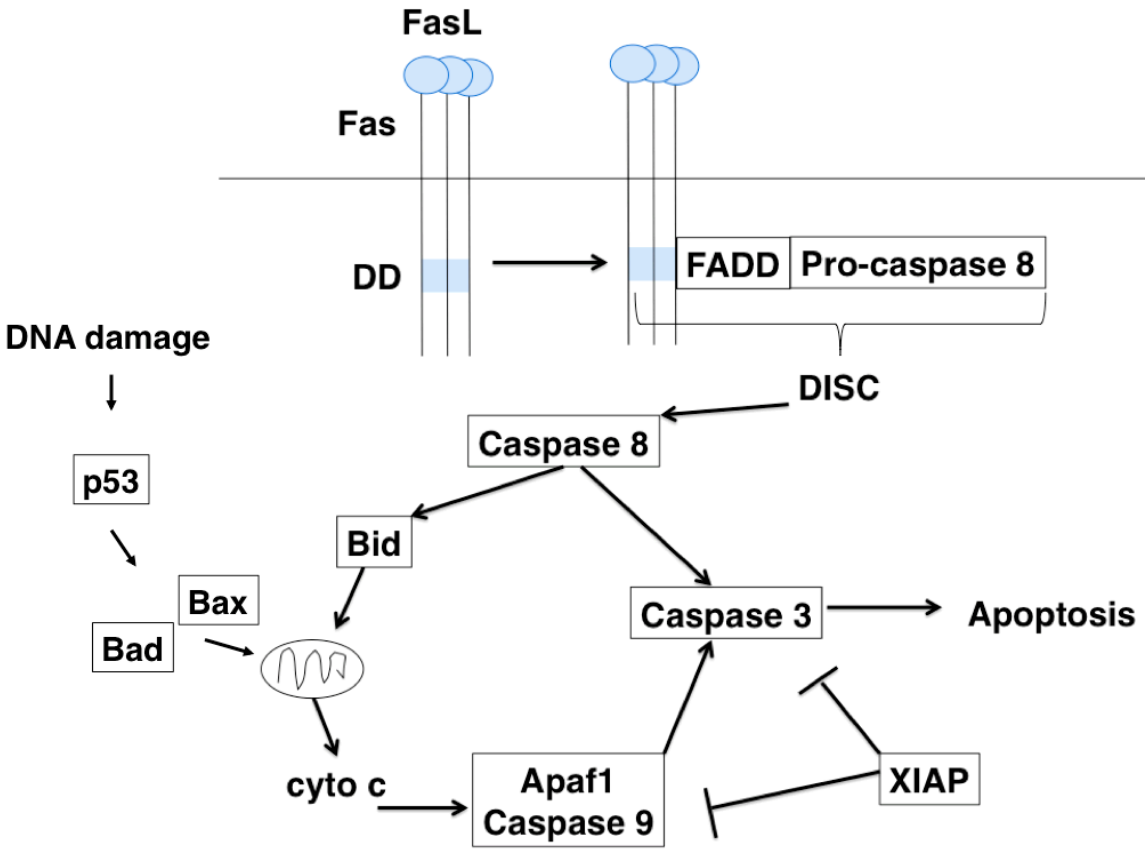

Figure 4.2 The apoptotic cascade. Apoptosis is initiated by extrinsic stimuli, involving death receptors, or by internal cellular stress, such as DNA damage. For receptor-mediated apoptosis FasL, for example, is produced by immune cells and ligates with the Fas receptor, recruiting FADD and pro-Caspase-8 to the death domain (DD) to form the DISC. Activated Caspase-8 stimulates Bid to induce the mitochondria, via Bax and Bak, to release Cytochrome *c*. Cytochrome *c* forms the apoptosome with Apaf1 and Caspase-9 affecting Caspase-3 activity, which leads to cells death. Similarly, intracellular stress, such as DNA damage, increases the activity of p53 to affect Bad and Bax to induce the mitochondria to release Cytochrome *c*. The XLP2 disease related protein XIAP has functional roles in apoptosis as it binds with and inhibit caspase activation[225,226].

Intracellular stress or the activation of Bid by Caspase-8, can increase the level of Bax and Bak oligomerization on the mitochondrial surface, creating pores that allow

Cytochrome *c* release[227,228]. Once released, Cytochrome *c* then binds to the apoptotic protease activating factor 1 (Apaf1) to form the apoptosome, which recruits Caspase-9[229] and activates downstream Caspase-3 to affect cell death. Caspase-3 activation, as an indicator of apoptosis, was measured in the *SAP*-null cells to determine the impact of *SAP*-defects on T cell apoptosis.

4.2 Results

Since XIAP and SAP contribute to the development of XLP, and XIAP has a recognized role in apoptosis, through its binding and inhibition of caspases[230], the initial question was whether cells deficient for *SAP* or *XIAP* had similar responses to apoptotic stimuli. To address this question in a comparative manner, Caspase-3 activity was measured after death receptor stimulation in RNAi silenced cells. Jurkat cells were transfected with siRNA targeting *SAP, XIAP*, or *GFP* as a negative control, and the samples were subsequently stimulated with activating anti-Fas antibody. Caspase-3 activity was assessed by measuring caspase-mediated cleavage of a fluorescently labeled target substrate. The results shown in figure 4.3 indicate that the suppression of both SAP and XIAP expression increased Caspase-3 activity following Fas stimulation compared to the control.

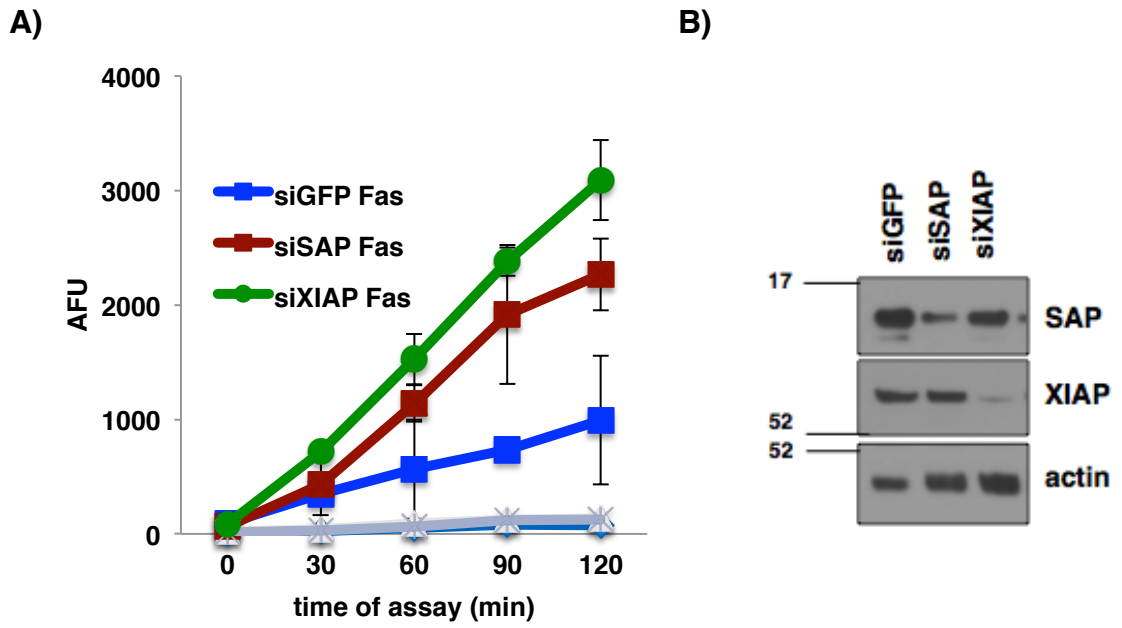

Figure 4.3 Caspase-3 activity with siRNA in Jurkat cells. A) Jurkat cells were transfected with siRNA against *SAP, XIAP*, or *GFP* as a negative control and incubated for 48 hours prior to treatment with an activating anti-Fas antibody (250 ng/mL). Six hours after stimulation, cells were measured for Caspase-3 activity. Representative data is shown for two experiments performed in triplicate with error bars indicating standard deviation ($p<0.004$ for 90 and 120 minute time points compared to siGFP). Grey bars indicated unstimulated samples. **B)** The Western blot for Jurkat cells transfected with the respective siRNA against anti-SAP and anti-XIAP antibodies illustrates the relative reduction in SAP and XIAP expression.

While it was anticipated that reduced XIAP expression would increase the levels of active Caspase-3, it was novel to see that *SAP* silencing by siRNA had a similar effect. Based on this data wild type and *SAP*-null Jurkat cells were also assessed for their cell death sensitivity to Fas. Similar to our findings in *SAP* silenced Jurkat cells, the *SAP*-null cells exhibited increased Caspase-3 activity to Fas treatment when compared to wild type (figure 4.4A). To further confirm increased Caspase-3 activity when *SAP* is defective, the wild type and *SAP*-null cells were stimulated with anti-Fas antibodies followed by Western blot analysis of Caspase-3

cleavage expression, a marker of caspase activation (figure 4.4B). These data demonstrated that there was no measurable Caspase-3 activity prior to stimulation in either cell type but, after treatment, the *SAP*-null cells exhibited higher levels of cleaved Caspase-3 activity, compared to wild type. This also suggested that *SAP*-deficiencies increase the amount of active Caspase-3 within the cell upon stimulation of Fas.

A)

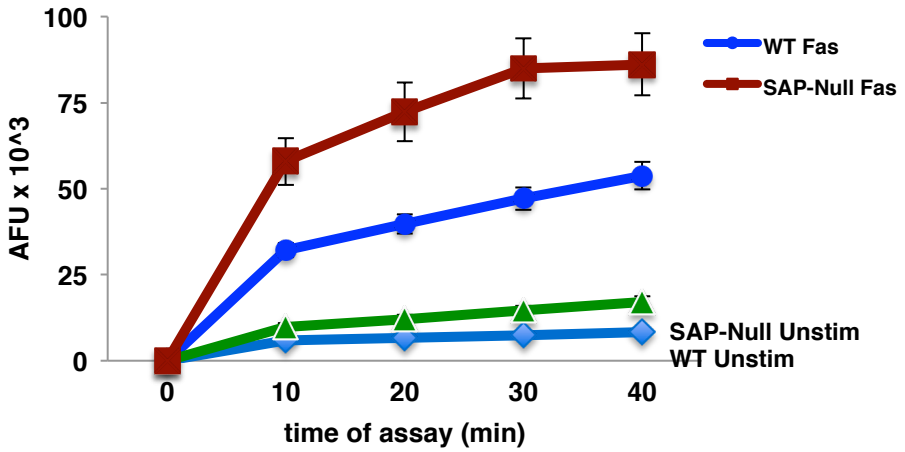

B)

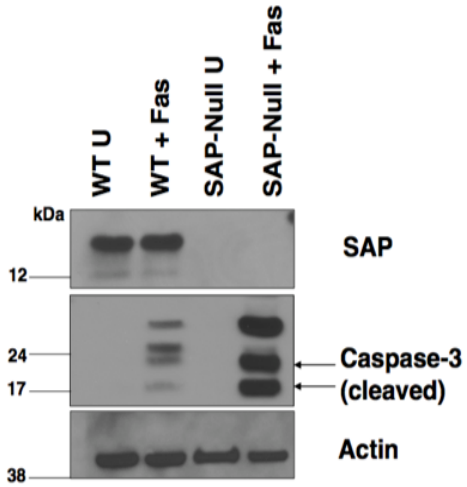

Figure 4.4 Increased Caspase-3 activity in SAP-null Jurkats. A) Cells were treated for 6 hours with activating anti-Fas antibody (250 ng/mL) prior to measuring caspase activity. Data are representative of three independent experiments with error bars indicating standard deviation. ($p<0.002$ at all time points between WT and SAP-null with Fas treatment. Lines at bottom of graph represent unstimulated SAP-null in green and WT in blue.) **B)** Cells were treated for 18 hours with anti-Fas antibody (250 ng/mL) prior to protein extraction and Western blotting using anti-SAP and anti-Caspase-3 antibodies.

The observation that Caspase-3 expression was elevated in *SAP*-deficient cells after Fas activation suggested that apoptosis might be higher in cells with *SAP* defects. To detect changes in cell viability upon Fas stimulation wild type and *SAP*-null cells were stimulated with activating anti-Fas antibody and viability was assessed by propidium iodide exclusion assay followed by flow cytometry. Indeed, *SAP*-deficient cells were less viable following Fas treatment as compared to wild type cells (figure 4.5A), suggesting that the *SAP*-null cells were more sensitive to Fas-mediated death. Although the results illustrated that the *SAP*-null cells have increased Caspase-3 activity (figure 4.4) and are less viable after Fas treatment (figure 4.5), it is possible that the observed decrease in viability was caspase-independent. T cell death independent of caspase activation or Cytochrome *c* release has previously been reported[231]. To confirm that the Fas-mediated sensitivity was caspase-dependent, cells were pre-treated with the pan-caspase inhibitor zVAD-fmk. Pre-treatment with zVAD-fmk blocked Fas-mediated cell death in the *SAP*-null cells (figure 4.5B), supporting the notion that the decreased viability in the *SAP*-deficient cells following Fas treatment resulted from a caspase-dependent mechanism.

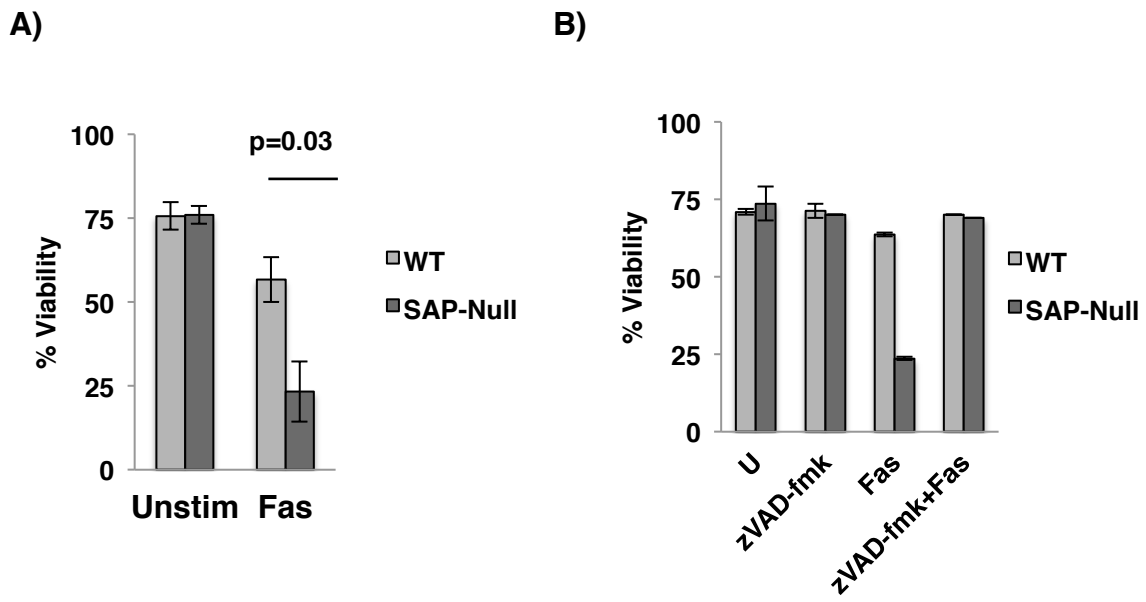

Figure 4.5 Fas-mediated cell death in *SAP*-null Jurkats. A) Cells were treated for 18 hours with activating anti-Fas (CD95) antibody (250 ng/mL) prior to measuring viability by PI exclusion and flow cytometry. Data represent the average of three independent experiments with error bars indicating standard deviation. **B)** Cells were pretreated for 1 hour with zVAD-fmk (10 μM) prior to the addition of activating anti-Fas and PI stain followed by flow cytometry, as described in A).

While these experiments demonstrated an increased sensitivity to Fas-mediated death, it was not yet proven to be a SAP-specific effect. In order to test that the increased sensitivity to Fas-mediated apoptosis was SAP-dependent, SAP expression was reconstituted in the *SAP*-null Jurkats using a FLAG-SAP plasmid, as discussed in chapter 3. The wild type, *SAP*-null, and SAP reconstituted cells were stimulated with activating anti-Fas antibodies, followed by viability assessment using propidium iodide exclusion and flow cytometry. While *SAP*-null cells exhibited increased sensitivity to Fas-mediated apoptosis, the SAP reconstituted cells did not (figure 4.6). Importantly, this viability was comparable to the viability observed in wild type cells, signifying a *SAP*-dependent effect.

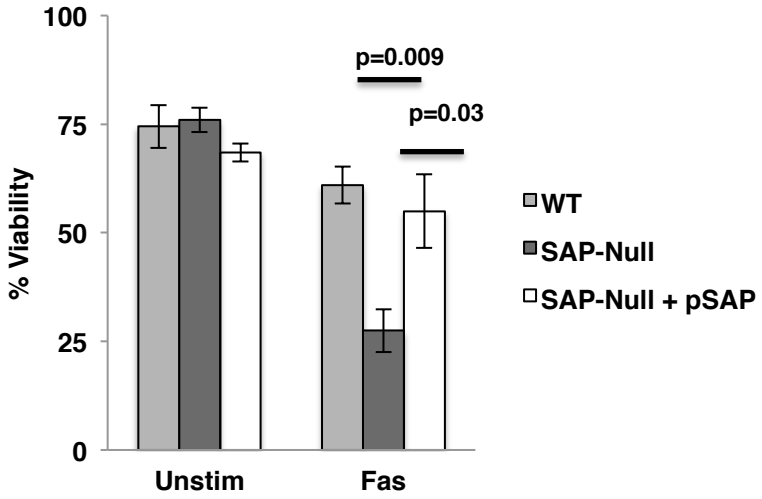

Figure 4.6 SAP reconstitution restores viability. Cells were treated for 18 hours with activating anti-Fas (CD95) antibody (250 ng/mL) prior to measuring viability by PI exclusion and flow cytometry. Data represent the average of two independent experiments with error bars indicating standard deviation.

To further test that the absence of SAP increased Caspase-3 activity, the wild type, *SAP*-null cells, and SAP reconstituted cells were stimulated with anti-Fas antibodies followed by analysis of Caspase-3 activity (figure 4.7A). The partial restoration of SAP expression resulted in decreased Caspase-3 activity following treatment compared to the *SAP*-null cells. Results indicated that the levels of Caspase-3 activity were between those of the wild type and SAP-deficient cells and this corresponds to the mixed population of SAP expressing and *SAP*-null cells in the partial rescue. There was no difference in the expression of full-length Caspase-3 between the cell types prior to stimulation (figure 4.7B) and these data suggest that the increased Capase-3 activity is a SAP-dependent effect.

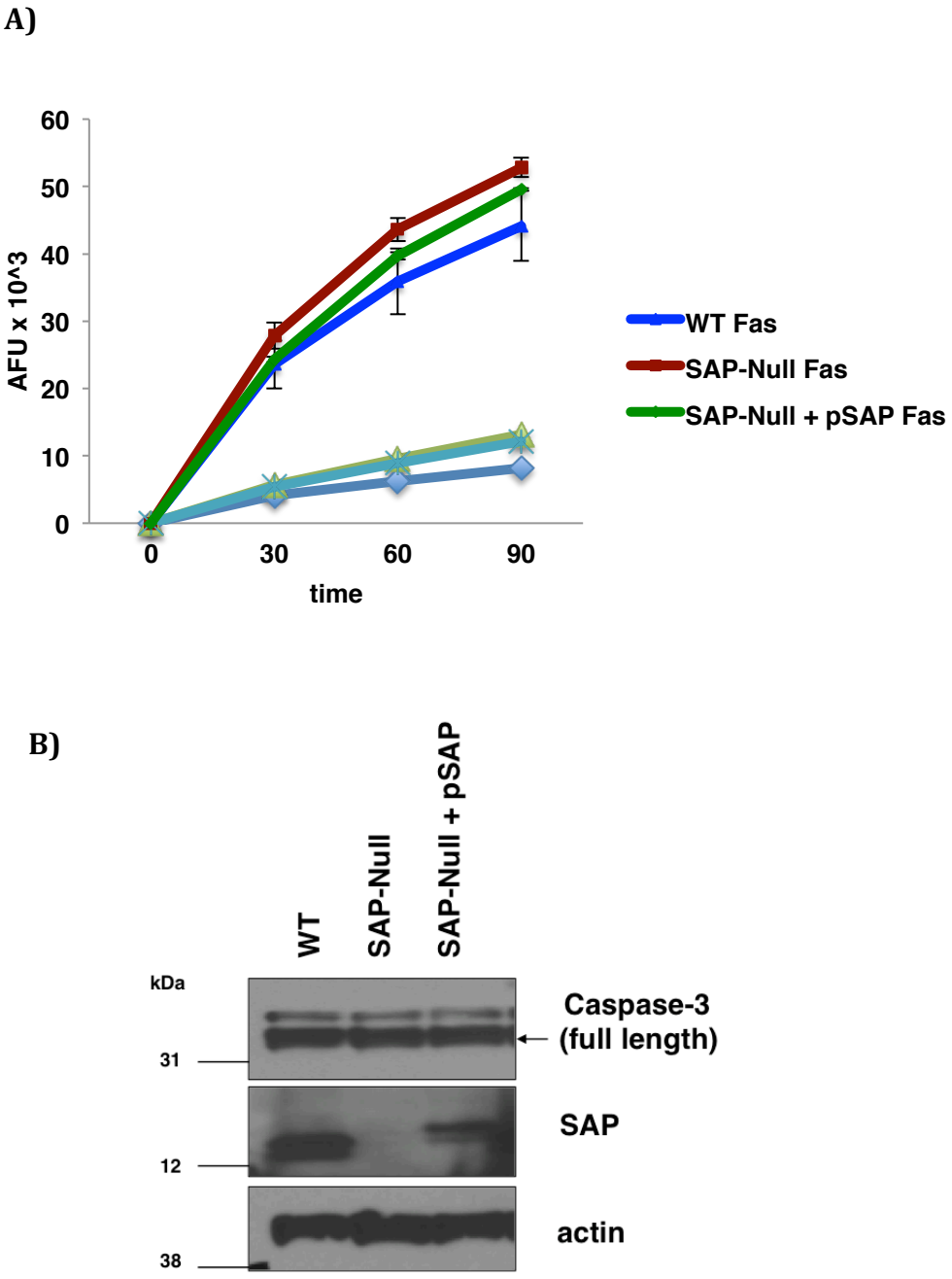

Figure 4.7 SAP reconstitution and Caspase-3. A) Cells were treated for 6 hours with activating anti-Fas antibody (250 ng/mL) prior to measuring caspase activity. ($p<0.04$ between WT and *SAP*-null with Fas treatment and between *SAP*-null cells and cells with SAP reconstitution.) **B)** Cells were analyzed by Western blot using anti-Caspase-3 (full-length) and anti-SAP antibodies.

To address the question of whether the observed increase in sensitivity to Fas-induced cell death in *SAP*-null cells was restricted to Fas-mediated death or a

more universal susceptibility to death stimuli, wild type and *SAP*-null cells were treated with various death inducing agents. Cells were incubated with the indicated concentrations of Fas, TNF and cycloheximide (CHX), or etoposide prior to measuring viability by PI exclusion and flow cytometry. TNF is a member of the TNF superfamily[232] that requires the addition of cycloheximide (CHX) to induce apoptosis[233], while etoposide is a topoisomerase II inhibitor that, as a consequence of inducing DNA damage, leads to the release of Cytochrome *c* from the mitochondria[234]. As shown in figure 4.8, the *SAP*-null cells exhibited increased sensitivity to Fas, TNF/CHX and etoposide treatment when compared to wild type cells, indicating that a deficiency in *SAP* confers a heightened, non-specific, sensitivity to cell death.

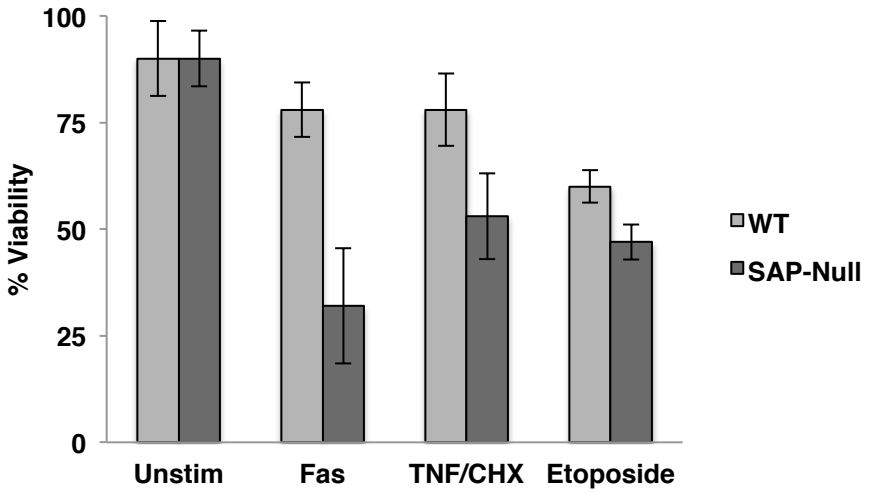

Figure 4.8 Increased sensitivity of *SAP*-null Jurkats to apoptotic stimuli. A) Cells were treated for 18 hours with activating anti-Fas (CD95) antibody (250 ng/mL), TNF (5 ng/mL) and cycloheximide (CHX) (2.5 ng/mL), or etoposide (20 μg/mL) prior to measuring viability by PI exclusion and flow cytometry. Data represent one of four independent experiments with error bars indicating standard deviation ($p<0.05$ for all treatment conditions).

4.3 Discussion

The analysis of SAP's role in T cell apoptosis demonstrated that *SAP* deficient Jurkat cells were more sensitive to apoptotic stimuli, as measured by cell viability and analysis of Caspase-3 activity. Initial results demonstrated that Fas stimulation in Jurkat cells with reduced XIAP and SAP expression led to increased Caspase-3 activity. These results were further supported by analyzing Caspase-3 activity and cleaved Caspase-3 levels, both of which were elevated in the *SAP*-null Jurkats compared to the wild type following Fas stimulation. Similarly, the *SAP*-null cells have heightened sensitivity to Fas-mediated apoptosis as shown by viability, and this cell death was caspase-dependent, demonstrated by the addition of a pan-caspase inhibitor. Restoration of SAP expression in the *SAP*-deficient cells rescued viability and provided resistance to Fas-mediated cell death.

The restoration of SAP expression in the *SAP*-null Jurkat cells decreased the activity of Caspase-3 following Fas stimulation (figure 4.7), but not to the level of the wild type. This could be explained by the partial rescue of SAP expression and that the population contains a mixture of cells with ectopic SAP expression and the *SAP*-null cells (figure 3.7). To determine which cells are responsible for the decrease in Caspase-3 activity, the bulk population would be stimulated with Fas followed by intracellular staining and flow cytometry analysis for SAP and Caspase-3 expression. This double staining approach would determine whether the SAP expressing cells are responsible for the decrease in Caspase-3 activity observed during the rescue experiment.

The increased sensitivity to other apoptotic stimuli observed in the *SAP*-deficient cells suggests a novel role of SAP in $CD4^+$ T cells. Sensitivity to apoptotic stimuli is a concern to maintain the proper balance of immune cells to respond to infections. A generalized sensitivity to apoptosis suggests involvement of the mitochondrial organelles. The elevated production of IFN-γ observed in the SAP-null cells (chapter 3) is a potential contributor to apoptosis as previous work has shown that overexpression of IFN-γ increased destabilization of the mitochondria by increased Bax levels[235] and, in stem cells, increased Caspase-3 mediated apoptosis[236]. While measuring Caspase-3 activity is an indicator of apoptosis, it does not specifically address changes in mitochondrial membrane potential. To address this, experiments were performed to assess the outer mitochondrial membrane potential and these results indicated that the membrane potential in the *SAP*-null Jurkat cells was lower than the wild type prior to Fas stimulation, but this difference was not observed following Fas treatment (data not shown). It was possible that unstimulated *SAP*-deficient cells had fewer mitochondria, accounting for the decreased mitochondrial membrane potential. However, subsequent analysis of the mitochondrial mass indicated that there was no difference in the total number of mitochondria among the cell types (Chang and Kim 2015, data not shown). These data suggest that the apoptotic sensitivity is not due to inherent mitochondrial defects due to *SAP*-deficiencies, but rather result from defects within the signaling cascades. Alternatively, it is possible that elevated calcium levels induce apoptosis[237] as high levels of calcium ions can disrupt the outer mitochondrial membrane potential to affect the release of Cytochrome *c* [238]. Selectively inhibiting

calcium mobilization followed by death receptor stimulation may indicate whether calcium mobilization is dispensable for *SAP*-mediated apoptotic sensitivity.

Suppression of *SAP* or *XIAP* demonstrated increased Caspase-3 activity upon Fas stimulation (figure 4.3). Considering that XLP results from mutations in either *SAP* or *XIAP*, two genes with no structural similarities, this suggests that these genes share a commonly deregulated pathway. While further studies are needed to fully appreciate this relationship, it is possible that the shared apoptotic sensitivity is responsible for the overlapping HLH phenotype.

Since the primary clinical presentation of XLP1 patients is often associated with infections, the relationship between SAP expression and response to various infections has been explored. More specifically, SAP expression in human $CD4^+$ T cells inversely correlated to IFN-γ levels after tuberculosis infection, again suggested that the presence of SAP disrupts IFN-γ production[199]. Although not directly tested by infecting the *SAP*-null Jurkat cells, an interesting study[190] monitored two brothers diagnosed with XLP1 for two years, and one brother had an acute EBV infection during the study while the other had previous exposure to the virus. Both brothers exhibited elevated IFN-γ levels throughout the study and not only did their $CD4^+$ T cells favor a Th1 phenotype but they had reduced numbers of $CD4^+$ T cells throughout the study[190], compared to EBV infected cells with normal SAP expression. Combining the observations in the *SAP*-null Jurkats with evidence in the literature, it is possible that *SAP* defects predispose $CD4^+$ cells to apoptosis and that the remaining T cells exhibit increased IFN-γ production.

Enhanced sensitivity to apoptosis is an intriguing observation, and clinical evidence has been shown in XLP1 patients. For example, a case report[239] quantifying lymphocytes of an EBV$^+$ infected XLP1 patient demonstrated a reduction of the total percentage of CD4$^+$ T cells compared to the SAP expressing EBV infected ranges[239]. These findings could also be explained by the increased sensitivity to cell death observed in the *SAP*-null cells (figure 4.5), suggesting that either fewer CD4$^+$ cells are produced or the cells are more sensitive to apoptosis, which may lead to fewer measurable cells.

The question was raised if the *SAP*-null cells were producing factors that influence cell viability that differ from *SAP*-expressing cells. To address this, conditioned media was prepared from the *SAP*-null and wild type Jurkat cells and was placed on the wild type Jurkat cells followed by measurement of cell viability (data not shown). This experiment showed that exposure to conditioned media from the *SAP*-null cells decreased the viability of the wild type cells, compared to cells exposed to the wild type conditioned media. This suggested that factors are being released by the *SAP*-deficient cells that affect cell viability. Future experiments using mass spectrometry could analyze the conditioned media to identify these death sensitizing factors.

Immune cells with increased sensitivity to death can have impaired abilities to respond to infection. Although EBV primarily infects B cells, CD4$^+$ T cells influence the control of the infected cells[240]. The *in vivo* presence of CD4$^+$ T cells during early EBV infection has been shown to decrease the appearance of rapidly proliferating transformed B cells that express CD23$^+$ on their surface[241]. In cultures depleted of

CD4+ T cells there was a marked increased in the presence of CD23+ B cells[242]. This suggests that CD4+ cells modulates the proliferation of EBV-infected B cells and when they are absent or in decreased quantities this contributes to B cell lymphoproliferation. This supports the hypothesis that *SAP*-deficient CD4+ T cells are more sensitive to apoptotic stimuli, particularly after an infection, and therefore fewer Th cells are able to provide support to B cells. Moreover, *in vitro* studies of XLP1 patient T cells have shown that *SAP*-deficient cells fail to induce B cells to efficiently produce antibodies[243], implying a decrease in the ability of B cells to clear EBV infection.

Interestingly, EBV infection itself has been shown to result in a decrease in *SAP* transcription presumably through a NF-κB dependent mechanism in cells with normal SAP expression[244], suggesting that EBV infection may decrease T cell signals by modulating SAP levels. This raises the question as to whether EBV infection would affect *SAP* expression and thus impair cytokine production and augment cell death. To assess the influence of EBV on *SAP* expression in T cells, the Jurkat cells can be transfected with the EBV-associated latent membrane protein 1 (LMP1)[245,246] followed by measurement of SAP expression and cytokine production following TCR stimulation. Also, it would be clinically relevant to determine whether EBV infections in XLP1 patients lead to a decreased total number of CD4+ T cells or if the *SAP* defects impair T cell signaling resulting in a decreased ability to kill infected cells. This may add insights as to EBV-dependent modulation of SAP expression and result in increased monitoring of CD4+ T cells in the clinic due to their sensitivity to cell death. Together, these studies reinforce the idea that *SAP* influences the

presence of $CD4^+$ T cells, as demonstrated in the reduction in viable *SAP*-null Jurkat cells following stimuli, and in patients following infection. These findings also underscore the importance of $CD4^+$ T cells in controlling the proliferation of EBV infected B cells.

4.4 Materials & Methods

Media. Jurkat cells were cultured in RPMI 1640 (Corning 15-041-CV) supplemented with 1% GlutaMax (Gibco 35050-061) and 10% FBS (Atlas) with incubation conditions at 37° and 5% CO_2.

Transfection of Jurkat Cells. Jurkat cells were electroporated using a BioRad Gene Pulser II (250 V and 975 μF) using 0.4 cm gap cuvettes (BioRad 1652088). 10^7 cells were transfected with 20 nM of each siRNA targeting *SAP, XIAP* or *GFP* control. For *SAP* reconstitution experiments, 10^7 *SAP*-null Jurkat cells were transfected with 10 μg of pEBB-SAP-FLAG and 1 μg of pBABE-puro selection plasmid. Forty-eight hours after transfection cells were maintained in 0.5 μg/mL of puromycin containing selection media.

Whole cell lysate preparation. Cells were harvested by centrifugation at 300 rpm for 5 minutes and resuspended in 100 μL of prepared radioimmunoprecipitation assay (RIPA) lysis solution per 10^6 cells. RIPA buffer consists of PBS containing 1% NP-40, 0.5% sodium-deoxycholate, and 0.1% sodium dodecyl sulfate (SDS). To prepare lysis solution, 10 mL of RIPA buffer was supplemented with 1 protease

inhibitor tablet (cOmplete Mini EDTA-free Roche 11836170001), 100 µL Na_3VO_4 (BioLab P0758S 100 mM), 10 µL of 1mM DTT, and 20 µL NaF (BioLab P0759S 500 mM). Cell lysates were incubated on ice for 10 minutes followed by a 10 minute centrifugation at 13000 rpm at 4°. Supernatants were stored at -80°.

Western blotting. Protein concentration was determined by using Pierce BCA kit against a known standard. Cytoplasmic extracts (25 µg) were prepared in LDS sample buffer (Invitrogen) and loaded on a 4-12% NuPage gel in a 1:20 MES running buffer. Following transfer, nitrocellulose membranes were blocked in 5% milk with TBS 0.1% Tween, followed by overnight incubation at 4° with the appropriate antibody. After washing, membranes were incubated with horseradish peroxidase-conjugated antibody for 1 hour at room temperature followed by visualization on chemiluminescence film. The following antibodies were used for Western blotting: rat anti-SAP (Cell Signaling #2805); goat-anti rat IgG-HRP (Santa Cruz-2006); mouse anti-FLAG M2 (Sigma 088K6018); anti-mouse IgG-HRP (Cell Signaling #7076S); HRP-conjugated actin (Abcam 20272); anti-rabbit full length Caspase-3 (Cell Signaling 9665); anti-rabbit cleaved Caspase-3 (Cell Signaling 9661); and mouse anti-XIAP (BD 610717).

Caspase-3 assay. Cells were synchronized on the day prior to the experiment by centrifugation and resuspension in fresh media. 2x10^5 cells per condition were unstimulated or stimulated with 250 ng/mL of activating anti-Fas (CD95 CH11 clone) for six hours with incubation at 37°. Cells were collected by centrifugation at

3000 rpm for 5 minutes and 50 µL of Biosource Caspase Assay Kit cell lysis buffer (BY01) was added, followed by a brief vortex and incubated on ice for 10 minutes. A 2X reaction buffer consisting of 800 µL of the BY01 buffer, 8 µL of 1M DTT, and 4 µL of DEVD-AFC was prepared. Fifty microliters of the reaction buffer was added to each well on a Costar 96-well black-sided clear bottom plate followed by 50 µL of the cell in lysis buffer. Assay was measured on a BioTek plate reader using an AutoAdjust Gain fluorescence program with bottom read set for excitation at 400 nm and emission at 505 nm. A kinetics program read every 5 minutes for the indicated time frames. Data was graphed using average fluorescence units.

Viability assay. Cells were untreated or incubated in the presence of 250 ng/mL. of activating anti-Fas (CD95 Clone CH11 Millipore 05-201) for 18 hours at 37°. Where indicated, cells were treated with z-VAD-fmk (Cayman 14463) at specified concentrations. Cells were harvested by centrifugation and resuspended in PBS plus 1% bovine serum albumin. Propidium iodide (PI), 2 µg/mL, was added just prior to analysis by flow cytometry using Accuri C6 machine at 500,000 threshold for 10,000 events.

Chapter 5 Discussion

5.1 Introduction

Although XLP is a disease that was first described in young males in the mid-1970s[27], there remain unknown aspects of how the disease develops into a spectrum of hematological deficiencies. Several previous studies have addressed the role of *SAP* in the disease using patient derived material, mouse models, or cell-based studies. However, there are many unanswered questions as to how *SAP*-defects impair T cell activation. There were several ways to address this question. Ideally, patient derived T cells would have provided an optimal way to examine signaling defects. However, the patient population is small and access to the materials extremely limits this approach. Several studies have used *Sap*-deficient mouse models to provide valuable insights into T cell differentiation and signaling defects. This approach has limitations in that mice have genetic differences from humans and, importantly, cannot be infected by EBV. Previous studies have used established cell lines to identify *SAP*-dependent effects using RNAi to disrupt SAP expression and elucidate signaling defects and protein interactions. However, this also has limitations by the transient nature of the *SAP* disruption and the incomplete effects of silencing the gene. The utilization of a TALEN-based gene editing approach presented the opportunity to create a *SAP*-null Jurkat cell line with a total disruption

of SAP expression and allowed the comparative analysis of the *SAP*-dependent effects on T cell signaling.

The work presented in this dissertation exclusively examined signaling in the Jurkat T leukemia line. Jurkat cells have been extensively used to characterize T cell signaling[247], but all established cell lines have limitations, so it is important to bear this in mind when interpreting observations. Jurkat cells have defects in the lipid phosphatases PTEN (phosphatase tensin homolog) and SHIP-1 (SH2-domain-containing inositol phosphatase)[248]. PTEN defects contribute to these cells being in a partially activated state, which may affect the basal activity of target genes that would not be observed in a naïve T cell. When SHIP-1 is bound to the SLAM receptor this inhibits T cell activation[249] and it is possible that the absence of this inhibitor abnormally activates Jurkat cells. However, Jurkat cells have been very useful to characterize T cell signaling in the past and provided a mechanism to assess the *SAP*-dependent signaling defects following TCR stimulation[107].

To more fully understand how SAP influences T cell signaling, future studies should be performed in primary T cells or patient derived material. However, Jurkat cells are useful for hypothesis generation and the identification of cellular characteristics that differ based on the presence or absence of SAP. As described in chapter 2, we used a TALEN-based gene editing approach to edit the *SAP* gene and eliminate SAP expression. These SAP-null Jurkat cells were used to interrogate T cell signaling alterations in cytokine production, transcription factor activity, and calcium mobilization, illustrated in chapter 3. In chapter 4 the sensitivity to death stimuli was examined in the *SAP*-null Jurkat cells, which further identified a *SAP*-

dependent increase in sensitivity to apoptosis. Together, our results signify specific *SAP*-dependent defects in T cell signaling, in Jurkat cells, which uncovered contributing factors to immune deregulation that apply to XLP1 patients. It is thought provoking to discuss how SAP regulates immune cell signaling in the context of the development of cancer. Further exploration of immune surveillance of pre-neoplastic cells in primary cells or other transformed cell lines would add powerful reinforcement to the findings within this dissertation and how they relate to the development of XLP.

5.2 Remaining questions regarding SAP-dependent effects on immune surveillance

Does SAP participate in T cell activation in the apparent absence of signaling by the SLAM family of co-receptors?

The observation that NFAT activity and IL-2 production was impaired in the *SAP*-null Jurkat cells following TCR stimulation was surprising. If SAP simply interacts with the SLAM receptor family and provides co-stimulation, the addition of CD3 and CD28 would have bypassed SAP defects and not altered the production of IL-2, as shown in figure 1.4.

The observed decreased in IL-2 production and transcription factor activity suggests that SAP is modulating other components of T cells signaling that are required during T cell activation that are independent of CD3/CD28 stimulation. One explanation is that SAP has SLAM independent roles by uncharacterized interactions with other PTKs within the signaling cascades, such as potential direct

engagement with ZAP-70 or LCK (figure 1.3). Alternately, the SLAM family of receptors are self-ligands, and direct cell-to-cell contact by immune cells may provide a background level of T cell stimulation in the absence of TCR activation through CD3. In this case, SLAM on the surface of Jurkat cells may be responding to interaction with other Jurkat cells leading to a basal level of SLAM activity. This may be an artifact of the cell model and would require further examination in patient derived material or primary T cells.

Another potential explanation for impaired T cell activation in cells with *SAP* defects is that SAP modulates the activity of other proteins with characterized roles in immune cells activation and development. Following TCR stimulation, integrin mediated actin mobilization leads to cytoskeletal shifts at the immune synapse[18]. The nucleotide exchange factor VAV-1 activates the Rho family GTPases that regulate the cytoskeletal reorganization following TCR stimulation[250]. During reorganization, PKC-θ moves to the lipid raft where it can activate NF-κB[251]. When VAV-1 is defective, this decreases NF-κB activation by impairing the recruitment of PKC-θ[252]. Notably, impaired NF-κB activation has been shown in *Sap*-deficient mice[111] and SAP has been shown to regulate VAV-1 activity in NK cells, in a FYN dependent manner[253]. Therefore, *SAP*-deficiencies may modulate VAV-1 activity and decrease the recruitment of PKC-θ leading to impaired NF-κB activation.

Studies engineering VAV-1 defects in Jurkat cells demonstrated that VAV-1 is required for NFAT activity and IL-2 production[254,255], both of which were deficient in the *SAP*-null Jurkats. VAV-1 deficient Jurkat cells exhibited elevated calcium influx, potentially due to opening of the calcium channels during TCR stimulation[256].

Although not directly tested, it is possible that the *SAP*-null Jurkat cells have VAV-1 impairments that are responsible for the observed cytokine, transcription factor, and calcium defects. This could explain the role of SAP in T cell activation that is independent of CD3/CD28 stimulation in both SLAM-dependent and –independent mechanisms. Additionally, the activity of the MAPK pathway was outside the scope of this study and defects in AP-1 formation cannot be excluded as contributing to the impaired defects observed in the *SAP*-null Jurkat cells.

Is XLP-1 associated lymphoma due to impaired immune surveillance?

Pre-cancerous cells develop characteristics that, when grown in absence of immune surveillance, can develop neoplastic phenotypes. Transformed cells activate intracellular signaling through tyrosine kinase domains and these activated cells avoid apoptosis. It is challenging to determine if growth signals are transmitted by autonomous signals within the cancer cell or from neighboring cells in a paracrine manner. Mutations in PTEN[257], which lead to the constitutive activation of PI3K are observed in several cancers[258]. Cancer cells also avoid apoptotic signaling by impairing extrinsic signaling through the modification of death receptors (i.e., Fas) or through intrinsic programs, which normally affect the mitochondrial membrane. One of the most commonly mutated gene is in the DNA damage sensor p53[259]. A subset of mutations in p53 are unable to up-regulate the BH3-containing proteins that inhibit the Bcl-2 family members[260,261]. The balancing of Bcl-2 (anti-apoptotic family) with pro-apoptotic signaling, such as Bax and Bak, regulate the overall apoptotic threshold[260]. However, since the *SAP*-null cells are more sensitive

to apoptosis, it is likely that the pre-cancerous non-SAP expressing B cells are the ones that must obtain additional capabilities to allow them to evade cell death. While it is likely that the cancer cells in XLP1-associated lymphoma also have developed the ability to evade apoptosis, the inherent *SAP*-dependent defects in T cell signaling could impair the surveillance abilities of immune cells themselves and these malfunctioning cells support conditions for pre-cancerous outgrowth. In this case, patients with XLP initiate the development of cancer due to malfunctioning immune cells rather than genetically predisposing B cells to neoplasia.

SAP-deficiencies increase the levels of IFN-γ production (figure 3.3) and this may contribute to an environment with persistent inflammation that is conducive to metastasis. Elevated IFN-γ production is thought to increase the relative numbers of macrophages and these cells secrete metalloproteinases that degrade the cellular matrix[262]. This facilitates invasion into the surrounding tissue and dissemination to distant sites, another characteristic in the formation of cancer. However, prior to invasion and metastasis, the pre-cancerous cell must actively evade immune surveillance.

It is not well understood how cancer cells evade a fully functional immune system and several studies have addressed how a pre-malignant cell avoids immune surveillance in immune deficiencies. The majority of viral-induced cancers are within immunocompromised individuals[65] and this suggests that mechanisms that control viral infection must become deregulated in order for cancer to develop or that persistent infection can lead to cancer development. Alternately, defective immune cells can become activated but they are ineffective at killing.

Histopathological examination of tumors have demonstrated that immune cells are present[66] yet they are ineffective at preventing tumor formation. XLP1 patients with EBV infection have been shown to have increased percentage and absolute quantities of CD8+ T cells and whether these cells are defective at killing target cells or whether the lack of SAP disturbs the ratios of CD4+ T cells available to assist B cell surveillance is unknown[239]. However, several murine studies have revealed an increased tumor burden when the $CD8^+$, $CD4^+$, or natural killer cells are perturbed[70,71].

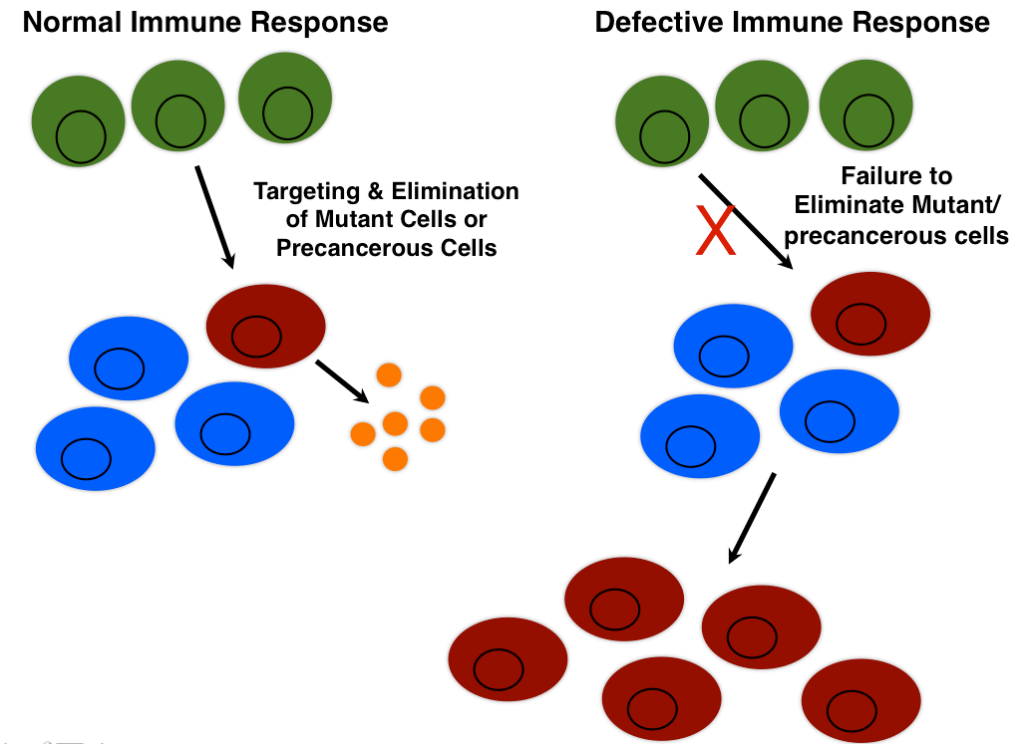

Figure 5.1 Immune surveillance defects contribute to cancer. It is possible that XLP-1 associated lymphoma results from a combination of events that allow the pre-cancerous non-SAP expressing B cell to avoid immune surveillance and the inability of SAP-deficient immune cells to detect or kill mutant cells.

Innate immune cells in particular are thought to secrete tumor promoting growth factors and activation inducing signals[67,68] or secrete reactive oxygen species that promote genetic mutations[69]. As previously discussed (chapter 1), tumor cells can secrete the pleiotropic transforming growth factor-β (TGF-β)[263], which can lead to abnormally high quantities of T_{reg} cells[264,265] limiting the expansion of CD4 and CD8 cells[265] and disrupt CTL activity by impairing perforin production[266,267]. Together, expression of TGF-β is another mechanism that cells can avoid immune surveillance as well as modulates the quantity, type, and functional capabilities of immune cells in the vicinity of the tumor.

Evidence presented in the *SAP*-null cells suggests that SAP defects contribute to defective immune responses (figure 5.1). Jurkat cells are a representative $CD4^+$ T cell lineage which, when *SAP* is defective, exhibit impaired cytokine production, transcription factor activity, and apoptotic sensitivity. The possibility exists that there are fewer total $CD4^+$cells compared to $CD8^+$ and NK cells. The impact of fewer $CD4^+$ T cells would be decreased Th1 cell production and a relative increase in the presence of CTLs. Elevated proportions of CTLs could be recruited to the virally infected T cells, generating the release of cytokines that promote the production of tumor growth factors (ie., EGF and VEGF) and matrix degrading enzymes[68], but the CTLs are unable to kill the infected immune cells. Thus, it is plausible that XLP1-associated lymphoma arises by impaired surveillance of EBV-infected B cells and the recruitment of CTLs that are ineffective at killing target promoting a tumor permissive environment. Together, data presented in this dissertation suggest that lack of SAP contributes to decreased activation of $CD4^+$ T cells through impaired

activation of NFAT. These T cells are more sensitive to cell death and are potentially unable to response to antigen. This contributes to persistent infection and a continually inflamed microenvironment that is conducive to the formation of cancer.

Three potential influences of SAP during the immune response can be envisioned, as illustrated in figure 5.2. In cells with normal SAP expression, pathogens stimulate the proliferation of immune cells (i.e., T and NK cells) followed by apoptosis of the target cell. First, the immune cells could be initially activated in response to the pathogen but they prematurely die due to increased sensitivity to apoptotic stimuli. The *SAP*-null Jurkat cells have increased sensitivity to cell death compared to the wild type cells and following exposure to pathogens activated T cells could be viable for a shorter time and unable to clear the infection resulting in persistent inflammation. Second, it is possible that *SAP*-deficient immune cells are not activated to affect killing of target cells. The lack of IL-2 production observed in the *SAP*-null cells suggests that there would be reduced proliferation of T cells and fewer immune cells would be available. Third, key immune cells may never be present within the organism due to SAP defects. Immune cells that do not develop cannot respond to antigen and this is best illustrated in XLP1 patients' inability to develop NKT cells[34]. Taken together, the role of SAP in the clearance of virally infected cells and how this contributes to the development of lymphoma is an area to further explore.

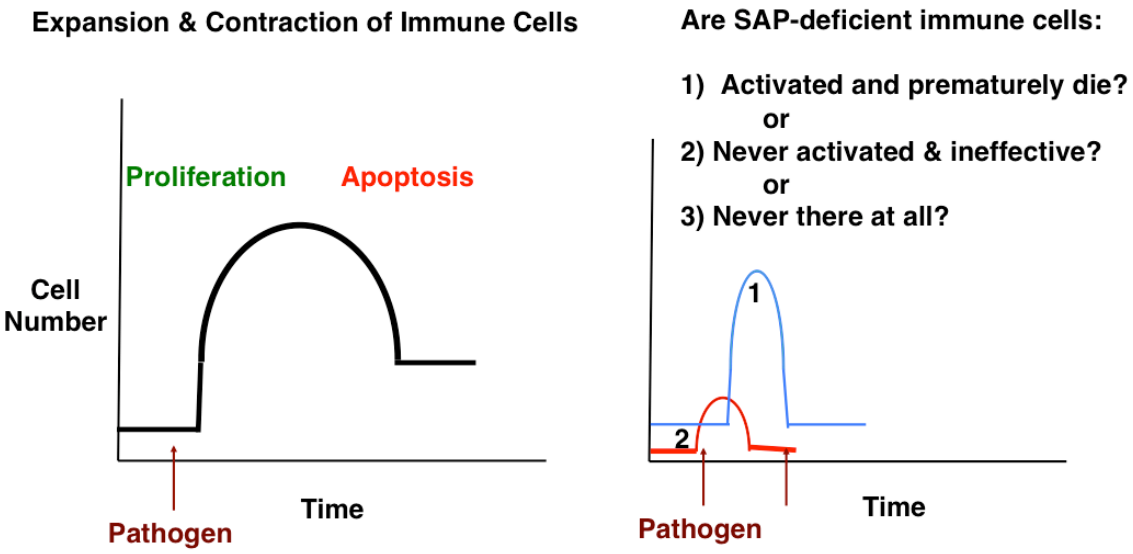

Figure 5.2 Proposed influence of SAP defects on immune cells. Immune cells proliferate in response to pathogens and this expansion is followed by death of the expanded immune cells to maintain immune homeostasis. Three potential defects, listed above, result from SAP defects and this could contribute to the abnormal numbers of immune cells and ineffective response to antigens leading to persistent inflammation.

Why do XLP2 patients not develop lymphoma?

XLP2 is caused by mutations in XIAP and results in similar clinical presentations to XLP1[28,41]. However, it remains unclear why *XIAP*-deficient patients do not develop lymphoma. XIAP expression is elevated in many types of cancers, including B cell lymphoma[268]. Tumors that upregulate the expression of XIAP[269] promote cell survival by inhibiting caspase activation. However, XIAP has an ascribed function[270] in the upregulation of cyclin D1 expression by the E3 ligase within the RING domain. One explanation of why XLP2 patients do not develop lymphoma could be that XIAP defects impair the expression of cyclin D1 and B cells are unable to proceed in the cell cycle and extensively proliferate. Whether the

absence of lymphoma in *XLP2* patients is due to increased death of B cells or impaired cell cycling remains to be determined. The observation of increased sensitivity to Fas mediated apoptosis in Jurkat cells with reduced XIAP expression (figure 4.3) supports that T cells are more sensitive to death and further studies are required to determine if this is also the case in B cells.

The examination of XIAP's role in T cell activation has not been explored in-depth. It is possible that XIAP, with ubiquitous expression, does not play a role in T cell signaling and immune cells from XIAP patients are competent to detect virally infected cells during immune surveillance and this prevents pre-neoplastic cells from accumulating. *Xiap*-deficient mice are able to form germinal centers while *Sap*-deficient mice cannot[6] and this suggests that XLP2 patients would be able to appropriately respond to EBV infection, which is not the case[28]. Further studies directly comparing the effects of TCR stimulation in a *XIAP*-null Jurkat cell would clarify whether defects in TCR activation are SAP specific or whether there are shared functional roles between XIAP and SAP.

EBV induces B-cell lymphoproliferation and the development of lymphoma in immunocompromised individuals[242]. Nikiforow, *et al* (2001) demonstrated that while $CD8^+$ T cells kill EBV infected cells, it is the $CD4^+$ T cells that limit the expansion of EBV-infected B cells and prevent their lymphoproliferation. While the mechanism is unclear, this is particularly relevant to the findings within this dissertation as the *SAP*-null cells have fewer proliferative (IL-2) cytokines and the $CD4^+$ cells are more sensitive to apoptosis. These potentially short-lived $CD4^+$ T cells with SAP defects are unable to control the proliferation of EBV-infected B cells.

Coupled with ineffective killing by CTLs, this could explain why XLP1 patients progress to lymphoma through a combination of early events of $CD4^+$ T cell surveillance and ineffective killing of B cells following infection. This could also explain why XLP2 patients do not present with lymphoma as there is no evidence to support that their T cell compartment is altered. However, the preliminary data demonstrating that decreased XIAP expression also increased apoptotic sensitivity in Jurkat cells requires further analysis to explore whether there are compensatory mechanisms for control of EBV infection due to the presence of functional SAP in their T cell populations.

Is apoptosis the shared pathway in XLP1 & XLP2 that contributes to HLH development?

SAP and XIAP appear to have similar cytoprotective properties in Jurkat cells. Results indicated that cells with either suppression of *SAP* or *XIAP* demonstrated increased Caspase-3 activity upon Fas stimulation (figure 4.3). XLP1 and XLP2 patients both develop HLH and it is possible that the increased apoptotic sensitivity observed in T cells contributes to this phenotype. As previously discussed (chapter 1) familial HLH patients have defects in CTL or NK cell killing of virally infected cells due to defects in genes related to the movement or release of cytotoxic granules. SAP defects are associated with defective cytotoxic activity of NK cells but it is unclear why XIAP patients develop HLH. It is plausible that XIAP defects increase the sensitivity of immune cells to undergo apoptosis and, in a manner similar to SAP

defects, result in fewer or short-lived CLTs or NK cells available to kill virally infected target cells.

Considering that XLP results from mutations in either of two genes, with no structural similarities, yet co-located at the same Xq25 locus, this suggests that these genes share a commonly deregulated pathway. This is an area that has not been explored, particularly in a comparative nature. Thus, two apparently functionally unrelated genes may contribute to the shared phenotype by deregulating the process of apoptosis.

5.3 Potential XLP1 therapy using engineered T cells

Within the XLP patient population, it is particularly challenging to find a matched donor for a curative bone marrow transplant and there are few treatment options available. There are several emergent techniques to encourage immune surveillance and the clearance of both infected or pre-neoplastic cells. For example, the use of chimeric antigen receptor T cells (CAR Ts)[271–273] in immunotherapy presents the opportunity to modify patient T cells with receptors that can recognize and target specific cells that would otherwise evade immune surveillance. An added benefit is the use of patient derived material to minimize rejection. CAR Ts contain the variable domains of the TCR[271–273] fused with T cell activation domains[272,273] and recognize, in the case of a B cell targeting CAR T, the CD19 receptor expressed by mature B cells[274]. Notably, this recognition is independent of the T cell receptor and does not require MHC presentation or recognition of a specific peptide by the T cell but, rather recognizes proteins expressed on the surface of B cells[275]. This is particularly important when using CAR Ts on patients that have acquired the ability

to downregulate MHC class I expression to escape T cell-mediated immune surveillance[58]. Low MHC-I expression levels rely on NK cells to target virally infected cells while high MHC-I expression supports recognition by TCR containing CTLs[59]. Should the patient's tumor cells have decreased MHC-I expression, the CAR Ts would be able to recognize the aberrant B cells and kill the target.

CAR T cells have shown promise in children and adults in promoting clinical remission and survivability[276], suggesting that CAR T cells could replace BMTs or offer a viable alternative to transplantation when a donor is unavailable. Specifically, the use of CAR T cells in B-cell lymphoma showed that 22/27 patients entered remission and half of these patients remained disease free during three years of follow-up[277]. Modulating the numbers of CAR T cells and using them in conjunction with chemotherapy seem to be effective against B cell lymphomas[278], but the therapy is not without risk.

Mortality has been documented[279] during CAR T therapy due to excessive cytokine production, particularly IFN-γ and TNF[279]. This is of particular concern in the context of increased IFN-γ production observed in the *SAP*-deficient Jurkat cells. XLP1 patients develop HLH during cytokine storms[39] and since this is a potential side effect of CAR T therapy, this raises questions as to its suitability for use in XLP patients. It is possible that CD19 CAR T cell treatment in XLP-associated lymphoma patients would exhibit further increased IFN-γ production and patients would require close monitoring and potential intervention with neutralizing IFN-γ antibodies. To combat the potential cytokine storm during CAR T therapy, it would be necessary to reintroduce SAP expression at the same time modifications are

made to the patient T cells. This could be done by several gene editing techniques, such as TALENs or CRISPR/Cas9. In theory, XLP1 patient CAR T cells with the reconstitution of SAP expression would not only correct the patient mutation but also target the aberrant B cell proliferation.

Particularly relevant to XLP1 patients, CAR T cells for EBV+ malignancies have been tested[280,281] as the CAR T cells recognize CD19 B cells with EBV peptides on their surface[282,283]. Again, without the restoration of SAP expression, these CAR T cells would be potentially ineffective at killing EBV infected B cells due to *SAP* dependent cytotoxic defects. However, tailoring a CAR T cell to recognize only EBV infected B cells would, in theory, have minimal effects on uninfected B cells and avoid the continual targeting of the entire B cell compartment. Targeting all B cells could result in decreased antibody production or hypogammaglobulinemia[284], a clinical characteristic observed in a portion of XLP patients. However, it is feasible to consider using modified CAR T cells in patients with XLP1-associated lymphomas to improve survivability.

5.4 Future studies using patient-derived T cells

Patient-derived T cells would be the ideal system to further analyze the *SAP*-dependent influences on T cell signaling. Initial experiments would focus on the apoptotic sensitivity as well as confirm the findings regarding cytokine defects and NFAT impairments discovered in the *SAP*-null cells using the developed intracellular staining and flow cytometry protocol (chapter 3) compared to donor T cells. Concurrently, the examination of Caspase expression in response to intrinsic and

extrinsic apoptotic stimuli would identify whether the results are reproducible in primary cells or whether these findings are specific to the *SAP*-null Jurkat cell.

There are several additional options to examine the *SAP*-dependent modulation of apoptosis. One mechanism malignant cells use to evade apoptosis is by upregulating the expression of the anti-apoptotic protein c-FLIP[285] (cellular FADD-like IL-1β-converting enzyme inhibitory protein). Stimulation of primary T cells normally increases c-FLIP expression, which blocks Caspase-8 activation during Fas mediated apoptosis[222]. Although this concept has not been explored in the context of *SAP* deficiencies, it is possible that c-FLIP expression is inhibited, though unknown interactions, and this increases the sensitivity to apoptosis compared to the wild type. Moreover, mice with Caspase-8 impairments having low responses to viral infections[16] and impaired T cell activation[16] characterized by decreased IL-2 production in response to CD3 stimulation[286,287]. It is unknown whether *SAP* defects influence Caspase-8 expression or activation, by modulating c-FLIP, but it is possible based on the characteristics observed in the *SAP*-null cells.

Activation induced cell death (AICD), a negative regulator of T cell activation, is another area of interest relevant to *SAP*-deficiencies. Activated T cells increase the transcription and export of Fas ligand (FasL) which can then kill the cell producing FasL or other immune cells within the vicinity that express the Fas receptor[288,289]. Studies introducing overexpression of SAP into B-LCL lines using retroviral delivery illustrated that the presence of SAP increased the number of dead cells following exposure to DNA damage inducing radiation while the wild type, non-SAP expressing cells, were more resistant to cell death[290]. Although radiation was not

specifically tested in the *SAP*-null Jurkat cells, the introduction of DNA damaging etoposide resulted in increased cell death compared to the wild type. This contrast in finding could be attributed to the overexpression of SAP inducing an effect that is not normally observed in the B cell lineage. Alternatively, this could mean that the apoptotic sensitivity is restricted to the $CD4^+$ Jurkat cells. Preliminary experiments demonstrated that the *SAP*-null Jurkat cells are less viable following TCR stimulation compared to the wild type cells (data not shown), but further analysis in primary T cells using either siRNA modulation of SAP expression or patient derived materials would elucidate the specific effects of SAP defects on T cell viability following TCR activation.

XLP1-associated lymphomas, similar to endemic Burkitt's lymphoma[46], occur in childhood and pediatric cancers suggest that defects occur during development. Although SAP is not known to regulate fetal development, it is possible that certain proteins that are expressed during development are aberrantly reactivated during childhood or by exposure to viruses. Particularly in hematopoietic malignancies these developmental proteins, called oncofetal antigens, have been shown to be expressed in cancer cells and not in normal tissues making them an attractive therapy for recognition by CTLs[291]. One such candidate is the B-cell tumor associated antigen ROR1 (receptor tyrosine kinase-like orphan receptor 1), expressed in embryonic stem cells and in B-cell lymphoma but absent in normal B cells[292]. There may be yet uncharacterized fetal proteins that are expressed by the lymphoma cells that promote a survival advantage or enhance cell proliferation in these patients. Determining whether ROR1 or other B cell related oncofetal antigens

are expressed in cells from XLP1-associated lymphomas would provide understanding of factors that influence a portion of SAP-deficient patients to develop cancer as well as identify markers that, when expressed, increase the likelihood of lymphoma development. These biomarkers could greatly improve the early diagnosis and potential survivability.

5.5 Final remarks

The studies presented in this dissertation demonstrated that lack of SAP impairs T cell signaling by altering cytokine production, NFAT transcription factor activity, calcium mobilization, and sensitivity to apoptosis. These changes potentially contribute to abnormal immune cell activation, as well as alter the number and type of cells that are able to respond to infectious agents. Furthermore, the analysis of the *SAP*-null Jurkat cells provided a composite analysis of traits, some of which have been previously associated with various XLP1 studies, attributable to *SAP*-dependent T cell signaling defects. This is the first study to systematically compare the *SAP*-dependent effects on T cell signaling in the same cell line, using this particular gene editing technology, and identified defects, which can be tested in XLP1 patients. Screening for these *SAP*-dependent effects in the clinic may improve survival of patients with undiagnosed *SAP* defects. Additionally, recognizing how SAP defects impair the ability of immune cells to recognize and eliminate pre-neoplastic cells will further enhance the understanding of how XLP1 patients develop lymphoma. Together the insights provided in this study functionally characterized *SAP*-dependent defects in T cell signaling with implications towards the etiology of the complex immunological disease known as XLP.

References

1. Sayos, J. *et al.* The X-linked lymphoproliferative-disease gene product SAP regulates signals induced through the co-receptor SLAM. *Nature* **395,** 462–9 (1998).

2. Coffey, a J. *et al.* Host response to EBV infection in X-linked lymphoproliferative disease results from mutations in an SH2-domain encoding gene. *Nat. Genet.* **20,** 129–35 (1998).

3. Nichols, K. E. *et al.* Inactivating mutations in an SH2 domain-encoding gene in X-linked lymphoproliferative syndrome. *Proc. Natl. Acad. Sci. U. S. A.* **95,** 13765–70 (1998).

4. Rigaud, S. *et al.* XIAP deficiency in humans causes an X-linked lymphoproliferative syndrome. *Nature* **444,** 110–4 (2006).

5. Filipovich, A. H., Zhang, K., Snow, A. L. & Marsh, R. a. X-linked lymphoproliferative syndromes: brothers or distant cousins? *Blood* **116,** 3398–408 (2010).

6. Rumble, J. M. *et al.* Phenotypic differences between mice deficient in XIAP and SAP, two factors targeted in X-linked lymphoproliferative syndrome (XLP). *Cell. Immunol.* **259,** 82–9 (2009).

7. Purtilo, D. *et al.* Epstein-Barr virus-induced diseases in boys with the X-linked lymphoproliferative syndrome (XLP): update on studies of the registry. *Am. J. Med.* **1,** 49–56 (1982).

8. Li, C., Schibli, D. & Li, S. The XLP syndrome protein SAP interacts with SH3 proteins to regulate T cell signaling and proliferation. *Cell Signal* **1,** 111–119 (2009).

9. National Institute of Allergy and Infectious Diseases: Primary Immunodeficiencies. *National Institute of Health* (2015). at <http://www.niaid.nih.gov/topics/immuneDeficiency/Understanding/Pages/quickFacts.aspx>

10. De Vries, E. *et al.* Patient-centered screening for primary immunodeficiency, a multi-stage diagnostic protocol designed for non-immunologists: 2011 update. *Clin. Exp. Immunol.* **167,** 108–119 (2012).

11. Notarangelo, L. Primary immunodeficiencies. *J. Allergy Clin. Immunol.* **125,** S182–94 (2010).

12. Van Der Burg, M. & Gennery, A. R. Educational paper: The expanding clinical and immunological spectrum of severe combined immunodeficiency. *Eur. J. Pediatr.* **170,** 561–571 (2011).

13. Buckley, R. Molecular defects in human severe combined immunodeficiency and approaches to immune reconstitution. *Annu. Rev. Immunol.* **22,** 625–655 (2004).

14. Kasahara, Y. *et al.* Novel Fas (CD95/APO-1) mutations in infants with a lymphoproliferative disorder. *Int. Immunol.* **10,** 195–202 (1998).

15. Miyawaki, T. Primary Immunodeficiencies inducing EBV-associated severe illnesses. *Iran. J. Allergy. Asthma. Immunol.* **3,** 51–57 (2004).

16. Salmena, L. *et al.* Essential role for caspase 8 in T-cell homeostasis and T-cell-mediated immunity. *Genes Dev.* **17,** 883–895 (2003).

17. Horne, A. *et al.* Characterization of PRF1, STX11, and UNC13D genotype-phenotype correlations in familial hemophagocytic lymphohistiocytosis. *Br. J. Haematol.* **143,** 75–83 (2008).

18. Gomez, T. S. & Billadeau, D. D. T cell activation and the cytoskeleton: you can't have one without the other. *Adv. Immunol.* **97,** 1–64 (2008).

19. Katano, H., Patera, A., Catalfamo, M., Jaffe, E. & Kimura, H. Chronic active Epstein-Barr virus infection associated with mutations in perforin that impair its maturation. *Blood* **103,** 1244–52 (2004).

20. Maillard, M., Cotta-de-Almedia, V. & Takeshima, F. The Wiskott-Aldrich syndrome protein is required for the function of $CD4^+CD25^+Foxp3^+$ regulatory T cells. *J. Exp. Med.* **204,** 381–391 (2007).

21. Humblet-Baron, S., Sather, B. & Anover, S. Wiskott-Aldrich syndrome protein is required for regulatory T cell homeostasis. *J. Clin. Invest.* **117,** 207–18 (2007).

22. Palenzuela, G., Bernard, F., Gardiner, Q. & Mondain, M. Malignant B cell non-Hodgkin's lympoma of the larynx in children with Wiskott Aldrich syndrome. *Int. J. Pediatr. Otorhinolaryngol.* **67,** 989–93 (2003).

23. Canioni, D. *et al.* Lymphoproliferative disorders in children with primary immunodeficiencies: immunological status may be more predictive of the outcome than other criteria. *Histopathology* **38,** 146–59 (2001).

24. Albert, M. *et al.* X-linked thrombocytopenia (XLT) due to WAS mutations: clinical characteristics, long-term outcome, and treatment options. *Blood* **115,** 3231–8 (2010).

25. Al-Herz, W. *et al.* Primary immunodeficiency diseases: an update on the classification from the international union of immunological societies expert committee for primary immunodeficiency. *Front. Immunol.* **22 April,** (2014).

26. Tangye, S. G. XLP: Clinical features and molecular etiology due to mutations in SH2D1A encoding SAP. *J. Clin. Immunol.* (2014). doi:10.1007/s10875-014-0083-7

27. Purtilo, D., Cassel, C., Yang, J. & Harper, R. X-linked recessive progressive combined variable immunodeficiency (Duncan's disease). *Lancet* **1,** 935–940 (1975).

28. Marsh, R. *et al.* XIAP deficiency: a unique primar immunodeficiency best classified as X-linked familial hemophagocytic lymphohistiocytosis and not as X-linked lymphoproliferative disease. *Blood* **116,** (2010).

29. Yang, X., Miyawaki, T. & Kanegane, H. SAP and XIAP deficiency in hemophagocytic lymphohistiocytosis. *Pediatr. Int.* 54447–54454 (2012).

30. Filippakopoulos, P., Muller, S. & Knapp, S. SH2 domains: modulators of nonreceptor tyrosine kinase activity. *Curr. Opin. Struct. Biol.* **19,** 643–649 (2009).

31. Latour, S. *et al.* Regulation of SLAM-mediated signal transduction by SAP, the X-linked lymphoproliferative gene product. *Nat. Immunol.* **2,** 681–690 (2001).

32. Veillette, A. *et al.* SAP expression in T cells, not in B cells, is required for humoral immunity. *Proc. Natl. Acad. Sci. U. S. A.* **105,** 1273–8 (2008).

33. Detre, C., Keszei, M., Romero, X., Tsokos, G. C. & Terhorst, C. SLAM family receptors and the SLAM-associated protein (SAP) modulate T cell functions. *Semin. Immunopathol.* **32,** 157–71 (2010).

34. Pachlopnik Schmid, J. *et al.* Clinical similarities and differences of patients with X-linked lymphoproliferative syndrome type 1 (XLP-1/SAP deficiency) versus type 2 (XLP-2/XIAP deficiency). *Blood* **117,** 1522–9 (2011).

35. Janka, G. Hemophagocytic lymphohistiocytosis: when the immune system runs amok. *Klin. Padiatr.* **221,** 278–285 (2009).

36. Beutel, K. *et al.* Infection of T lymphocytes in Epstein-Barr virus-associated hemophagocytic lymphohistiocytosis in children of non-Asian origin. *Pediatr. Blood Cancer* **53,** 184–190 (2009).

37. Yang, X. *et al.* Characterization of Epstein-Barr virus (EBV)-infected cells in EBV-associated hemophagocytic lymphohistiocytosis in two patients with X-linked lymphoproliferative syndrome type 1 and type 2. *Herpesviridae* **3,** (2012).

38. Siminas, S., Caswell, M. & Kenny, S. E. Hemophagocytic lymphohistiocytosis mimicking surgical symptoms and complications: Lessons learned from four cases. *J. Pediatr. Surg.* **48,** 1514–1519 (2013).

39. Xu, X. J. *et al.* Diagnostic accuracy of a specific cytokine pattern in hemophagocytic lymphohistiocytosis in children. *J. Pediatr.* **160,** 984–990.e1 (2012).

40. Gross, T. *et al.* Cure of X-linked lymphoproliferative disease (XLP) with alogenic hematopoietic stem cell transplantation (HSCT): report from the XLP registry. *Bone Marrow Transpl.* 17741–17744 (1996).

41. Filipovich, A., Johnson, J., Zhang, K. & Marsh, R. Lymphoproliferative Disease, X-Linked. *NCBI Bookshelf* (2013). at <ncbi.nlm.nih.gov>

42. Damgaard, R. B. *et al.* Disease-causing mutations in the XIAP BIR2 domain impair NOD2-dependent immune signalling. *EMBO Mol. Med.* **5,** 1278–1295 (2013).

43. Strahm, B. *et al.* Recurrent B-cell non-Hodgkin's lymphoma in two brothers with X-linked lymphoproliferative disease without evidence for Epstein-Barr virus infection. *Br. J. Haematol.* **108,** 377–382 (2000).

44. Brandau, O. *et al.* Epstein-Barr virus-negative boys with non-Hodgkin lymphoma are mutated in the SH2D1A gene, as are patients with X-linked lymphoproliferative disease (XLP). *Hum. Mol. Genet.* **8,** 2407–13 (1999).

45. Burkitt, D. A sarcoma involving the jaws in African children. *Br. J. Surg.* **46,** 218–223 (1958).

46. Pelengaris, S., Khan, M. & Evan, G. c-MYC: more than just a matter of life and death. *Nat. Rev. Cancer* **2,** 764–76 (202AD).

47. Orem, J., Mbidde, E. & Lambert, B. Burkitt's lymphoma in Africa, a review of the epidemiology and etiology. *Afr. Health Sci.* **7,** 166–175 (2007).

48. Palendira, U. *et al.* Molecular pathogenesis of EBV susceptibility in XLP as revealed by analysis of female carriers with heterozygous expression of SAP. *PLoS Biol.* **9,** e1001187 (2011).

49. Harrington, D. S., Weisenburger, D. D. & Purtilo, D. T. Malignant lymphoma in the X-linked lymphoproliferative syndrome. *Cancer* **59,** 1419–1429 (1987).

50. Nagy, N., Klein, G. & Klein, E. To the genesis of Burkitt lymphoma: regulation of apoptosis by EBNA-1 and SAP may determine the fate of Ig-myc translocation carrying B lymphocytes. *Semin. Cancer Biol.* **19,** 407–10 (2009).

51. Rezaei, N., Mahmoudi, E., Aghamohammadi, A., Das, R. & Nichols, K. E. X-linked lymphoproliferative syndrome: a genetic condition typified by the triad of infection, immunodeficiency and lymphoma. *Br. J. Haematol.* **152,** 13–30 (2011).

52. Taniguchi, M., Harada, M., Kojo, S., Nakayama, T. & Wakao, H. The regulatory role of Vα14 NKT cells in innate and acquired immune response. *Annu. Rev. Immunol.* **21,** 483–513 (2003).

53. Parolini, S. *et al.* X-linked lymphoproliferative disease. 2B4 molecules displaying inhibitory rather than activating function are responsible for the inability of natural killer cells to kill Epstein-Barr virus-infected cells. *J. Exp. Med.* **192,** 337–346 (2000).

54. Tangye, S. *et al.* Cutting edge: human 2B4, an activating NK cell receptor, recruits the protein tyrosine phosphatase SHP-2 and the adaptor signaling protein SAP. *J. Immunol.* **162,** 6981–6985 (1999).

55. Coffey A. *et al.* Host response to EBV infection in X-linked lymphoproliferative disease results from mutations in an SH2-domain encoding gene. *Nat Genet* **20,** 129–135 (1998).

56. Bechtel, D., Kurth, J., Unkel, C. & Kuppers, R. Transformation of BCR-deficient germinal-center B cells by EBV supports a major role of the virus in the pathogenesis of Hodgkin and posttransplantation lymphomas. *Blood* **106,** 4345–4350 (2005).

57. Hanahan, D. & Weinberg, R. Hallmarks of cancer: The next generation. *Cell* **144,** 646–674 (2011).

58. Bubenik, J. Tumor MHC class I downregulation and immunotherapy. *Oncol Rep* **10,** 2005–8 (2003).

59. Bubenik, J. MHC class I down-regulation: tumor escape from immune surveillance? *Int. J. Oncol.* **25,** 487–91 (2004).

60. Petersen, J., Morris, C. & Solheim, J. Virus evasion of MHC class I molecule presentation. *J. Immunol.* **171,** 4473–4478 (2003).

61. Schwartz, O., Marechal, V., Gall, S., Lemonnier, F. & Heard, M. Endocytosis of major histocompatability complex class I molecues is induced by the HIV-1 Nef protein. *Nat. Med.* **2,** 338–342 (1996).

62. Howcroft, T., Strebel, K., Martin, M. & Singer, D. Repression of MHC class I gene promoter activity by two-exon Tat of HIV. *Science (80-.).* **160,** 1320 (1993).

63. Lin, J. *et al.* Epstein-Barr virus LMP2A suppresses MHC class II expression by regulating the B-cell transcription factors E47 and PU.1. *Blood* **125,** (2015).

64. Garrido, C. *et al.* MHC class I molecules act as tumor suppressor genes regulating the cell cycle gene expression, invasion and intrinsic tumorigenicity of melanoma cells. *Carcinogenesis* **33,** 687–693 (2012).

65. Vajdic, C. & van Leeuwen, C. Cancer incidence and risk factors after solid organ transplantation. *Int. J. Cancer* **125,** 1747–1754 (2009).

66. Pages, F. *et al.* Immune infiltration in human tumors: a prognostic factor that should not be ignored. *Oncogene* **29,** 1093–1102 (2010).

67. DeNardo, D., Andreu, P. & Coussens, L. Interactions between lymphocytes and myeloid cells regulate pro- versus anti-tumor immunity. *Cancer metastasis Rev.* **29,** 309–316 (2010).

68. Qian, B. & Pollard, J. Macrophage diversity enhances tumor progression and metastasis. *Cell* **141,** 39–51 (2010).

69. Grivennikov, S., Greten, F. & Karin, M. Immunity, inflammation, and cancer. *Cell* **140,** 883–899 (2010).

70. Teng, M., Swann, J., Koebel, C., Schreiber, R. & Smyth, M. Immune-mediated dormancy: an equilibrium with cancer. *J. Leukoc. Biol.* **84,** 988–993 (2008).

71. Kim, R., Emi, M. & Tanabe, K. Cancer immunoediting from immune surveillance to immune escape. *Immunology* **121,** 1–14 (2007).

72. Mroczek, E., Weisenburger, D., Grierson, H., Markin, R. & Purtillo, D. Fatal infectious mononucleosis and virus-associated hemophagocytic syndrome. *Arch Pathol Lab Med* **111,** 530–535 (1987).

73. Wegener, A. *et al.* The T cell receptor/CD3 complex is composed of at least two autonomous transduction modules. *Cell* **68,** 83–95 (1992).

74. Bernard, A., Lamy, A. & Alberti, I. The two-signal model of T-cell activation after 30 years. *Transplantation* **15,** S31–35 (2002).

75. Linsley, P. & Ledbetter, J. The role of the CD28 receptor during T cell responses to antigen. *Annu. Rev. Immunol.* **11,** 191–212 (1993).

76. Bour-Jordan, H. & Blueston, J. CD28 function: a balance of costimulatory and regulatory signals. *J. Clin. Immunol.* **22,** 1–7 (2002).

77. Pages, F. *et al.* Two distinct intracytoplasmic regions of the T-cell adhesion molecule CD28 participate in phosphatidylinositol 3-kinase association. *J Biol Chem* **271,** 9403–9 (1996).

78. Harada, Y. *et al.* A single amino acid alteration in cytoplasmic domain determines IL-2 promoter activation by ligation of CD28 but not inducible costimulator (ICOS). *J. Exp. Med.* **197,** 257–62 (2003).

79. Robey, E. *et al.* Thymic selection in CD8 transgenic mice supports an instructive model for commitment to a CD4 or CD8 lineage. *Cell* **64,** 99–107 (1991).

80. Germain, R. T-cell development and the CD4-CD8 lineage decision. *Nat. Rev. Immunol.* **2,** 309–322 (2002).

81. Von Boehmer, H. & Fehling, H. Structure and function of the pre-T cell receptor. *Annu. Rev. Immunol.* **15,** 433–452 (1997).

82. Raulet, D., Garman, R., Saito, H. & Tonegawa, S. Developmental regulation of T-cell receptor gene expression. *Nature* **314,** 103–107 (1985).

83. Snodgrass, H., Dembic, Z., Steinmetz, M. & von Boehmer, H. Expression of T-cell antigen receptor genes during fetal development in the thymus. *Nature* **315,** 232–233 (1985).

84. Calpe, S. *et al.* The SLAM and SAP gene families control innate and adaptive immune responses. *Adv. Immunol.* **97,** 177–250 (2008).

85. Engel, P., Eck, M. & Terhorst, C. The SAP and SLAM families in immune responses and X-linked lymphoproliferative disease. *Nat. Rev. Immunol.* **3,** 813–821 (2003).

86. Morra, M. *et al.* Structural basis for the interaction of the free SH2 domain EAT-2 with SLAM receptors in hematopoietic cells. *EMBO J.* **20,** 5840–5852 (2001).

87. Hwang, P. M. *et al.* A 'three-pronged' binding mechanism for the SAP/SH2D1A SH2 domain: Structural basis and relevance to the XLP syndrome. *EMBO J.* **21,** 314–323 (2002).

88. Poy, F. *et al.* Crystal structures of the XLP protein SAP reveal a class of SH2 domains with extended, phosphotyrosine-independent sequence recognition. *Mol. Cell* **4,** 555–561 (1999).

89. Shlapatska, L. M. *et al.* CD150 association with either the SH2-containing inositol phosphatase or the SH2-containing protein tyrosine phosphatase is regulated by the adaptor protein SH2D1A. *J. Immunol.* **166,** 5480–5487 (2001).

90. Cambier, J. The awesome power of the immunoreceptor tyrosine-based activation motif (ITAM). *J. Immunol.* **155,** 3281–3285 (1995).

91. Veillette, A. SLAM-family receptors: immune regulators with or without SAP-family adaptors. *Cold Spring Harb. Perspect. Biol.* **2,** (2010).

92. Jordan, M., Singer, A. & Koretzky, G. Adaptors as central mediators of signal transduction in immune cells. *Nat. Immunol.* **4,** 110–116 (2003).

93. Thomas, S. & Brugge, J. Cellular functions regulated by Src family kinases. *Annu. Rev. Cell Dev. Biol.* **13,** 513–609 (1997).

94. Latour, S. *et al.* Binding of SAP SH2 domain to FynT SH3 domain reveals a novel mechanism of receptor signalling in immune regulation. *Nat. Cell Biol.* **5,** 149–154 (2003).

95. Chan, B. *et al.* SAP couples Fyn to SLAM immune receptors. *Nat. Cell Biol.* **5,** 155–160 (2003).

96. Tavano, R. *et al.* CD28 and lipid rafts coordinate recruitment of Lck to the immunological synapse of human T lymphocytes. *J. Immunol.* **173,** 5392 (2004).

97. Simons, K. & Toomre, D. Lipid rafts and signal transduction. *Nat. Rev. Mol. Cell Biol.* **1,** 31–41 (2000).

98. Huse, M. The T-cell-receptor signaling network. *J. Cell Sci.* **122,** 1269–1273 (2009).

99. Palacios, E. H. & Weiss, A. Function of the Src-family kinases, Lck and Fyn, in T-cell development and activation. *Oncogene* **23,** 7990–8000 (2004).

100. Koch, C., Anderson, D., Moran, M., Ellis, C. & Pawson, T. SH2 and SH3 domains: elements that control interactions of cytoplasmic signaling proteins. *Science (80-.).* **252,** 668–674 (1991).

101. Nunez-Cruz, S. *et al.* Differential requirement for the SAP-Fyn interaction during NK T cell development and function. *J. Immunol.* **181,** 2311–2320 (2008).

102. Pelosi, M. *et al.* Tyrosine 319 in the interdomain B of ZAP-70 is a binding site for the Src homology 2 domain of Lck. *J. Biol. Chem.* **274,** 14229–14237 (1999).

103. Chan, C., Iwashima, M., Turck, C. & Weiss, A. ZAP-70: a 70 kd protein-tyrosine kinase that associates with the TCR zeta chain. *Cell* **71,** 649–662 (1992).

104. Zhang, W., Sloan-Lancaster, J., Kitchen, J., Trible, R. & Samelson, L. LAT: The ZAP-70 tyrosine kinase substrate that links T cell receptor to cellular activation. *Cell* **92,** 83–92 (1998).

105. Zhang, W. *et al.* Association of Grb2, Gads, and phospholipase C-γ1 with phosphorylated LAT tyrosine residues: Effect of LAT tyrosine mutations on T cell antigen receptor-mediated signaling. *J. Biol. Chem.* **275,** 23355–23361 (2000).

106. Muscolini, M. *et al.* Phosphatidylinositol 4-phosphate 5-kinase activation critically contributes to CD28-dependent signaling responses. *J. Immunol.* **190,** 5279–5286 (2013).

107. Abraham, R. & Weiss, A. Jurkat T cells and development of the T-cell receptor signalling paradigm. *Nat. Rev. Immunol.* **4,** 301–8 (2004).

108. Veillette, A. SLAM-family receptors: immune regulators with or without SAP-family adaptors. *Cold Spring Harb. Perspect. Biol.* **2,** 1–15 (2010).

109. Cannons, J. & Schwartzberg, P. Fine-tuning lymphocyte regulation: What's new with tyrosine kinases and phosphatases? *Curr. Opin. Immunol.* **16,** 296–303 (2004).

110. Sun, Z. *et al.* PKC-θ is required for TCR-induced NF-κB activation in mature but not immature T lymphocytes. *Nature* **404,** 402–7 (2000).

111. Cannons, J. L. *et al.* Biochemical and genetic evidence for a SAP-PKC-θ interaction contributing to IL-4 regulation. *J. Immunol.* **185,** 2819–27 (2010).

112. Wang, D. *et al.* A requirement for CARMA1 in TCR-induced NF-κB activation. *Nat. Immunol.* **3,** 830–835 (2002).

113. Thome, M., Charton, J., Pelzer, C. & Hailfinger, S. Antigen Receptor Signaling to NF-κB via CARMA1, BCL10, and MALT1. *Cold Spring Harb. Perspect. Biol.* **2,** a003004–a003004 (2010).

114. Hara, H. *et al.* The MAGUK family protein CARD11 is essential for lymphocyte activation. *Immunity* **18,** 763–775 (2003).

115. Ghosh, S., May, M. J. & Kopp, E. B. NF-κB and Rel proteins: evolutionarily conserved mediators of immune responses. *Annu. Rev. Immunol.* **16,** 225–260 (1998).

116. Mikoshiba, K. & Hattori, M. Perspective IP3 receptor-operated calcium entry. *Cell Calcium* **3,** 3–6 (2000).

117. Feske, S. Immunodeficiency due to defects in store-operated calcium entry. *Annu. NY Acad. Sci.* **1238,** 74–90 (2011).

118. Chin, D. & Means, A. Calmodulin: A prototypical calcium sensor. *Trends Cell Biol.* **10,** 322–328 (2000).

119. Klein, S., Waite, B., Donnell, S., Yoder, J. & Shea, M. Regulation of calcineurin by domain-specific interactions with calmodulin. *Biophysj* **104,** 100a (2013).

120. Crabtree, G. & Olson, E. NFAT signaling: choreographing the social lives of cells. *Cell* **109,** 67–79 (2002).

121. Palkowitsch, L. *et al.* The Ca2+-dependent phosphatase calcineurin controls the formation of the Carma1-Bcl10-Malt1 complex during T cell receptor-induced NF-κB activation. *J. Biol. Chem.* **286,** 7522–7534 (2011).

122. Sanzone, S. *et al.* SLAM-associated protein deficiency causes imbalanced early signal transduction and blocks downstream activation in T cells from X-linked lymphoproliferative disease patients. *J. Biol. Chem.* **278,** 29593–9 (2003).

123. Heissmeyer, V. *et al.* Calcineurin imposes T cell unresponsiveness through targeted proteolysis of signaling proteins. *Nat. Immunol.* **5,** 255–265 (2004).

124. Shibasaki, F. & McKeon, F. Calcineurin Functions in Ca^{2+}-activated cell death in mammalian cells. *J. Cell Biol.* **131,** 735–743 (1995).

125. Okkenhaug, K. & Rottapel, R. Grb2 forms an inducible protein complex with CD28 through a Src homology 3 domain-proline interaction. *J Biol Chem* **273,** 21194–202 (1998).

126. Karin, M. The regulation of AP-1 activity by mitogen-activated protein kinases. *J Biol Chem* **270,** 16483–16486 (1995).

127. Jain, J., Valge-archer, V. & Ra, A. Analysis of the AP-1 sites in the IL-2 promoter. *J Immunol* **148**, 1240–1250 (1992).

128. Kamps, M., Corcoran, L., LeBowitz, J. & Baltimore, D. The promoter of the human interleukin-2 gene contains two octamer-binding sites and is partially activated by the expression of Oct-2. *Mol. Cell. Biol.* **10,** 5464–5472 (1990).

129. Gu, C. *et al.* The X-linked lymphoproliferative disease gene product SAP associates with PAK-interacting exchange factor and participates in T cell activation. *Proc. Natl. Acad. Sci. U. S. A.* **103,** 14447–14452 (2006).

130. Pasquier, B. *et al.* Defective NKT cell development in mice and humans lacking the adapter SAP, the X-linked lymphoproliferative syndrome gene product. *J. Exp. Med.* **201,** 695–701 (2005).

131. Nichols, K. E. *et al.* Regulation of NKT cell development by SAP, the protein defective in XLP. *Nat. Med.* **11,** 340–345 (2005).

132. Hu, J., Havenar-Daughton, C. & Crotty, S. Modulation of SAP dependent T:B cell interactions as a strategy to improve vaccination. *Curr. Opin. Virol.* **3,** 363–70 (2013).

133. Veillette, A. Immune regulation by SLAM family receptors and SAP-related adaptors. *Nat. Rev. Immunol.* **6,** 56–66 (2006).

134. Ma, C., Nichols, K. & Tangye, S. Regulation of cellular and humoral immune responses by the SLAM and SAP families of molecules. *Annu. Rev. Immunol.* **25,** 337–379 (2007).

135. Cannons, J. SAP regulates T cell-mediated help for humoral immunity by a mechanism distinct from cytokine regulation. *J. Exp. Med.* **203,** 1551–1565 (2006).

136. MacLennan, I. Germinal centers. *Annu. Rev. Immunol.* **12,** 117–39 (1994).

137. Natkunam, Y. The biology of the germinal center. *ASH Educ. B.* **2007,** 210–215 (2007).

138. Thorbecke, G., Amin, A. & Tsiagbe, V. Biology of germinal centers in lymphoid tissue. *FASEB J* **8,** 832–40 (1994).

139. Qi, H., Cannons, J., Klauschen, F., Schwartzberg, P. & Germain, R. SAP-controlled T-B cell interactions underlie germinal centre formation. *Nature* **455,** 764–769 (2008).

140. Rajewsky, K. Clonal selection and learning in the antibody system. *Nature* **381,** 751–758 (1996).

141. Hess, J., Laumen, H., Muller, K. & Wirth, T. Molecular genetics of the germinal center reaction. *J. Cell Physiol.* **177,** 525–534 (1998).

142. Baumjohann, D. *et al.* Persistent antigen and germinal center B cells sustain T follicular helper cell responses and phenotype. *Immunity* **38,** 596–605 (2013).

143. Yusuf, I. *et al.* Germinal center T follicular helper cell IL-4 production is dependent on signaling lymphocytic activation molecule receptor (CD150). *J. Immunol.* **185,** 190–202 (2010).

144. Kamperschroer, C., Dibble, J., Meents, D., Schwartzberg, L. & Swain, S. SAP is required for Th cell function and for immunity to influenza. *J. Immunol.* **177,** 5317–5327 (2006).

145. Veillette, A. *et al.* SAP expression in T cells, not in B cells, is required for humoral immunity. *Proc. Natl. Acad. Sci. U. S. A.* **105,** 1273–1278 (2008).

146. Shaffer, A., Rosenwald, A. & Staudt, L. Lymphoid malignancies: the dark side of B-cell differentiation. *Nat. Rev. Immunol.* **2,** 920–932 (2002).

147. Stamatopoulous, K., Belessi, C. & Papadaki, T. Somatic hypermutation patterns in germinal center B cell malignancies. *Hematology* **8,** 319–328 (2003).

148. Al-Alem, U. *et al.* Impaired Ig class switch in mice deficient for lymphoproliferative disease gene Sap. *Blood* **106,** 2069–2075 (2005).

149. Morra, M. & Al., E. Defective B cell responses in the absence of SH2D1A. *PNAS* **102**, 4819–4823 (2005).

150. Nichols, K. & Etal. Inactivating mutations in an SH2 domain-encoding gene in X-linked lymphoproliferative syndrome. *Mol. Cell. Biol.* **95,** 13765–13770 (1998).

151. Dong, Z. & Veillette, A. How do SAP family deficiencies compromise immunity? *Trends Immunol.* **31,** 295–302 (2010).

152. Czar, M. J. *et al.* Altered lymphocyte responses and cytokine production in mice deficient in the X-linked lymphoproliferative disease gene SH2D1A/DSHP/SAP. *Proc. Natl. Acad. Sci. U. S. A.* **98,** 7449–7454 (2001).

153. Yin, L. *et al.* Mice deficient in the X-linked lymphoproliferative disease gene sap exhibit increased susceptibility to murine gammaherpesvirus-68 and hypo-gammaglobulinemia. *J. Med. Virol.* **71,** 446–455 (2003).

154. Crotty, S. *et al.* SAP is required for generating long-term humoral immunity. *Nature* **421,** 282–287 (2003).

155. Sumegi, J. *et al.* Correlation of mutations of the SH2D1A gene and Epstein-Barr virus infection with clinical phenotype and outcome in X-linked lymphoproliferative disease. *Blood* **96,** 3118–3125 (2000).

156. Chen, G. *et al.* Signaling lymphocyte activation molecule-associated protein is a negative regulator of the CD8 T cell response in mice. *J. Immunol.* **175,** 2212–2218 (2005).

157. Bloch-Queyrat, C. *et al.* Regulation of natural cytotoxicity by the adaptor SAP and the Src-related kinase Fyn. *JEM* **202,** 181–192 (2005).

158. Dong, Z. & Veillette, A. Essential role of SAP family adaptors in natural killer cell surveillance of hematopoietic cells. *Nat. Immunol.* **10,** 973–980 (2009).

159. Katz, G., Krummey, S., Larsen, S., Stinson, J. & Snow, A. SAP facilitates recruitment and activation of LCK at NTB-A receptors during restimulation-induced cell death. *J. Immunol.* **192,** 4202–9 (2014).

160. Chen, G. *et al.* Increased proliferation of $CD8^+$ T cells in SAP-deficient mice is associated with impaired activation-induced cell death. *Eur. J. Immunol.* **37,** 663–74 (2007).

161. Booth, C. *et al.* X-linked lymphoproliferative disease due to SAP / SH2D1A deficiency : a multicenter study on the manifestations , management , and outcome of the disease *Blood* **117,** 53–62 (2010).

162. Boch, J. & Bonas, U. *Xanthomonas* AvrBs3 family-type III effectors: discovery and function. *Annu. Rev. Phytopathol.* **48,** 419–436 (2010).

163. Boch, J. *et al.* Breaking the code of DNA binding specificity of TAL-type III effectors. *Science* **326,** 1509–1512 (2009).

164. Mussolino, C. *et al.* TALENs facilitate targeted genome editing in human cells with high specificity and low cytotoxicity. *Nucleic Acids Res.* **42,** 6762–6773 (2014).

165. Wyman, C. & Kanaar, R. DNA double-strand break repair: all's well that ends well. *Annu. Rev. Genet.* **40,** 363–383 (2006).

166. Scholze, H. & Boch, J. TAL effectors are remote controls for gene activation. *Curr. Opin. Microbiol.* **14,** 47–53 (2011).

167. Bogdanove, A. & Voytas, D. TAL effectors: customizable proteins for DNA targeting. *Science* **333,** 1843–1846 (2011).

168. Moscou, M. & Bogdanove, A. A simple cipher governs DNA recognition by TAL effectors. *Science* **326,** 1501 (2009).

169. Gifford, C. *et al.* Clinical flow cytometric screening of SAP and XIAP expression accurately identifies patients with SH2D1A and XIAP/BIRC4 mutations. *Clin. Cytom.* **86**, 263-71 (2014).

170. Sander, J, *et al.* Zinc Finger Targeter (ZiFiT): an engineered zinc finger/target site design tool. *Nucleic Acids Res.* **35,** W599–605 (2007).

171. Sander, J. *et al.* ZiFiT (Zinc Finger Targeter): an updated zinc finger engineering tool. *Nucleic Acids Res.* **38,** W462–468 (2010).

172. Buel, E., Schwartz, M. & LaFountain, M. Capillary electrophoresis STR analysis: comparison to gel-based systems. *J Forensic Sci* **43,** 164–170 (1998).

173. Lazaruk, K. *et al.* Genotyping of forensic short tandem repeat (STR) systems based on sizing precision in a capillary electrophoresis instrument. *Electrophoresis* **19,** 86–93 (1998).

174. Butler, J., Buel, E., Crivellente, F. & McCord, B. Forensic DNA typing by capillary electrophoresis using the ABI Prism 310 and 3100 genetic analyzers for STR analysis. *Electrophoresis* **25,** 1397–1412 (2004).

175. Marx, V. Cell-line authentication demystified. *Nat. Methods* **11,** 483–488 (2014).

176. ATCC STR Database. at <www.atcc.org/STR Database.aspx>

177. Altschul, S. *et al.* Gapped BLAST and PSI-BLAST: a new generation of protein database search programs. *Nucleic Acids Res* **25,** 3389–3402 (1997).

178. Cho, S. W. *et al.* Analysis of off-target effects of CRISPR Cas-derived RNA-guided endonucleases and nickases *Genome Res.* **24,** 132–141 (2014). doi:10.1101/gr.162339.113.Freely

179. Gammon, K. Gene therapy editorial control. *Nature* **515,** S11–S13 (2014).

180. Kling, J. CRISPR less reliable than alternatives. *BioTechniques* June (2013).

181. Osborn, M. J. *et al.* TALEN-based gene correction for epidermolysis bullosa. *Mol. Ther.* **21,** 1151–9 (2013).

182. Ma, N. *et al.* Transcription activator-like effector nuclease (TALEN)-mediated Gene correction in integration-free β–thalassemia induced pluripotent stem cells. *J. Biol. Chem.* **288,** 34671–34679 (2013).

183. Engel, P., Eck, M. J. & Terhorst, C. The SAP and SLAM families in immune responses and X-linked lymphoproliferative disease. *Nat. Rev. Immunol.* **3,** 813–21 (2003).

184. Schmid, J. *et al.* Clinical similarities and differences of patients with X-linked lymphoproliferative syndrome type 1 (XLP-1 / SAP deficiency) versus type 2 (XLP-2 / XIAP deficiency). *Blood* **117,** 1–3 (2011).

185. Shinozaki, K. *et al.* Activation-dependent T cell expression of the X-linked lymphoproliferative disease gene product SLAM-associated protein and its assessment for patient detection. *Int. Immunol.* **14,** 1215–1223 (2002).

186. Chen, F. *et al.* High-frequency genome editing using ssDNA oligonucleotides with zinc-finger nucleases. *Nat. Methods* **8,** 753–755 (2011).

187. Feng, Y., Zhang, S. & Huang, X. A robust TALENs system for highly efficient mammalian genome editing. *Sci. Rep.* **4,** 3632 (2014).

188. Gadue, P., Morton, N. & Stein, P. The Src family tyrosine kinase Fyn regulates natural killer T cell development. *J. Exp. Med.* **190,** 1189–1196 (1999).

189. Lewis, J. *et al.* Distinct interactions of the X-linked lymphoproliferative syndrome gene product SAP with cytoplasmic domains of members of the CD2 receptor family. *Clin. Immunol.* **100,** 15–23 (2001).

190. Cannons, J. L. *et al.* SAP regulates Th2 differentiation and PKC-θ-mediated activation of NF-κB1. *Immunity* **21,** 693–706 (2004).

191. Graham, D. B. *et al.* Ly9 (CD229)-deficient mice exhibit T cell defects yet do not share several phenotypic characteristics associated with SLAM- and SAP-deficient mice. *J. Immunol.* **176,** 291–300 (2006).

192. Valdez, P. a. *et al.* NTB-A, a new activating receptor in T cells that regulates autoimmune disease. *J. Biol. Chem.* **279,** 18662–18669 (2004).

193. Sanzone, S. *et al.* SLAM-associated protein deficiency causes imbalanced early signal transduction and blocks downstream activation in T cells from X-linked lymphoproliferative disease patients. *J. Biol. Chem.* **278,** 29593–9 (2003).

194. Baldanzi, G. *et al.* SAP-mediated inhibition of diacylglycerol kinase α regulates TCR-induced diacylglycerol signaling. *J. Immunol.* **187,** 5941–51 (2011).

195. Schoenborn, J. & Wilson, C. Regulation of interferon-γ during innate and adaptive immune responses. *Adv. Immunol.* **96,** 41–101 (2007).

196. Henter, J. I. *et al.* Hypercytokinemia in familial hemophagocytic lymphohistiocytosis. *Blood* **78,** 2918–2922 (1991).

197. Solomou, E., Visconte, V., Gibellini, F. & Young, N. SAP (SH2D1A), the immunomodulator deficient in X-linked lymphoproliferative syndrome (XLP), is profoundly decreased in aplastic anemia: an immunologic link between constitutional and acquired bone marrow failure. in *ASH Annual Meeting* 1141 (2006).

198. Romagnani, S. The Th1/Th2 paradigm. *Immunol. Today* **18,** 263–266 (1997).

199. Pasquinelli, V. *et al.* Expression of signaling lymphocytic activation molecule-associated protein interrupts IFN-γ production in human tuberculosis. *J. Immunol.* **172,** 1177–1185 (2004).

200. Ritchie, M. F., Samakai, E. & Soboloff, J. STIM1 is required for attenuation of PMCA-mediated Ca^{2+} clearance during T-cell activation. *EMBO J.* **31,** 1123–1133 (2012).

201. Cosman, D. Control of messenger RNA stability. *Immunol. Today* **8,** 16–17 (1987).

202. Chen, C., Ezzeddine, N. & Shyu, A. Messenger RNA half-life measurements in mammalian cells. *Methods Enzymol.* **448,** 335–357 (2008).

203. Zubiaga, A., Belasco, J. & Greenberg, M. The nonamer UUAUUUAUU is the key AU-rich sequence motif that mediates mRNA degradation. *Mol. Cell. Biol.* **15,** 2219–2230 (1995).

204. Macian, F. NFAT proteins: key regulators of T-cell development and function. *Nat. Rev. Immunol.* **5,** 472–484 (2005).

205. Kaminuma, O. *et al.* Differential contribution of NFATc2 and NFATc1 to TNF–α gene expression in T cells. *J. Immunol.* **180,** 319–326 (2008).

206. Pan, F. *et al.* Feedback inhibition of calcineurin and Ras by a dual inhibitory protein carabin. *Nature* **445,** 433–436 (2007).

207. Schickel, J. N. *et al.* Carabin deficiency in B cells increases BCR-TLR9 costimulation-induced autoimmunity. *EMBO Mol. Med.* **4,** 1261–1275 (2012).

208. NovImmune. Long-term follow-up of HLH patient who received treatment with NI-0501, an anti-interferon γ monoclonal antibody. (2014). at <https://clinicaltrials.gov/ct2/show/NCT02069899?term=ni0501&rank=1>

209. Mosmann, T. & Sad, S. The expanding universe of T-cell subsets: Th1, Th2 and more. *Immunol. Today* **17,** 138–46 (1996).

210. Szabo, S. *et al.* Distinct effects of T-bet in Th1 lineage commitment and IFN-γ production in CD4 and CD8 T cells. *Science (80-.).* **295,** 338–342 (2002).

211. Nurieva, R. *et al.* Bcl6 mediates the development of T follicular helper cells. *Science* **325,** 1001–5 (2009).

212. Oestreich, K. J., Huang, A. C. & Weinmann, A. S. The lineage-defining factors T-bet and Bcl-6 collaborate to regulate Th1 gene expression patterns. *J. Exp. Med.* **208,** 1001–1013 (2011).

213. Choi, Y. *et al.* ICOS receptor instructs T follicular helper cell versus effector cell differentiation via induction of the transcriptional repressor Bcl6. *Immunity* **34,** 932–46 (2011).

214. Rudensky, A. Y., Gavin, M. & Zheng, Y. FOXP3 and NFAT: partners in tolerance. *Cell* **126,** 253–256 (2006).

215. Galluzi, L. & Kroemer, G. Necroptosis: a specialized pathway of programmed necrosis. *Cell* **135,** 1161–1163 (2008).

216. Zong, W. & Thompson, C. Necrotic death as a cell fate. *Genes Dev.* **20,** 1–15 (2006).

217. Alnemri, E. *et al.* Human ICE/CED-3 protease nomenclature. *Cell* **18,** 171 (1996).

218. Nicholson, D. & Thornberry, N. Caspases: killer proteases. *Trends Biochem. Sci.* **8,** 299–306 (1997).

219. Oehm, A. *et al.* Purification and molecular cloning of the APO-1 cell surface antigen, a member of the tumor necrosis factor growth factor receptor superfamily. *J. Biol. Chem.* **267,** 10709-15 (1992).

220. Chinnaiyan, A., O'Rourke, K., Tewari, M. & Dixit, V. FADD, a novel death domain-containing protein, interacts with the death domain of Fas and initiaties apoptosis. *Cell* **81,** 505–512 (1995).

221. Muzio, M. *et al.* FLICE, a novel FADD-homologous ICE/CED-3-like protease, is recruited to the CD95 (Fas/APO-1) death-inducing signaling complex (DISC). *Cell* **85,** 817–827 (1996).

222. Scaffidi, C. *et al.* Two CD95 (APO-1/Fas) signaling pathways. *EMBO J.* **17,** 1675–1687 (1998).

223. Enari, M., Talanian, R., Wong, W. & Nagata, S. Sequential activation of ICE-like and CPP32-like proteases during Fas-mediated apoptosis. *Nature* **380,** 723–726 (1996).

224. Orth, K., O'Rourke, K., Salvesen, G. S. & Dixit, V. M. Molecular ordering of apoptotic mammalian CED-3/ICE-like proteases. *J. Biol. Chem.* **271,** 20977–20980 (1996).

225. Deveraux, Q. L. *et al.* Cleavage of human inhibitor of apoptosis protein XIAP results in fragments with distinct specificities for caspases. *EMBO J.* **18,** 5242–5251 (1999).

226. Takahashi, R. *et al.* A single BIR domain of XIAP sufficient for inhibiting caspases. *J. Biol. Chem.* **273,** 7787–7790 (1998).

227. Oltvai, Z., Milliman, C. & Korsmeyer, S. Bcl-1 heterodimerizes in vivo with a conserved homolog, Bax, that accelerates programmed cell death. *Cell* **74,** 609–619 (1993).

228. Hu, Y., Benedict, M., Ding, L. & Nunez, G. Role of Cytochrome *c* and dATP/ATP in Apaf-1-mediated Caspse-9 activation and apoptosis. *EMBO J.* **18**, 3586-95 (1999).

229. Zou, H., Li, Y., Liu, X. & Wang, X. An APAF-1 Cytochrome *c* multimeric complex is a functional apoptosome that activates procaspase-9. *J. Biol. Chem.* **274,** 11549–11556 (1999).

230. Scott, F. L. *et al.* XIAP inhibits Caspase-3 and -7 using two binding sites: evolutionarily conserved mechanism of IAPs. *EMBO J.* **24,** 645–655 (2005).

231. Holler, N. *et al.* Fas triggers an alternative, Caspase-8-independent cell death pathway using the kinase RIP as effector molecule. *Nat Immunol* **1,** 489–495 (2000).

232. Lin, Y. *et al.* Tumor Necrosis Factor-induced nonapoptotic cell death requires receptor-interacting protein-mediated cellular reactive oxygen species accumulation. *J. Biol. Chem.* **279,** 10822–10828 (2004).

233. Tang, D., Lahti, J., Grenet, J. & Kidd, V. Cycloheximide-induced T-cell death is mediated by a Fas-associated death domain-dependent mechanism. *J. Biol. Chem.* **274,** 7245–7252 (1999).

234. Karpinich, N., Tafani, M., Rothman, R., Russo, M. & Farber, J. The course of etoposide-induced apoptosis from damage to DNA and p53 activation to mitochondrial release of Cytochrome *c*. *J. Biol. Chem.* **277,** 16547–16552 (2002).

235. De Saint Jean, M., Brignole, F., Feldmann, G., Goguel, A. & Baudouin, C. Interferon-γ induces apoptosis and expression of inflammation-related proteins in Chang conjunctival cells. *Investig. Ophthalmol. Vis. Sci.* **40,** 2199–2212 (1999).

236. Liu, Y. *et al.* Mesenchymal stem cell-based tissue regeneration is governed by recipient T lymphocytes via IFN-γ and TNF-α. *Nat Med* **17,** 1594–1601 (2011).

237. Orrenius, S., Zhivotovsky, B. & Nicotera, P. Regulation of cell death: the calcium-apoptosis link. *Nat. Rev. Mol. Cell Biol.* **4,** 552–565 (2003).

238. Pinton, P., Giorgi, C., Siviero, R., Zecchini, E. & Rizzuto, R. Calcium and apoptosis: ER-mitochondria Ca^{2+} transfer in the control of apoptosis. *Oncogene* **27,** 6407–6418 (2008).

239. Gulez, N. *et al.* X-linked lymphoproliferative syndrome and common variable immunodeficiency may not be differentiated by SH2D1A and XIAP/BIRC4 genes sequence analysis. *Case Rep. Med.* **2011,** 121258 (2011).

240. Carbone, A., Gloghini, A. & Dotti, G. EBV-associated lymphoproliferative disorders: classification and treatment. *Oncologist* **13,** 577–585 (2008).

241. Calender, A. *et al.* Epstein-Barr virus (EBV) induces expression of B-cell activation markers on in vitro infection of EBV-negative B-lymphoma cells. *PNAS* **84,** 8060–8064 (1987).

242. Nikiforow, S., Bottomly, K. & Miller, G. $CD4^+$ T-cell effectors inhibit Epstein-Barr virus-induced B-cell proliferation. *J. Virol.* **75,** 3740–3752 (2001).

243. Ma, C. S. *et al.* Impaired humoral immunity in X-linked lymphoproliferative disease is associated with defective IL-10 production by $CD4^+$ T cells. *J. Clin. Invest.* **115,** 1049–1059 (2005).

244. Chuang, H. C. *et al.* Epstein-Barr virus LMP1 inhibits the expression of SAP gene and upregulates Th1 cytokines in the pathogenesis of hemophagocytic syndrome. *Blood* **106,** 3090–3096 (2005).

245. Ahsan, N., Kanda, T., Nagashima, K. & Takada, K. Epstein-Barr virus transforming protein LMP1 plays a critical role in virus production *J. Virol.* **79,** 4415–4424 (2005).

246. Liebowitz, D., Kopan, R., Fuchs, E., Sample, J. & Kieff, E. An Epstein-Barr virus transforming protein associates with vimentin in lymphocytes. *Mol. Cell. Biol.* **7,** 2299–2308 (1987).

247. Irving, B. & Weiss, A. The cytoplasmic domain of the T cell receptor ζ chain is sufficient to couple to receptor-associated signal transduction pathways. *Cell* **64,** 891–901 (1991).

248. Abraham, R. T. & Weiss, A. Jurkat T cells and development of the T-cell receptor signalling paradigm. *Nat. Rev. Immunol.* **4,** 301–308 (2004).

249. Rhee, I. & Veillette, A. Protein tyrosine phosphatases in lymphocyte activation and autoimmunity. *Nat. Immunol.* **13,** 439–47 (2012).

250. Altman, A. & Villalba, M. Protein kinase C-θ: it's all about location, location, location. *Immunol. Rev.* **192,** 53–63 (2003).

251. Schmitz, M. L., Bacher, S. & Dienz, O. NF-κB activation pathways induced by T cell costimulation. *FASEB J.* **17,** 2187–2193 (2003).

252. Reynolds, L. F. *et al.* Vav1 transduces T cell receptor signals to the activation of phospholipase C-γ1 via phosphoinositide 3-kinase-dependent and -independent pathways. *J. Exp. Med.* **195,** 1103–1114 (2002).

253. Dong, Z. *et al.* The adaptor SAP controls NK cell activation by regulating the enzymes Vav-1 and SHIP-1 and by enhancing conjugates with target cells. *Immunity* **36,** 974–85 (2012).

254. Cao, Y. *et al.* Pleiotropic defects in TCR signaling in a Vav-1-null Jurkat T-cell line. *EMBO J.* **21,** 4809–4819 (2002).

255. Tybulewicz, V., Ardouin, L., Prisco, A. & Reynolds, L. Vav1: a key signal transducer downstream of the TCR. *Immunol. Rev.* **192,** 42–52 (2003).

256. Lewis, R. Calcium signaling mechanisms in T lymphocytes. *Annu. Rev. Immunol.* **19,** 497–521 (2001).

257. Yuan, T. & Cantley, L. PI3K pathway alterations in cancer: variations on a theme. *Oncogene* **27,** 5497–5510 (2008).

258. Jiang, B. & Liu, L. PI3K/PTEN signaling in angiogenesis and tumorigenesis. *Adv. Cancer Res.* **102,** 19–65 (2009).

259. Juntilla, M. & Evan, G. p53-a jack of all trade but master of none. *Nat. Rev. cancer* **9,** 821–829 (2009).

260. Adams, J. & Cory, S. The Bcl-2 apoptotic switch in cancer development and therapy. *Oncogene* **26,** 1324–1337 (2007).

261. Willis, S. & Adams, J. Life in the balance: how BH3-only proteins induce apoptosis. *Curr. Opin. Cell Biol.* **17,** 617–625 (2005).

262. Kessenbrock, K., Plaks, V. & Werb, Z. Matrix metalloproteinases: regulators of the tumor microenvironment. *Cell* **141,** 52–67 (2010).

263. Yoshimura, A. & Muto, G. TGF-β function in immune suppression. *Curr. Top. Microbiol. Immunol.* **350,** 127–47 (2011).

264. Wahl, S., Swisher, J., McCartney-Francis, N. & Chen, W. TGF-β: the perpetrator of immune suppression by regulatory T cells and suicidal T cells. *J. Leukoc. Biol.* **76,** 15–24 (2004).

265. Mougiakakos, D., Choudhury, A., Lladser, A., Kiessling, R. & Johansson, C. Regulatory T cells in cancer. *Adv. Cancer Res.* **107,** 57–117 (2010).

266. Smyth, M., Strobl, S., Young, H., Ortaldo, J. & Ochoa, A. Regulation of lymphokine-activated killer activity and pore-forming protein gene expression in human peripheral blood $CD8^+$ T lymphocytes. *J. Immunol.* **146,** 3289–97 (1991).

267. Yang, L., Pang, Y. & Moses, H. TGF-β and immune cells: an important regulatory axis in the tumor microenvironment and progression. *Trends Immunol.* **31,** 220–227 (2010).

268. Kashkar, H. *et al.* XIAP-mediated caspase inhibition in Hodgkin's lymphoma-derived B cells. *J. Exp. Med.* **198,** 341–347 (2003).

269. Van Themsche, C., Chaudhry, P., Leblanc, V., Parent, S. & Asselin, E. XIAP gene expression and function is regulated by autocrine and paracrine TGF-β signaling. *Mol. Cancer* **9,** 216 (2010).

270. Cao, Z. *et al.* X-linked inhibitor of apoptosis protein (XIAP) regulation of cyclin D1 protein expression and cancer cell anchorage-independent growth via its E3 ligase-mediated protein phosphatase 2A/c-Jun axis. *J. Biol. Chem.* **288,** 20238–20247 (2013).

271. Park, T., Rosenberg, S. & Morgan, R. Treating cancer with genetically engineered T cells. *Trends Biotechnol.* **29,** 550–557 (2011).

272. Kershaw, M., Teng, M., Smyth, M. & Darcy, P. Supernatural T cells: genetic modification of T cells for cancer therapy. *Nat. Rev. Immunol.* **5,** 928–940 (2005).

273. Sadelain, M., Brentjens, R. & Rivière, I. The promise and potential pitfalls of chimeric antigen receptors. *Curr. Opin. Immunol.* **21,** 215–223 (2009).

274. Nadler, L. M. *et al.* B4, a human B lymphocyte-associated antigen expressed on normal, mitogen-activated, and malignant B lymphocytes. *J. Immunol.* **131,** 244–250 (1983).

275. Restifo, N., Dudley, M. & Rosenberg, S. Adoptive immunotherapy for cancer: harnessing the T cell response. *Nat. Rev. Immunol.* **12,** 269–281 (2012).

276. Maude, S. L. *et al.* Chimeric antigen receptor T cells for sustained remissions in leukemia. *N. Engl. J. Med.* **371,** 1507–1517 (2014).

277. Kochenderfer, J. *et al.* Anti-CD19 CAR T cells administered after low-dose chemotherapy can induce remissions of chemotherapy-refractor diffuse large B-cell lymphoma. in *American Society of Hematology* Abstract 550 (2014).

278. Brower, V. The CAR T-cell race. *The Scientist* (2015).

279. Turtle, C. *et al.* Therapy of B cell malignancies with CD19-specific chimeric antigen receptor-modified T cells of defined subset composition. in *American Society of Hematology* Abstract 384 (2014).

280. Bollard, C. M. *et al.* Complete responses of relapsed lymphoma following genetic modification of tumor-antigen presenting cells and T-lymphocyte transfer. *Blood* **110,** 2838–2845 (2007).

281. Bollard, C., Rooney, C. & Heslop, H. T-cell therapy in the treatment of post-transplant lymphoproliferative disease. *Nat Rev Clin Oncol* **9,** 510–9 (2012).

282. Micklethwaite, K. P. *et al.* Derivation of human T lymphocytes from cord blood and peripheral blood with antiviral and antileukemic specificity from a single culture as protection against infection and relapse after stem cell transplantation. *Blood* **115,** 2695–2703 (2010).

283. Terakura, S. *et al.* Generation of CD19-chimeric antigen receptor modified CD8+ T cells derived from virus-specific central memory T cells *Blood* **119,** 72–82 (2012).

284. Kochenderfer, J. & Rosenberg, S. Treating B-cell cancer with T cells expressing anti-CD19 chimeric antigen receptors. *Nat. Rev. Clin. Oncol.* **10,** 267–76 (2013).

285. Safa, A. & Pollok, K. Targeting the anti-apoptotic protein c-FLIP for cancer therapy. *Cancers (Basel)* **3,** 1639–71 (2011).

286. Alam, A., Cohen, L., Aouad, S. & Sekaly, R. Early activation of caspases during T lymphocyte stimulation results in selective substrate cleavage in nonapoptotic cells. *JEM* **190,** 1879–1890 (1999).

287. Kennedy, N., Katoaka, T., Tschopp, J. & Budd, R. Caspase activation is required for T cell proliferation. *JEM* **190,** 1891–1896 (1999).

288. Zhang, J. *et al.* Regulation of Fas ligand expression during activation-induced cell death in T cells by p38 mitogen-activated protein kinase and c-Jun NH2-terminal kinase. *J. Exp. Med.* **191,** 1017–1030 (2000).

289. Maher, S., Toomey, D., Condron, C. & Bouchier-Hayes, D. Activation-induced cell death: The controversial role of Fas and Fas ligand in immune privilege and tumour counterattack. *Immunol. Cell Biol.* **80,** 131–137 (2002).

290. Nagy, N. *et al.* The proapoptotic function of SAP provides a clue to the clinical picture of X-linked lymphoproliferative disease. *PNAS* **106,** 11966–11971 (2009).

291. Siegel, S. *et al.* Induction of cytotoxic T-cell responses against the oncofetal antigen-immature laminin receptor for the treatment of hematologic malignancies. *Blood* **102,** 4416–4423 (2003).

292. Hudecek, M. *et al.* The B-cell tumor associated antigen ROR1 can be targeted with T cells modified to express a ROR1-specific chimeric antigen receptor. *Blood* **116,** 4532–41 (2010).